RESSALVA

Atendendo solicitação do autor, o texto completo desta **Tese** será disponibilizado somente a partir de 29/01/2021.

UNIVERSIDADE ESTADUAL PAULISTA "JÚLIO DE MESQUITA FILHO"
FACULDADE DE CIÊNCIAS FARMACÊUTICAS
DEPARTAMENTO DE CIÊNCIAS BIOLÓGICAS

RONE APARECIDO DE GRANDIS

Avaliação toxicogenética e estudo dos mecanismos de resposta antiproliferativa de metalofármacos de rutênio contendo bioligantes naftoquinônicos em modelos celulares tumorais convencionais e em 3D

ARARAQUARA
2020

RONE APARECIDO DE GRANDIS

Avaliação toxicogenética e estudo dos mecanismos de resposta antiproliferativa de metalofármacos de rutênio contendo bioligantes naftoquinônicos em modelos celulares tumorais convencionais e em 3D

Tese apresentada à Faculdade de Ciências Farmacêuticas da UNESP, como parte das exigências do Programa de Pós-Graduação em Biociências e Biotecnologia Aplicadas à Farmácia, para obtenção do título de Doutor.

Orientador: Prof. Dr. Fernando Rogério Pavan

ARARAQUARA

2020

De Grandis, Rone Aparecido.
D321a Avaliação toxicogenética e estudo dos mecanismos de resposta antiproliferativa de metalofármacos de rutênio contendo bioligantes naftoquinônicos em modelos celulares tumorais convencionais e em 3D / Rone Aparecido De Grandis. – Araraquara: [S.n.], 2020.
163 f. : il.

Tese (Doutorado) – Universidade Estadual Paulista. "Júlio de Mesquita Filho". Faculdade de Ciências Farmacêuticas. Programa de Pós Graduação em Biociências e Biotecnologia Aplicadas à Farmácia.

Orientador: Fernando Rogério Pavan.

1. Câncer. 2. Lapachol. 3. Complexo de rutênio. 4. Apoptose. 5. ERO. I. Pavan, Fernando Rogério, orient. II. Título.

Diretoria do Serviço Técnico de Biblioteca e Documentação - Faculdade de Ciências Farmacêuticas
UNESP - Campus de Araraquara

CAPES: 33004030081P7
Esta ficha não pode ser modificada

UNIVERSIDADE ESTADUAL PAULISTA

Câmpus de Araraquara

CERTIFICADO DE APROVAÇÃO

TÍTULO DA TESE: Avaliação toxicogenética e estudo dos mecanismos de resposta antiproliferativa de metalofármacos de rutênio contendo bioligantes naftoquinônicos em modelos celulares tumorais convencionais e em 3D

AUTOR: RONE APARECIDO DE GRANDIS
ORIENTADOR: FERNANDO ROGERIO PAVAN

Aprovado como parte das exigências para obtenção do Título de Doutor em BIOCIÊNCIAS E BIOTECNOLOGIA APLICADAS À FARMÁCIA, área: Análises Clínicas pela Comissão Examinadora:

Prof. Dr. FERNANDO ROGERIO PAVAN
Departamento de Ciências Biológicas / FCF- UNESP - Araraquara

Profa. Dra. DENISE CRISPIM TAVARES
Departamento de Ciências Biológicas / Universidade de Franca

Prof. Dr. LUIS OCTÁVIO REGASINI
Departamento de Química e Ciências Ambientais / Ibilce/ Unesp/ São José do Rio Preto

Profa. Dra. FLÁVIA APARECÍDA RESENDE NOGUEIRA
Departamento de Ciências Biológicas e da Saúde / Universidade de Araraquara - UNIARA

Prof. Dr. CLEVERTON ROBERTO DE ANDRADE
Departamento de Fisiologia e Patologia / FOAR- UNESP - Araraquara

Araraquara, 29 de janeiro de 2020

Dedico especialmente este trabalho aos meus pais e à minha irmã, por todo o amor, o apoio e o incentivo durante todas as etapas de minha vida.

AGRADECIMENTOS

A conclusão deste trabalho finaliza um importante ciclo na minha vida profissional, um ciclo marcado por enriquecedores momentos vividos enquanto aluno de pós-graduação. Ao longo dos anos dedicados à pesquisa, em muitas situações contei com pessoas especiais que contribuíram direta ou indiretamente para a conclusão deste trabalho. À essas pessoas, deixo registrado meus sinceros agradecimentos:

Ao meu orientador ***Prof. Dr. Fernando Rogério Pavan*** pela orientação, pela amizade e pela oportunidade concedida ao abrir as portas de seu laboratório. Sou muito grato por ter me acolhido e caminhado ao meu lado durante as dificuldades desta trajetória.

À minha orientadora ***Profa. Dra. Lusânia Maria Greggi Antunes***, pela orientação, pelo apoio, pelo respeito, pelo carinho e também pela imensa contribuição para meu amadurecimento profissional e pessoal.

Ao ***Prof. Dr. Alzir Azevedo Batista***, pelo apoio, pela simpatia, pelos momentos de descontração e de ensinamento que ultrapassaram os limites da universidade.

Às minhas orientadoras de iniciação científica e mestrado, professoras doutoras, ***Ticiana Capote, Raquel Caminaga, Flávia Resende*** e ***Eliana Varanda***, pelas muitas oportunidades oferecidas e por me introduzirem ao fascinante campo da pesquisa científica.

Aos professores, ***Dr. Adelino de Godoy Neto***, ***Dra. Denise Tavares*** e ***Dra. Paula Barbugli***, pelas imprescindíveis colocações durante o exame geral de qualificação.

Aos ***professores membros da banca examinadora***, pela disponibilidade e pelas contribuições para este trabalho.

À ***FAPESP*** pela concessão da bolsa de doutorado e pelo suporte financeiro oferecido para a realização deste trabalho.

À ***CAPES*** pelo suporte financeiro oferecido, bem como ao ***CNPq*** e à ***FAEPA/HCFMRP***.

Aos colegas do Laboratório de Pesquisa de Fármacos contra Tuberculose da FCF/UNESP, ***Débora***, ***Camila M.***, ***Mari***, ***Ana Carolina***, ***Manu***, ***Rachel***, ***Giulia***, ***Camila G.***, ***Gabi***, ***Júlia*** e ***Mel***, pela recepção amigável, pelo excelente ambiente de trabalho, pela amizade e pelos momentos de descontração.

Aos colegas do Laboratório de Nutrigenômica da FCFRP/USP, ***Patrick***, ***Ana Rita***, ***Katiuska***, ***Diego***, ***Lívia***, ***Xandão*** e ***Joana D'Arc***, pela convivência harmoniosa, por todo auxílio prestado nas atividades de pesquisa, pela amizade e por fazerem os dias em Ribeirão Preto mais leves e agradáveis.

Aos funcionários do Departamento de Genética da FMRP/USP, do Departamento de Análises Clínicas e Toxicológicas da FCFRP/USP e do Departamento de Ciências Biológicas da FCF/UNESP, por toda a atenção, o apoio, a dedicação e a simpatia.

A todos meus amigos, principalmente: ***Jéssica***, ***Larissa***, ***Mariane***, ***Flávia S.***, ***Roberta***, ***Matheus***, ***Marina***, ***Maria Clara***, ***Patrick*** e minhas amigas de infância ***Érica*** e ***Flávia***, minha gratidão pela verdadeira amizade, pelos conselhos, pelas conversas, pelo apoio e pelos momentos de descontração.

Ao meu companheiro, ***Wellington Marques***, por todos os momentos felizes que passamos juntos, pelo amor, pelo carinho, pelo respeito e pela cumplicidade. Obrigado por toda a compreensão, a paciência e o incentivo durante meu doutorado.

À minha família, especialmente à ***Izilda, minha mãe***, por seus gestos solidários, pelo amor e pelo carinho que me ensinaram os limites da vida, por ter investido e acreditado sempre na educação e por ter me incentivado a trilhar os caminhos do conhecimento. Amo você!

"Conheça todas as teorias, domine todas as técnicas, mas ao tocar uma alma humana, seja apenas outra alma humana." Carl Jung

APOIO E SUPORTE FINANCEIRO

Este trabalho foi realizado com o apoio financeiro das seguintes entidades e instituições:

- Fundação de Amparo à Pesquisa do Estado de São Paulo – FAPESP (Proc. N° 2016/22429-7 e 2018/00168-0).

- Coordenação de Aperfeiçoamento de Pessoal de Nível Superior – CAPES (Código de Financiamento 001).

- Conselho Nacional de Desenvolvimento Científico e Tecnológico – CNPq.

- Faculdade de Ciências Farmacêuticas da UNESP – FCF/UNESP.

- Faculdade de Ciências Farmacêuticas de Ribeirão Preto – FCFRP/USP

NORMATIZAÇÃO ADOTADA

Este documento foi elaborado de acordo com:

- Referências: Associação Brasileiras de Normas Técnicas (ABNT) - NBR 6023/2018.

- Biblioteca da Faculdade de Ciências Farmacêuticas do câmpus de Araraquara, UNESP. Diretrizes para apresentações de dissertações e teses, 2020.

RESUMO

DE GRANDIS, Rone Aparecido. **Avaliação toxicogenética e estudo dos mecanismos de resposta antiproliferativa de metalofármacos de rutênio contendo ligantes naftoquinônicos em modelos celulares tumorais convencionais e em 3D**. 163p, Tese - Faculdade de Ciências Farmacêuticas, Universidade Estadual Paulista, Araraquara, 2020.

Recentemente, complexos de rutênio têm ocupado lugar de destaque na busca por novas terapias anticâncer em razão de sua potencialidade de ação, seletividade em tecido tumoral e toxicidade inferior aos complexos de platina, atualmente utilizados na clínica. A diversidade de seus ligantes é fundamental para que esses metalofármacos atinjam múltiplos alvos biológicos e assim, superem as limitações das terapias existentes. Uma abordagem para moléculas multialvo é a combinação de ligantes bioativos com propriedades antitumorais comprovadas, como os derivados de naftoquinonas naturais. Baseados nisso, esse estudo propôs a avaliação e caracterização das propriedades toxicogenéticas e antitumorais de oito novos complexos de rutênio contendo os ligantes naturais lapachol e lausona. De maneira geral, a série de complexos fosfínicos apresentou satisfatória atividade antiproliferativa frente a diferentes linhagens celulares tumorais, em especial para células derivadas de carcinoma de próstata. Os valores de IC_{50} desses complexos foram consideravelmente menores do que os valores encontrados para a cisplatina, no qual foi observada atividade até 28 vezes mais seletiva, em relação a esse fármaco. Além disso, os ensaios de eficiência clonogênica sugerem que a substituição do ligante bipy pela phen aumenta a atividade dos compostos, induzindo a perda da clonogenicidade das células tumorais de próstata DU-145. Os complexos fosfínicos também apresentaram atividade antiproliferativa em modelos celulares em três dimensões (3D). Nesses ensaios, os complexos contendo o ligante lapachol demonstraram atividade citotóxica independente do estado de hipóxia encontrado no interior dos esferoides. Ademais, os resultados indicam que o complexo DP-LP é capaz de permear através do esferoide tumoral e desestabilizar as agregações celulares, resultando na perturbação das interações célula-matriz. De fato, o complexo DP-LP desencadeia apoptose em células DU-145 acompanhado de um acúmulo de células na fase G2/M, o que é consistente com a inibição da atividade da proteína AURORA-B. O mecanismo central relacionado com esses efeitos é de que a presença do lapachol no complexo DP-LP promova a geração de espécies reativas intracelulares que podem causar danos ao DNA. A fragmentação do DNA, evidenciada pelo ensaio do cometa pode ativar sistemas de reparos de DNA que mantém as células no *checkpoint* G2/M devido a diminuição da expressão do gene *AURKB*. Além disso, os danos ao DNA configuram o estímulo que desencadeia a ativação de caspases que conduz as células DU-145 à apoptose. Em suma, os resultados encontrados neste estudo contribuem para a seleção e elucidação das propriedades antiproliferativas e citotóxicas de novos compostos, demonstrando que a coordenação do lapachol em complexos fosfínicos de rutênio(II) possibilita a formação de complexos com potencial de impacto na área de saúde tendo como alvo o tratamento do câncer.

Palavras-chave: câncer, lapachol, complexo de rutênio, apoptose, ERO.

ABSTRACT

DE GRANDIS, Rone Aparecido. **Toxicogenetic evaluation and study of antiproliferative response mechanisms of ruthenium-based metallodrugs containing naphthoquinones ligands in tumor cells growing in conventional and 3D systems**. 163p, Thesis – School of Pharmaceutical Sciences, São Paulo State University, Araraquara, 2020.

Recently, ruthenium complexes have occupied a leading position in the search for new anti-cancer therapies due to their potential of action, selectivity in tumor tissues and less toxicity compared to current platinum complexes. The diversity of ligands is crucial for these complexes to reach multiple biological targets and thus, overcome the limitation of contemporary therapies. One approach for multi-target molecules is the combination of bioactive ligands with recognized antitumor properties, such as natural naphthoquinones. Based on this, this study had proposed the evaluation and characterization of toxicogenetics and antitumor properties of eight new ruthenium complexes containing the natural ligands lapachol and lawsone. In general, the phosphinic series showed satisfactory antiproliferative activity against different cell lines, especially prostate carcinoma-derived cells. The IC_{50} values of these complexes were considerably lower than the values found for cisplatin. Furthermore, it was observed up to 28-fold selective for the complexes than cisplatin. Also, clonogenic assay suggests that the replacement of bipy ligand for phen increases the compound activity, inducing loss of DU-145 cells clonogenicity. Phosphinic complexes also described antiproliferative activities in three-dimensional (3D) cell models. In these assays, the lapachol-complexes have demonstrated cytotoxic activity independent of the hypoxia found in the spheroids. Besides, the results suggest that the DP-LP complex goes through the spheroid and destabilizes the cell aggregates, resulting in disruption of matrix-cell interactions. The DP-LP complex triggers apoptosis in DU-145 cells accompanied by an increase of cells in the G2 / M phase, which is consistent with the inhibition of AURORA-B protein activity. The central mechanism related to these effects is the presence of lapachol in DP-LP, which promotes the generation of intracellular reactive species that can cause DNA damage. DNA fragmentation, evidenced by comet assay, could activate the DNA repair systems that maintain the cells in the G2 / M checkpoint, due to a decrease of the AURKB gene expression. Also, DNA damage could activate caspases that conducted the DU-145 cells to apoptosis. In summary, the results found in this study contributed to the selection and elucidation of antiproliferative and cytotoxic properties of new compounds. We demonstrate the coordination of lapachol in a phosphinic ruthenium complex allowed the formation of compounds with potential impact in health targeting cancer treatment.

Keywords: cancer, lapachol, ruthenium complex, apoptosis, ROS.

LISTA DE ILUSTRAÇÕES

Figura 1. As 10 marcas registradas do câncer e seus possíveis alvos terapêuticos. 18

Figura 2. Principais adutos formados por meio da interação do cisplatina com o DNA.....22

Figura 3. Distribuição seletiva preferencial de íons de rutênio por meio da transferrina..... 25

Figura 4. Fórmulas estruturais dos complexos de rutênio NAMI-A, KP1019 e RAPTA-C. 26

Figura 5. Fórmulas estruturais dos principais grupos de quinonas. 28

Figura 6. Ipê-roxo (*Tabebuia avellanedae* Lor, Bignoniaceae) do Instituto de Química de Araraquara - UNESP e a fórmula estrutural do lapachol 29

Figura 7. Henna (*Lawsonia inermis* L.) e a fórmula estrutural da lausona 31

Figura 8. Células tumorais cultivadas em microambientes em 3D expressam diferentes sinais celulares que alteram suas respostas ao meio.. 35

Figura 9. Representação esquemática da microplaca de 96 poços no ensaio de citotoxicidade da resazurina 42

Figura 10. Viabilidade celular (%) da linhagem não-tumoral FGH após o tratamento de 24 horas com os complexos de rutênio 59

Figura 11. Viabilidade celular (%) da linhagem não-tumoral PNT-2 após o tratamento de 24 horas com os complexos de rutênio. 60

Figura 12. Viabilidade celular (%) da linhagem tumoral A549 após o tratamento de 24 horas com os complexos de rutênio. 60

Figura 13. Viabilidade celular (%) da linhagem tumoral Caco-2 após o tratamento de 24 horas com os complexos de rutênio. 61

Figura 14. Viabilidade celular (%) da linhagem tumoral DU-145 após o tratamento de 24 horas com os complexos de rutênio. 61

Figura 15. Viabilidade celular (%) da linhagem tumoral HepG2 após o tratamento de 24 horas com os complexos de rutênio. 62

Figura 16. Viabilidade celular (%) da linhagem tumoral MDA-MB-231 após o tratamento de 24 horas com os complexos de rutênio. 62

Figura 17. Viabilidade celular (%) da linhagem tumoral PC-3 após o tratamento de 24 horas com os complexos de rutênio. 63

Figura 18. Avaliação da citotoxicidade pelo ensaio de sobrevivência clonogênica em células DU-145. 68

Figura 19. Efeitos dos complexos na viabilidade de esferoides multicelulares tumorais (EMT) de células DU-145..... 71

Figura 20. Efeito do complexo DP-LP no crescimento de esferoides multicelulares tumorais (EMT) de células DU-145..... 72

Figura 21. Efeito dos complexos DB-LP e DP-LP na possível indução da apoptose em células tumorais de próstata DU-145..... 75

Figura 22. Imagens representativas dos núcleos de células DU-145 duplamente marcadas com Hoechst 33342 e PI..... 77

Figura 23. Efeito do complexo DP-LP sobre a cinética de ciclo celular de células DU-145..... 78

Figura 24. Efeito do complexo DP-LP nos níveis de espécies reativas intracelulares 81

Figura 25. (A) Níveis de ERO após 24 horas de tratamento com complexo DP-LP nas concentrações de 0,5, 1 e 2 μM na ausência (-) ou na presença (+) do antioxidante NAC (5 mM). (B) Viabilidade celular de células DU-145 avaliadas pelo ensaio de Alamar blue após 24 horas de incubação com diferentes concentrações do complexo DP-LP na ausência (-) ou na presença (+) do antioxidante NAC. 82

Figura 26. (A) Imagens representativas dos tratamentos de 24 horas durante a análise do ensaio do cometa das células DU-145. Aumento de 200x. (B) *Tail Intensity* (% de DNA na cauda) dos 300 nucleoides avaliados da linhagem tumoral DU-145, após o tratamento com o complexo DP-LP. 87

Figura 27. Imagem representativa do tratamento com 1,0 μM do complexo por 24 horas em células DU-145 do ensaio do cometa. 88

Figura 28. (A) Imagens representativas dos tratamentos de 24 horas durante a análise do ensaio do cometa das células PNT-2. Aumento de 200x. (B) *Tail Intensity* (% de DNA na cauda) dos 300 nucleoides avaliados da linhagem não-tumoral PNT-2, após o tratamento com o complexo DP-LP 90

Figura 29. Imagens representativas de células DU-145 marcadas com Hoechst 33342 (núcleo) e FITC (citoplasma). 94

Figura 30. Espectros de emissão de fluorescência dos complexos BB-LP (A), BP-LP (B), DB-LP (C) e DP-LP (D), na presença de quantidades crescentes de CT-DNA . 98

Figura 31. Mobilidade por eletroforese de DNA do plasmídeo pBR322 com quantidades crescentes de complexos BB-LP e BP-LP (A), e os complexos DB-LP e DP-LP (B), após 18 horas de incubação a 37 ° C..... 100

Figura 32. Espectros de emissão do Hoechst, CT-DNA, contendo diferentes relações molares [complexo]/[CT-DNA]..... 101

Figura 33. Gel de eletroforese capilar e número de integridade de RNA (RIN) do RNA total extraído das células DU-145. 103

Figura 34. Expressão das proteínas PARP, PARP-clivada, caspase-3 clivada, caspase-9 clivada, caspase-8 clivada, AURORA-B e do controle endógeno β-actina em células DU-145 analisada por western blot..... 112

Figura 35. Valores obtidos na análise pelo programa Scion Image, referentes às médias dos valores de expressão proteica e seu desvio padrão.....114

LISTA DE TABELAS

Tabela 1. Complexo de Ru-naftoquinonas sintetizados pelo Laboratório de Estrutura e Reatividade de Compostos Inorgânicos da Universidade Federal de São Carlos (UFSCar). 38

Tabela 2. Média dos valores de log P e da IC50 (μM) dos complexos de Ru-naftoquinonas, precursores e ligantes nas linhagens celulares tumorais A549, Caco-2, DU-145, HepG2, MDA-MB-231, PC-3 e nas linhagens não-tumorais FGH e PNT-2. 64

Tabela 3. Índices de seletividade dos complexos de Ru-naftoquinonas e da cisplatina calculados pela razão dos valores de IC50 em células não-tumorais e tumorais.....66

Tabela 4. Frequência de micronúcleos (MNi) e índice de proliferação pelo bloqueio da citocinese (CBPI) em cultura de células DU-145 após 24 horas de tratamento com o complexo DP-LP. 93

Tabela 5. Frequência de micronúcleos (MNi) e índice de proliferação pelo bloqueio da citocinese (CBPI) em cultura de células PNT-2 após 24 horas de tratamento com o complexo DP-LP. 96

Tabela 6. Quantidade de RNA total dos grupos controle, dos grupos de células tratadas com o complexo DP-LP e razões A260/A280 e A260/A280. 102

Tabela 7. Efeito do complexo de rutênio DP-LP sobre a expressão gênica de células DU-145. 105

SUMÁRIO

CAPÍTULO 1

1. INTRODUÇÃO **17**
1.1 O Câncer **17**
1.2 Quimioterapia anticâncer **20**
1.3 Complexos de Rutênio **24**
1.4 Ligantes naftoquinônicos **27**
1.5 Busca por novos candidatos anticâncer **32**
2. OBJETIVOS **37**
2.1 Objetivo geral **37**
2.2 Objetivos específicos **37**
3. MATERIAL E MÉTODOS **38**
3.1 Síntese dos complexos **38**
3.1.1 Determinação do Coeficiente de Partição (log *P*) **40**
3.2. Linhagens Celulares **40**
3.3 Avaliação da viabilidade celular e atividade citotóxica **41**
3.3.1 Ensaio redox da resazurina (Alamar blue**)** **41**
3.3.2 Ensaio de sobrevivência clonogênica **43**
3.3.3 Inibição do crescimento de esferoides tumorais cultivados em 3D **44**
3.4 Avaliação dos mecanismos de morte celular **45**
3.4.1 Ensaio de marcação com Anexina V / Iodeto de propídeo **45**
3.4.2 Análise da cinética de ciclo celular **46**
3.4.3 Determinação dos níveis de espécies reativas intracelulares **46**
3.5 Avaliação da instabilidade genômica e interação com o DNA **49**
3.5.1 Atividade genotóxica **49**
3.5.2 Atividade mutagênica **50**
3.5.3 Estudos de interação com o DNA **52**
3.6 Análise da expressão transcricional e traducional de genes envolvidos com a atividade antiproliferativa **53**
3.7 Análise dos resultados **58**
4. RESULTADOS E DISCUSSÃO **59**
4.1 Avaliação da viabilidade celular e atividade citotóxica **59**
4.2 Avaliação dos mecanismos de morte celular **74**
4.3 Avaliação da instabilidade genômica e interação com o DNA **85**
4.4 Análise da expressão transcricional e traducional de genes envolvidos com a atividade antiproliferativa **101**
5. CONCLUSÃO **118**
6. REFERÊNCIAS BIBLIOGRÁFICAS **120**

CAPÍTULO 2

1. PUBLICAÇÕES REFERENTES À TESE **142**
2. PRODUÇÃO BIBLIOGRÁGICA NO PERÍODO DO DOUTORADO **157**

Capítulo 1

1. INTRODUÇÃO

1.1 O Câncer

O câncer atinge a humanidade desde os tempos pré-históricos, embora sua prevalência tenha aumentado acentuadamente nas últimas décadas. O registro escrito considerado como o primeiro relato da doença aparece em manuscritos egípcios, como no papiro de Edwin Smith, possivelmente escrito por Imhotep, médico-arquiteto egípcio, do ano de 1600 a.C. (FAGUET, 2015). Após o declínio das civilizações egípcia e grega, a medicina romana tornou-se hegemônica, especialmente com Hipócrates, considerado o pai da medicina (460-360 a.C.). Em seus escritos, são retratadas doenças produtoras de massas ("*onkos"*) e nódulos úlcerantes e não cicatrizantes que variavam de processos benignos a malignos ("*karkinos*") (FAGUET, 2015). No entanto, apenas no início do século 20, a introdução de novas ferramentas científicas permitiu que médicos e pesquisadores explorassem antigas e novas hipóteses sobre a natureza do câncer, levando a um progresso significativo no estudo oncológico (BLACKADAR, 2016).

Hoje, sabe-se que o processo de formação do câncer decorre de mudanças genéticas e epigenéticas que alteram o funcionamento interno da célula e a maneira como ela se relaciona com o meio externo (COOPER, 2000). As células tumorais podem se originar em diferentes tecidos, à medida que crescem e se dividem. Esse crescimento está habilmente regulado por centenas de genes que controlam sua proliferação. No entanto, quando essas células acumulam mutações nos vários genes que regulam o equilíbrio desses processos, dá-se início à carcinogênese (COOPER, 2000). As células tumorais apresentam ainda uma série de características que as diferem das células não-tumorais, como: autossuficiência em

sinais de crescimento, resistência a sinais inibitórios de crescimento, resistência à morte celular, permitindo a imortalidade replicativa e a indução de angiogênese. Essas características permitem o crescimento tumoral e são comuns tanto a tumores benignos quanto malignos. No entanto, somente os tumores malignos possuem a capacidade de invadir novos tecidos e órgãos distantes, promovendo a metástase (YOKOTA, 2000).

O desenvolvimento das várias características tipicamente associadas às células tumorais depende da aquisição de alterações nos seus genomas (HANAHAN; WEINBERG, 2011). As marcas registradas do câncer (Figura 1), descritas por Hanahan & Weinberg (2000), correspondem a essas capacidades funcionais adquiridas pelas células tumorais, que as permitem escapar dos mecanismos de defesa anticâncer existentes no interior das células e dos tecidos e, assim, se sobreporem às células sadias.

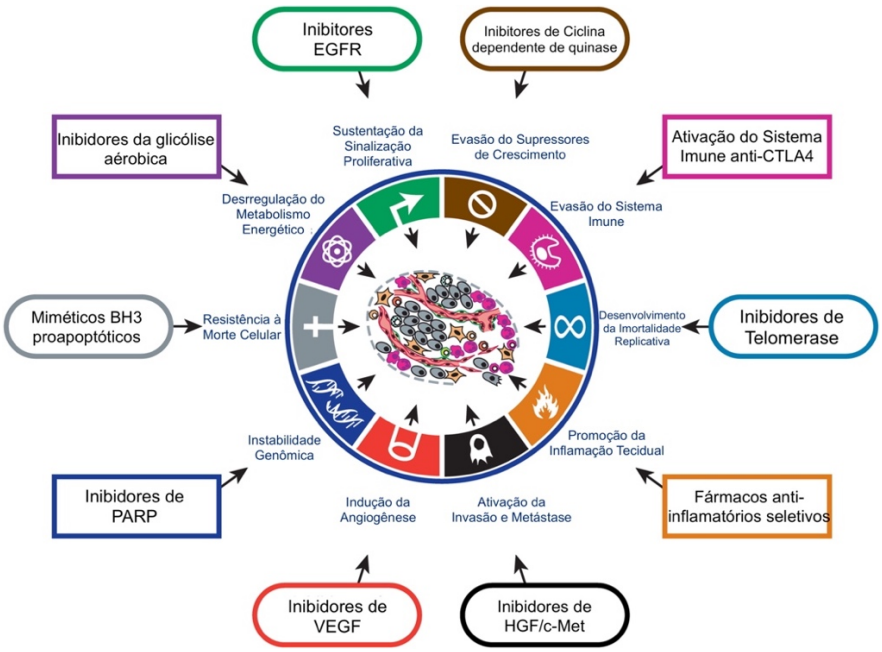


Figura 1. As 10 marcas registradas do câncer e seus possíveis alvos terapêuticos. Adaptado de Hanahan & Weinberg (2011).

A instabilidade genômica está presente na maioria dos cânceres humanos e em todos os seus estádios de desenvolvimento, desde lesões pré-cancerosas até cânceres em fases avançadas (HANAHAN; WEINBERG, 2000). De acordo com os resultados da pesquisa do Projeto Genoma do Câncer, a maioria das células tumorais possuem cerca de 60 mutações acumuladas (FORBES et al., 2015). Logo, o câncer pode ser definido como doença genética, ou seja, causada por alterações em genes que controlam a funcionalidade das células, especialmente como elas crescem e se dividem (NCI, 2015; SIEGEL et al., 2016). Devido às suas características malignas e a alta taxa de incidência na população, o câncer é hoje considerado um dos mais importantes problemas de saúde pública mundial (SIEGEL et al., 2017).

De acordo com o último relatório da IARC, agência da Organização Mundial da Saúde (OMS) de pesquisa sobre o câncer, estima-se que em 2030 pode-se esperar 22 milhões de casos incidentes de câncer e quase 17 milhões de mortes, tornando-se, assim, a principal causa de mortes em todo o mundo (IARC, 2018). A incidência e mortalidade do câncer estão crescendo rapidamente em todo mundo. As razões são complexas, mas refletem o aumento da longevidade e crescimento da população, bem como as mudanças de hábitos associadas ao desenvolvimento econômico (BRAY et al., 2018). No Brasil, o risco de desenvolver a doença até os 75 anos é de cerca de 20%. Ou seja, em média, uma em cada cinco pessoas terá câncer até os 75 anos, excetuando-se os cânceres de pele não-melanoma, que costumam ser excluídos das estatísticas por terem uma alta incidência, mas bom prognóstico (INCA, 2018).

A partir da década de 1960, vários fatores produziram uma rápida transição epidemiológica, expondo cada vez mais a população ao risco de doenças crônicas.

Especificamente no Brasil, aspectos como o aumento da renda, industrialização, mecanização da produção, urbanização, novos estilos de vida, melhor acesso à alimentação em geral, incluindo alimentos processados e globalização de hábitos não saudáveis, favoreceram à exposição da população a fatores de risco que podem aumentar as chances de uma pessoa desenvolver câncer (JEMAL et al., 2010). Como resultado desse processo, no Brasil, o câncer é a segunda causa mais comum de mortes, após doenças cardíacas e cerebrovasculares (BARBOSA et al., 2015). O Instituto Nacional do Câncer (INCA), estimou para o biênio 2018-2019 a ocorrência de cerca de 600.000 casos novos de câncer no país. Os tipos mais recorrentes são os de próstata nos homens (68.220 casos novos por ano), e os de mama nas mulheres (59.700 casos novos por ano) (INCA, 2018).

Tradicionalmente, a terapia de combate ao câncer tem sido baseada no princípio de que as células tumorais encontram-se frequentemente em divisão, sendo, portanto, mais sensíveis do que as células sadias à interferência na síntese de DNA e mitose. Assim, foram desenvolvidos ao longo dos anos múltiplas classes de agentes antineoplásicos destinados a interferir nas unidades formadoras na síntese do DNA e mitose, ou causar danos no DNA e instabilidade cromossômica, promovendo, portanto, a citotoxicidade e a morte celular programada (apoptose) (GOLAN, 2016).

1.2 Quimioterapia anticâncer

A quimioterapia é a forma de tratamento sistêmico do câncer que usa medicamentos denominados genericamente de quimioterápicos antineoplásicos - sejam eles quimioterápicos propriamente ditos, hormonioterápicos, bioterápicos, imunoterápicos, alvoterápicos - que são administrados continuamente ou a

intervalos regulares, que variam de acordo com os esquemas terapêuticos (LACERDA, 2001). Especificamente no tratamento anticâncer, a quimioterapia possui a capacidade de induzir a apoptose ou de abrandar o ritmo da divisão das células (LUNDQVIST et al., 2015). Ela é possivelmente a terapia oncológica que pode ser mais explorada, na medida em que podem ser testadas as capacidades de indução de morte celular de inúmeros compostos.

Atualmente, mais de 100 medicamentos são utilizados na quimioterapia de tratamento do câncer, seja isoladamente ou em combinação com outros fármacos (AMERICAN CANCER SOCIETY, 2019). No Sistema Único de Saúde (SUS) a área de oncologia é estruturada para atender de forma integral e integrada os pacientes que necessitam de tratamento. Logo, os hospitais oncológicos habilitados na alta complexidade em oncologia no SUS são os responsáveis pelo fornecimento de medicamentos antineoplásicos que eles, livremente, padronizam, adquirem e fornecem aos pacientes (MINISTÉRIO DA SAÚDE, 2013).

Os antineoplásicos podem ser classificados de acordo com suas diferentes atividades farmacológicas, sendo estes: (1) agentes alquilantes, que atuam por meio da formação de ligações covalentes com o DNA, impedindo sua replicação; (2) antimetabólicos, que interferem nas vias metabólicas envolvidas na síntese do DNA; (3) antagonistas de hormônios, que inibem o crescimento de células responsivas à esteroides; (4) imunoterápicos, que auxiliam o sistema imunológico a identificar e combater células tumorais; (5) inibidores mitóticos, que levam à paralisação da divisão celular; (6) inibidores de quinases, que impedem a proliferação e (7) agentes alvo-dirigidos, que atuam em receptores ou proteínas citoplasmáticas relacionadas com vias de proliferação ou sobrevivência celular (ESPINOSA et al., 2003; GOLAN, 2016).

Dentre as diversas opções quimioterapêuticas, o composto inorgânico *cis*-[diaminodicloroplatina(II)], denominado como cisplatina, é um dos fármacos citotóxicos mais utilizados devido à sua eficácia no tratamento de vários tipos de câncer (ALDOSSARY, 2019; DASARI; BERNARD TCHOUNWOU, 2014). A cisplatina foi o primeiro complexo de platina aprovado pelo *Food and Drug Administration* (FDA) em 1978 para o tratamento do câncer e, junto com a carboplatina e oxaliplatina, representam os principais metalofármacos baseados em platina utilizados no tratamento do câncer (KELLAND, 2007).

A interação que complexos de platina possuem com o DNA, leva a distorção da molécula e consequentemente quebra. Assim chamados agentes alquilantes, são capazes de substituir em outra molécula, um átomo de hidrogênio por um radical alquil e dessa forma, se ligam ao DNA de modo a impedir a separação das fitas, fenômeno este indispensável para a replicação (Figura 2) (KELLAND, 2007; SIKOV, 2015).

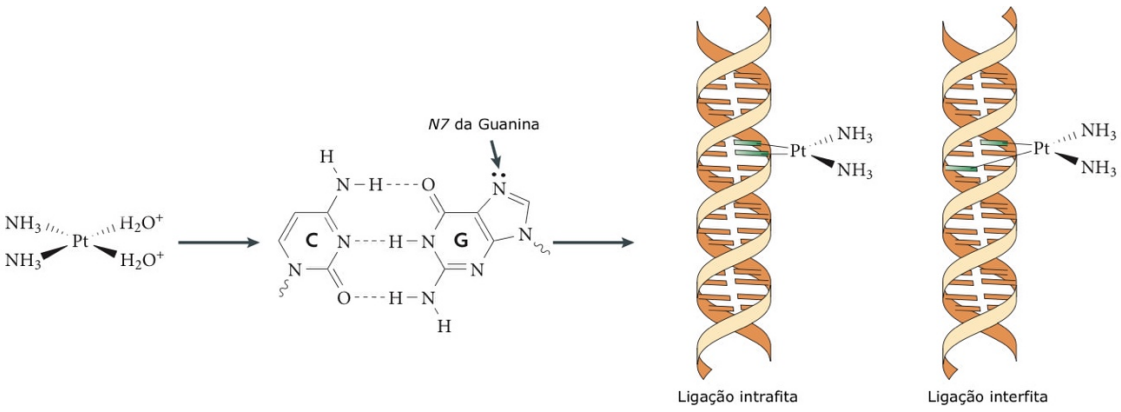


Figura 2. Principais adutos formados por meio da interação do cisplatina com o DNA. A molécula hidrolisada pode causar interação 1,2-intrafita ou 1,3-interfitas. Adaptado de Kelland, 2007.

Contudo, sua inespecificidade dá-se por afetar as células em todas as fases do ciclo celular (INCA, 2016; VAN RIJT; SADLER, 2009). A resistência tumoral é uma limitação importante do tratamento medicamentoso à base de platina. A

resistência adquirida a esses fármacos pode ocorrer por meio de três mecanismos principais: aumento de sua degradação e desativação antes que ele atinja o DNA nuclear, diminuição de sua captação pelas células tumorais e aumento da proficiência do sistema de reparo de DNA dessas células (AMABLE, 2016).

Todos os medicamentos à base de platina, exibem uma série de efeitos adversos graves devido à sua baixa seletividade pelo tecido canceroso sobre o tecido normal. A baixa seletividade apresentada é devida aos altos requerimentos nutricionais das células em proliferação. Logo, enquanto esses fármacos são absorvidos pelas células tumorais de crescimento rápido, elas também são absorvidas em outros tecidos que estão crescendo rapidamente, como as membranas mucosas da boca, garganta, estômago e intestinos, o que leva à toxicidade gastrointestinal. Além disso, a medula óssea é afetada, o que pode resultar na redução da produção de glóbulos brancos e vermelhos, bem como os folículos capilares e pilosos, o que significa que o tratamento com esses fármacos pode resultar em alopecia e ototoxicidade (OUN et al., 2018).

Na busca por fármacos mais seletivos, outros centros metálicos em substituição à platina têm atraído o interesse dos pesquisadores (MUHAMMAD; GUO, 2014; OTT; GUST, 2007; ZHANG; LIPPARD, 2003). Algumas características têm sido investigadas com o intuito de se alcançar efeitos farmacológicos mais eficazes e seguros. Dentre elas, pode-se destacar a presença de sítios de coordenação adicionais, mudanças no estado de oxidação, alterações na afinidade do ligante pelo metal e a possibilidade de utilização da terapia fotodinâmica (ALBANI et al., 2014; PRESA et al., 2015). Nessas circunstâncias, deu-se início ao estudo de complexos de rutênio como possíveis agentes antitumorais mais seguros (ALLARDYCE; DYSON, 2016).

1.3 Complexos de Rutênio

O rutênio (Ru) tem recebido destaque como centro metálico de novos complexos anticâncer devido as suas propriedades químicas. Sua variedade de estados de oxidação e estabilidade com diversos ligantes, tem atraído o interesse na busca de novos metalofármacos. O centro metálico é predominantemente hexacoordenado, de geometria octaédrica, o que permite a formação de uma enorme gama de complexos, cujo potencial redox pode ser modificado com a variação de seus ligantes e, com isso, ser modulado a fim de se atingir a eficácia desejada em potenciais novos medicamentos (ALLARDYCE; DYSON, 2001; BRABEC; KASPARKOVA, 2018).

Esse elemento possui baixa toxicidade quando comparado com outros metais, como a platina. Além disso, sua capacidade de mimetizar o ferro na ligação com proteínas plasmáticas garante ao rutênio benefícios importantes de transporte nos sistemas biológicos (ALLARDYCE; DYSON, 2001). A semelhança entre esses dois metais pode explicar a capacidade do rutênio se ligar à transferrina e à albumina. Essas proteínas são as responsáveis por transportar o ferro do plasma para os tecidos, principalmente os que estão em maior divisão e que por isso, possuem necessidades aumentadas do elemento (ANTONARAKIS; EMADI, 2010). Devido a alta taxa de divisão celular nos tumores, e consequente expressão de receptores para transferrina, estudos *in vivo* reportaram o aumento de 2 a 12 vezes na concentração de rutênio em células tumorais em comparação com as células não-tumorais (SAVA; BERGAMO, 2000). Esta deposição seletiva é facilitada pelo transporte via transferrina pelo sangue, conforme sugerido por Sava et al. (1990) que baseou-se na necessidade exacerbada de ferro das células tumorais. Considera-se então, que uma vez absorvido, o rutênio liga-se à transferrina presente

no plasma e seja disponibilizado aos tecidos na forma de um complexo rutênio-transferrina (Figura 3). Essas características tornam os complexos de Ru bem aceitos para a aplicação medicinal.

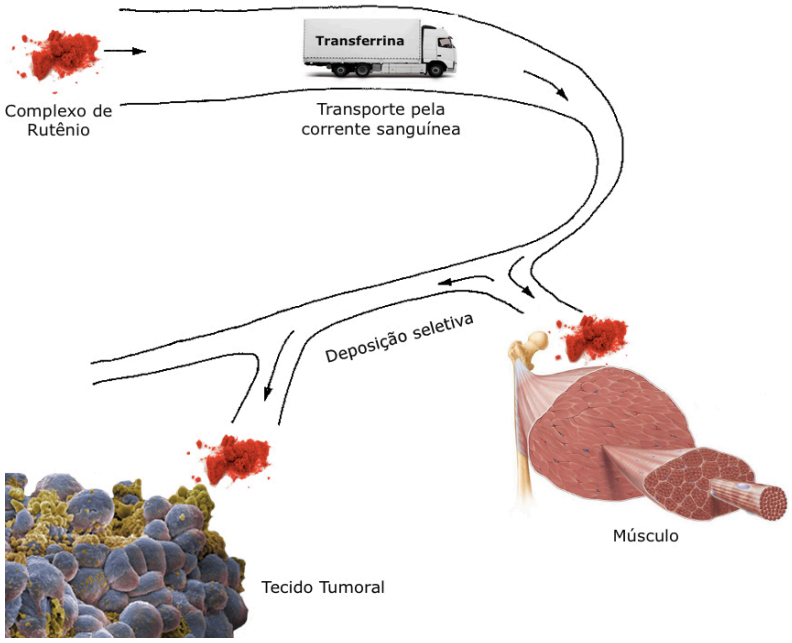


Figura 3. Distribuição seletiva preferencial de íons de rutênio por meio da transferrina. Adaptado de Sava et al. (1990).

Ao longo dos últimos anos, alguns complexos de Ru destacaram-se por apresentar significativas propriedades antitumorais e antimetastáticas (ALLARDYCE; DYSON, 2001; ZORZET et al., 2000). Por exemplo, alguns complexos de Ru como NAMI-A (*trans*-[$RuCl_4$(1H-imidazol)(DMSO-S)]), KP1019 (*trans*-[$RuCl_4$(1H-in-dazole)$_2$]) e RAPTA-C (Ru(η^6-C_6H_5Me)(pta)Cl_2) (Figura 4) apresentaram resultados satisfatórios em ensaios pré-clínicos e clínicos de fase I ou II.

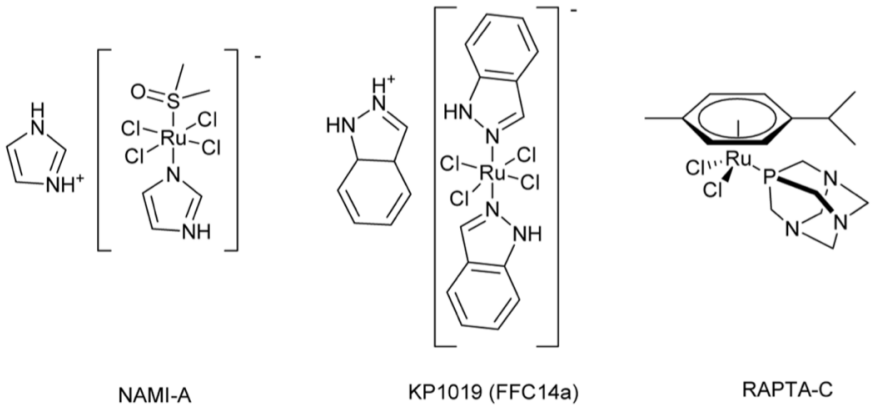


Figura 4. Fórmulas estruturais dos complexos de rutênio NAMI-A, KP1019 e RAPTA-C. (OTT; GUST, 2007).

O NAMI-A (acrônimo de *New Antitumor Metastasis Inhibitor*) foi primeiro complexo de Ru a entrar em ensaios clínicos. Esse complexo apresenta baixa citotoxicidade *in vitro*, no entanto, estudos *in vivo* evidenciaram seu potencial antitumoral. Sua principal característica é afetar a mobilidade das células tumorais, demonstrando, portanto, atividade antimetastática. Seu mecanismo de ação ainda não é conhecido, mas estudos têm indicado a capacidade do complexo em modificar a espessura da matriz extracelular e os processos de angiogênese, impedindo que as células tumorais invadam tecidos vizinhos e os vasos sanguíneos (RADEMAKER-LAKHAI et al., 2004). O NAMI-A completou em 2014 a fase II dos testes clínicos no Instituto de Câncer da Holanda (LEIJEN et al., 2015).

O complexo KP1019 apresentou em estudos pré-clínicos, promissora atividade contra tumores colorretais resistentes à quimioterapia padrão. Seu mecanismo de ação mostra-se semelhante ao do cisplatina, ou seja, interage com o DNA desestabilizando-o; no entanto, com menor intensidade que a do derivado de platina. Esse complexo é considerado um pró-fármaco, uma vez que inibe o crescimento tumoral após ativação por redução do seu centro metálico de Ru(III) para Ru(II), dadas as condições de hipóxia do tumor. Estudos farmacocinéticos em

humanos apresentaram resultados semelhantes daqueles verificados para o NAMI-A, ou seja, respostas satisfatórias em termos de ligação com proteínas plasmáticas e de eliminação (BERGAMO et al., 2015).

O RAPTA-C é um complexo de Ru(II) do tipo "*piano stool*", ou seja, possui estrutura similar a um banco de piano, com a presença do ligante PTA (1,3,5-triaza-7-fosfoadamantano). Esse ligante permite a ativação do complexo em ambiente hipóxico, o mesmo encontrado nos tumores sólidos. O complexo apresenta elevada seletividade para células tumorais e propriedades antimetastáticas promissoras. Estudos pré-clínicos demonstraram sua capacidade de modular o citoesqueleto celular diminuindo a capacidade das células invadirem e migrarem para outros tecidos (LEE et al., 2017).

Outros estudos apontam uma variedade de complexos de Ru com promissora atividade antitumoral, apresentando mecanismos de intercalação com o DNA (RAMADEVI et al., 2015), como inibidores das DNA-topoisomerases I e II (He et al., 2015), inibidores da viabilidade de células tumorais *in vitro* (VIJAYAN et al., 2014) e também, atividade antitumoral *in vivo* (WEISS et al., 2014). Esses resultados provêm do desenho de complexos com variados ligantes que conferem à estrutura uma química bastante diversificada. A diversidade dos ligantes é fundamental para que esses complexos atinjam múltiplos alvos biológicos e, assim, superem as limitações das terapias existentes. Uma abordagem para moléculas multialvo é a combinação de ligantes bioativos com propriedades antitumorais comprovadas, como os derivados de quinonas.

1.4 Ligantes naftoquinônicos

As quinonas são um grupo de substâncias orgânicas consideradas pelo *U.S National Cancer Institute* (NCI) como uma classe importante, biologicamente validada, para o desenvolvimento de novas moléculas com atividade antitumoral (MARX et al., 2003). Muitos medicamentos anticâncer, indispensáveis clinicamente, possuem uma porção quinona em sua molécula. As antraciclinas (doxorrubicina, daunorrubicina e mitoxantrona), mitomicina-c e bleomicina, são alguns exemplos de fármacos chave na quimioterapia para tratamento de muitas neoplasias malignas (AVENDAÑO; MENÉNDEZ, 2008). Os efeitos citotóxicos das quinonas estão relacionados com diferentes mecanismos, tais como: intercalação e indução de quebras do DNA, inibição das enzimas topoisomerases e geração de radicais livres (KUBANIK et al., 2016).

As quinonas podem ser divididas em três grupos em razão de diferenças em suas estruturas moleculares, tomando-se como critério o tipo de sistema aromático que sustenta o anel quinônico. Assim, têm-se: as benzoquinonas – um anel benzênico, as naftoquinonas – um anel naftalênico e as antraquinonas – um anel antracênico, como mostrado na Figura 5.

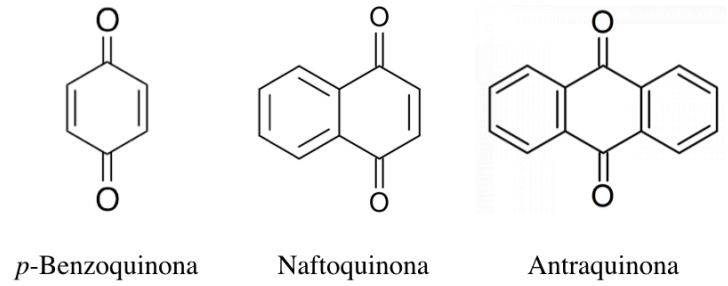


Figura 5. Fórmulas estruturais dos principais grupos de quinonas. Fonte: PubChem Compound.

Um grupo representativo de compostos quinônicos naturais, amplamente encontrados em plantas, fungos e bactérias, são as 1,4-naftoquinonas. Tais

naftoquinonas, como lapachol e lausona, têm apresentado efeitos farmacológicos promissores em linhagens celulares tumorais (EPIFANO et al., 2014; ORAMAS-ROYO et al., 2013). O lapachol (2-hidroxi-3-(3-metil-2-butenil)-1,4-naftoquinona) é uma alquil naftoquinona que ocorre em várias espécies de plantas da família Bignoniaceae, com destaque para o Ipê-roxo, também conhecido como 'Pau d'Aco' (Figura 6) (HUSSAIN; GREEN, 2017). Esse composto foi isolado pela primeira vez em 1882 pelo químico italiano Emanuele Paterno da espécie *Tabebuia avellanedae* Lor (Bignoniaceae) e posteriormente encontrado em vários outros gêneros pertencentes às famílias Plumbaginaceae, Verbenaceae, Caesalpiniaceae e Proteaceae (EPIFANO et al., 2014). O extrato do Ipê-roxo é utilizado por populações do interior do Brasil devido as suas propriedades anti-inflamatórias, antimicrobianas e antiparasitárias (GÓMEZ CASTELLANOS et al., 2009). O lapachol é, de fato, uma naftoquinona com estabelecida atividade antimicrobiana (SOUZA et al., 2013), antifúngica (MEDEIROS et al., 2010), antimalárica (BRANDÃO et al., 2018), antileishmanial (COSTA et al., 2017), anti-inflamatória (LIRA et al., 2008) e anticâncer (HUSSAIN; GREEN, 2017; HUSSAIN et al., 2007).

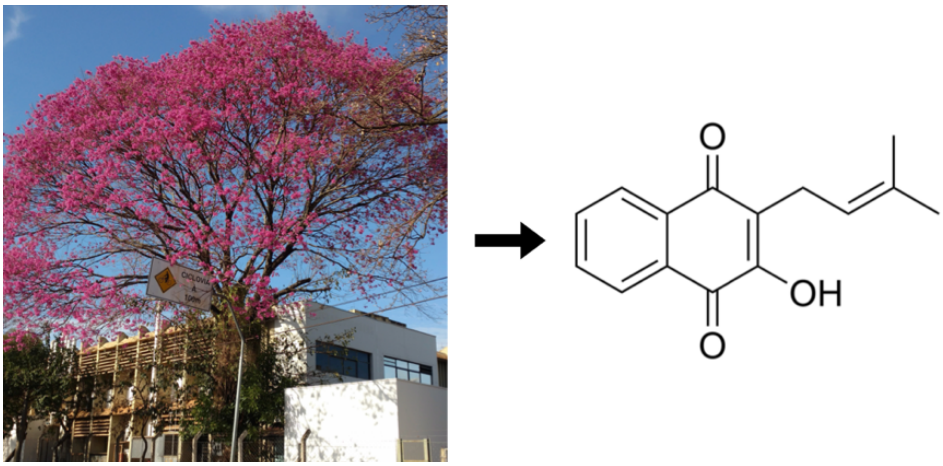


Figura 6. Ipê-roxo do Instituto de Química de Araraquara - UNESP e a fórmula estrutural do lapachol. Foto: José Luiz da Silva, 2018.

Os primeiros relatos anticâncer do lapachol foram reportados em 1968, em que esse composto apresentou efeitos promissores contra tumores murinos, fomentando, inclusive, estudos clínicos em humanos (ALMEIDA, 2009). No entanto, em 1974, o NCI descontinuou os ensaios devido à falta de atividade significativa mesmo em grandes doses orais (ARAÚJO et al., 2002; BLOCK et al., 1974). Apesar disso, o lapachol foi utilizado isoladamente em um pequeno estudo com 9 pacientes portadores de câncer, no qual o tratamento foi capaz de reduzir o tamanho dos tumores e a sensação de dor, além de alcançar a remissão completa do câncer em 3 desses pacientes (HUSSAIN; GREEN, 2017). Acredita-se que a atividade antitumoral do lapachol está relacionada com a interação do anel naftoquinônico com os ácidos nucléicos, o que leva à inibição da replicação do DNA (HUSSAIN et al., 2007). Devido a sua atividade antiproliferativa, o lapachol é um candidato de destaque para estudos de modificação estrutural e para o uso como ligante em complexos metálicos, promovendo, assim, novos compostos com atividade aprimorada. Recentemente, (OLIVEIRA et al., 2017a) reportaram a síntese de complexos metálicos de rutênio contendo lapachol, sendo observados resultados animadores, sugerindo que o uso do rutênio é relevante para melhorar a atividade do lapachol.

A lausona (2-hidroxi-1,4-naftoquinona) (Figura 7) é o principal constituinte da Henna, uma planta intrinsecamente ligada às culturas antigas do norte da África e da Ásia (BADONI et al., 2014). Seu extrato de cor intensa é utilizado para fins cosméticos e medicinais, sendo destacadas suas propriedades antifúngicas, antibacterianas, antiparasitárias e anticâncer (LÓPEZ-LÓPEZ et al., 2014; OLIVEIRA et al., 2018). O extrato aquoso das folhas da Henna foi capaz de regredir tumores induzidos por potentes carcinógenos em ratos, bem como a administração oral do

mesmo promoveu efeitos supressores em tumores sólidos de Ehrlich em camundongos (RAJA et al., 2009; ZUMRUTDAL; OZASLAN, 2012). Diferentes tipos de extratos das folhas da Henna também apresentam citotoxicidade para uma série de linhagens celulares humanas como, carcinoma de cólon (Colo-205 e Caco-2), carcinoma hepatocelular (HepG2) e leucemia mielóide (HL60) (SINGH; LUQMAN, 2014). Esses estudos indicam que a atividade antiproliferativa dos extratos deve-se à lausona, seu componente majoritário.

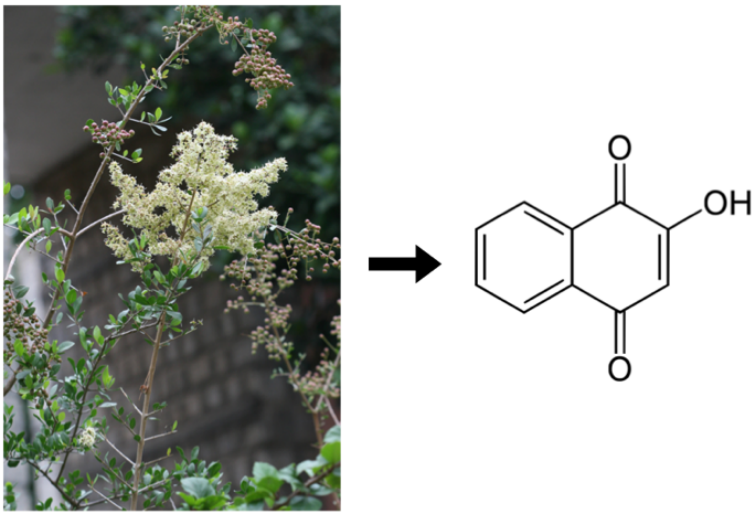


Figura 7. Henna e a fórmula estrutural da lausona. Foto: Herbarium of Indian Institute of Science, 2015.

Um dos principais mecanismos que confere à lausona essa atividade é sua capacidade de inibir a enzima DNA-topoisomerase II (COELHO-CERQUEIRA et al., 2014) e gerar radicais semiquinona que podem formar espécies reativas de oxigênio (ERO) no ambiente intracelular (CASTRO et al., 2008). Tem se observado que quinonas são eficientes geradoras de oxigênio singleto ($^1O_2$), entre outras formas de ERO (OURIQUE et al., 2015; RAJENDRAN, 2015) que podem causar danos oxidativos nas bases do DNA. No entanto, os derivados de naftoquinonas, lapachol e lausona apresentam resultados ainda pouco claros sobre sua atividade genotóxica (COELHO-CERQUEIRA et al., 2014). O grupo hidroxila vizinho à carbonila permite

que o lapachol e a lausona sejam capazes de se ligar potencialmente a íons metálicos em diferentes estados de oxidação, coordenando metais de uma forma bidentada, o que lhes permite desempenhar um papel essencial em sistemas biológicos (PRADHAN et al., 2012). De fato, alguns complexos metálicos contendo essas naftoquinonas como ligantes têm apresentado atividade biológica promissora contra linhagens tumorais (OLIVEIRA et al., 2017b; ORAMAS-ROYO et al., 2013). Estudos de Spoerlein-Guettler et al. (2014) apresentaram a síntese de complexos de Ru(II) com plumbagina, uma naftoquinona extraída de plantas do gênero *Plumbago*, que se mostraram eficazes em células tumorais resistentes a cisplatina. Recentemente, Kosiha et al. (2017) apresentaram novos complexos de Cobre(II), Zinco(II), Níquel(II) e Cobalto(II) contendo naftoquinonas, que induziram a morte de células tumorais, por meio de mecanismos envolvendo estresse oxidativo e clivagem do DNA.

1.5 Busca por novos candidatos anticâncer

À medida que o câncer se torna uma doença mais recorrente na população, a demanda por novas terapias aumenta. Nas últimas décadas, grandes investimentos foram feitos na pesquisa e desenvolvimento (P&D) de medicamentos oncológicos (AVORN, 2015). Entretanto, em comparação com outras classes de medicamentos, os candidatos anticâncer apresentam mais falhas quando chegam aos estágios finais dos estudos clínicos, o que torna o investimento bastante dispendioso (DIMASI; GRABOWSKI, 2007). Uma das razões que justificam esses desacertos é a de que os estudos pré-clínicos carecem de eficiência quando se trata de identificar compostos que podem alterar os estágios de desenvolvimento e progressão do câncer (OCANA et al., 2011).

Geralmente, os estudos de triagem pré-clínica para agentes anticâncer envolvem a identificação de compostos citotóxicos em linhagens celulares imortalizadas cultivadas em monocamada. De fato, a P&D de fármacos anticâncer tem se focado em agentes citotóxicos. O NCI desenvolveu no final nos anos 80 um painel de *screening in vitro* para fármacos anticâncer contendo 60 linhagens celulares tumorais humanas (NCI60), destinado a substituir o uso de tumores animais transplantáveis, até então muito utilizado (SHOEMAKER, 2006). Esse *screening* atualmente utiliza 60 linhagens tumorais diferentes, derivadas de cânceres de pulmão, cólon, sistema nervoso central, ovário, mama, próstata e rim, além de leucemia e melanoma (NCI, 2015). Esse painel contribuiu significantemente para a descoberta de novos agentes antitumorais como o bortezomibe aprovado pelo FDA em 2003 (SHOEMAKER, 2006), e o mesilato de eribulina, aprovado em 2010 para o tratamento do câncer de mama (CORTES et al., 2011). Em vista disso, a avaliação da citotoxicidade *in vitro* mostra-se uma ferramenta importante para a seleção de novas moléculas que interagem com alvos celulares tumorais específicos. No entanto, sabe-se que as respostas celulares baseadas em culturas convencionais, em duas-dimensões (2D), não podem reproduzir as funções teciduais *in vivo,* particularmente nos microambientes heterotípicos de tumores sólidos (LABARBERA et al., 2012).

A cultura de células convencional ocorre em superfícies tratadas de poliestireno que permitem a adesão celular ao substrato plástico. Essa configuração representa inadequadamente o complexo ambiente fisiológico em três-dimensões (3D), em que as células interagem umas com as outras e com a matriz extracelular (MEC) (EDMONDSON et al., 2014). Portanto, os sistemas convencionais não reproduzem a heterogeneidade dos tumores *in vivo*, e, como consequência, as

culturas em monocamadas podem perder a capacidade de responder aos fármacos anticâncer de maneira relevante (FANG; EGLEN, 2017). Uma abordagem promissora para lidar com altas taxas de falhas dos estudos pré-clínicos é o desenvolvimento de culturas de células em 3D, que refletem com maior fidelidade o comportamento celular em tecidos vivos (ANTONI et al., 2015).

A formação de esferoides celulares tumorais em 3D possibilita a reprodução de muitas características fisiologicamente relevantes dos tumores *in vivo*, incluindo os processos de interações célula-célula e MEC-célula, hipóxia e necrose central do tumor (LAMHAMEDI-CHERRADI et al., 2014). Além da resistência celular aos fármacos, as culturas de esferoides em 3D podem ajudar a prever a penetração dos agentes, que é uma importante causa de resistência em tumores, frequentemente negligenciada nos estudos pré-clínicos (VERJANS et al., 2018).

A importância do uso de modelos tumorais em 3D foi destacada por um estudo de Tung et al. (2011), em que os autores observaram respostas distintas dos fármacos anticâncer, 5-fluorouracil (5-FU) e tirapazamina, nos diferentes modelos de cultura de células de carcinoma epitelial humano (A-431). Os esferoides 3D das células A-431 mostraram-se viáveis mesmo após o tratamento com 5-FLU, que é um fármaco bem caracterizado por inibir a proliferação celular, enquanto as células cultivadas em 2D não sobreviveram após o tratamento. Esse resultado decorre do fato de que as culturas de células cultivadas em monocamadas proliferam-se a uma taxa relativamente uniforme aderidas ao substrato plástico, favorecendo a captação e a ação da 5-FLU. Por outro lado, os esferoides têm uma menor taxa de proliferação, tornando-os menos suscetíveis ao efeito genotóxico do quimioterápico. Em paralelo, observou-se que a tirapazamina foi extremamente eficiente em impedir o crescimento dos esferoides, ao passo que ela apresentou pouca atividade nas

células cultivadas em modelo convencional. Esse efeito deve-se ao mecanismo de ação desse pro-fármaco que é ativado em baixos níveis de oxigênio. Os esferoides exibem regiões de hipóxia no seu interior (Figura 8), tal como ocorre em tumores sólidos *in vivo*, onde a tirapazamina pode ser ativada e desempenhar sua atividade citotóxica.

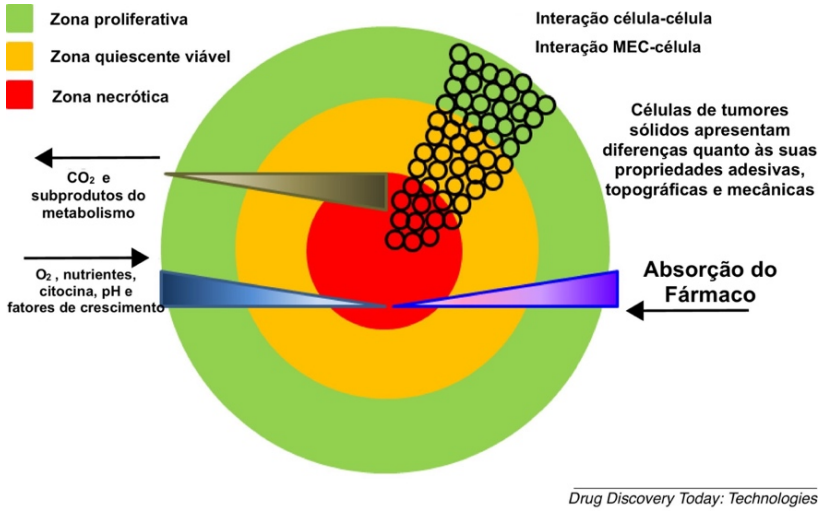


Figura 8. Células tumorais cultivadas em microambientes em 3D expressam diferentes sinais celulares que alteram suas respostas ao meio. Adaptado de Sant & Johnston (2017).

As repostas dos fármacos às células cultivadas em 2D ou 3D não estão somente relacionadas com as zonas diferenciais de proliferação ou disponibilidade de oxigênio. Vários estudos relatam diferenças significativas nos perfis de expressão de genes e proteínas, no metabolismo, e na comunicação celular entre os dois modelos (EDMONDSON et al., 2014; LUCKERT et al., 2016; VANTANGOLI et al., 2016). De fato, o uso de esferoides multicelulares tumorais tem representado um excelente modelo *in vitro* para *screening* de novos fármacos anticâncer, por permitir um estudo mais acurado sobre interações com proteínas, sinalização celular e expressão gênica (THEODORAKI et al., 2015).

Uma estratégia explorada por nosso grupo de pesquisa que contribui para o rastreio de novos candidatos anticâncer, consiste no uso de compostos com

atividade biológica conhecida e que possam ser combinados por meio da coordenação com metais, a fim de atingir múltiplos alvos biológicos da célula tumoral. Neste sentido, a complexação de ligantes com propriedades anticâncer ao metal rutênio pode favorecer a atividade do complexo formado, além de reduzir seus efeitos colaterais indesejados. Isto posto, nos últimos anos, nosso grupo de pesquisa em parceria com o Laboratório de Estrutura e Reatividade de Compostos Inorgânicos da Universidade Federal de São Carlos (LERCI/UFSCAr), encontrou uma série de complexos fosfínicos e bipiridínicos, com resultados bastante satisfatórios contra uma série de doenças e, em especial, contra o câncer (CUNHA et al., 2018; DE CAMARGO et al., 2016; DE GRANDIS et al., 2017; OLIVEIRA et al., 2017a; PIRES et al., 2018). A atividade de alguns compostos foi mais de 100 vezes superior à cisplatina para algumas linhagens tumorais humanas, demonstrando atuar por diferentes mecanismos de ação. Diante desses resultados, buscamos neste trabalho, caracterizar as atividades citotóxicas, genotóxicas e os possíveis mecanismos de resposta antiproliferativa de novos complexos de rutênio contendo ligantes fosfínicos, bipiridínicos e os ligantes lapachol e lausona, a fim de definir seu potencial como candidatos à terapia anticâncer.

5. CONCLUSÃO

Com base nos resultados obtidos neste projeto de pesquisa, nas condições empregadas neste estudo, podemos concluir que os complexos de fórmula geral [Ru(L)(dppm)(N-N)]PF_6 apresentaram satisfatória atividade antiproliferativa e citotóxica em diversas células tumorais, com destaque para células derivadas de câncer de próstata. Acreditamos que a atividade citotóxica encontrada para essa série de complexos seja devida a presença do ligante difenilfosfinometano (dppm) que melhorou não apenas a lipofilicidade dos complexos, como também sua atividade citotóxica. Além disso, os ensaios de sobrevivência clonogênica mostraram que a substituição do ligante bipiridina pela fenantrolina aumentou a atividade dos compostos, o que levou à perda da clonogenicidade das células DU-145. Nossos estudos também demonstraram o complexo DP-LP é capaz de permear através de esferoides de células DU-145 cultivadas em três dimensões e desestabilizar as agregações celulares, resultando na perturbação das interações célula-matriz e, por fim, na morte celular. De fato, o complexo DP-LP desencadeia apoptose em células DU-145 acompanhado de um acúmulo de células na fase G2/M, o que é consistente com a inibição da atividade da proteína AURORA-B. O mecanismo central relacionado com esses efeitos é de que a presença do lapachol no complexo DP-LP promova a geração de espécies reativas intracelulares que podem causar danos ao DNA. A fragmentação do DNA, evidenciada pelo ensaio do cometa pode ativar sistemas de reparos de DNA que mantém as células no *checkpoint* G2/M devido a diminuição da expressão do gene *AURKB*. Além disso, os danos ao DNA configuram o estímulo que desencadeia a ativação de caspases que conduz as células DU-145 à apoptose. Em suma, os resultados encontrados neste estudo contribuem para a seleção e elucidação das propriedades antiproliferativas e citotóxicas de novos compostos, demonstrando que a coordenação do lapachol em

complexos fosfínicos de rutênio(II) possibilita a formação de complexos com potencial de impacto na área de saúde tendo como alvo o tratamento do câncer.

6. REFERÊNCIAS BIBLIOGRÁFICAS

ADAN, A.; BARAN, Y. K. AND Y. Cell Proliferation and Cytotoxicity Assays. **Current Pharmaceutical Biotechnology**, 2016, v. 17, n. 14, p. 1213-1221, 2016.

ADDEPALLI, M. K. et al. RNAi-mediated knockdown of AURKB and EGFR shows enhanced therapeutic efficacy in prostate tumor regression. **Gene Therapy**, v. 17, n. 3, p. 352–359, 2009.

ALBANI, B. A. et al. Marked improvement in photoinduced cell death by a new tris-heteroleptic complex with dual action: Singlet oxygen sensitization and ligand dissociation. **Journal of the American Chemical Society**, v. 136, n. 49, p. 17055–17101, 2014.

ALDOSSARY, S. A. Review on pharmacology of cisplatin: Clinical use, toxicity and mechanism of resistance of cisplatin. **Biomedical and Pharmacology Journal**, v. 12, n. 1, p. 7–15, 2019.

ALLARDYCE, C. S.; DYSON, P. J. Ruthenium in medicine: Current clinical uses and future prospects. **Platinum Metals Review**, v. 45, n. 2, p. 62–69, 2001.

ALLARDYCE, C. S.; DYSON, P. J. Metal-based drugs that break the rules. **Dalton Trans.**, v. 45, n. 8, p. 3201–3209, 2016.

ALMEIDA, E. R. DE. Preclinical and Clinical Studies of Lapachol and Beta-Lapachone. **The Open Natural Products Journal**, v. 2, n. 1, p. 42–47, 20 abr. 2009.

AMABLE, L. Cisplatin resistance and opportunities for precision medicine. **Pharmacological research**, v. 106, p. 27–36, abr. 2016.

AMERICAN CANCER SOCIETY, A. **Chemotherapy Drugs : How They Work?**. Disponível em: < https://www.cancer.org/treatment>. Acesso e 23 de dez de 2019.

ANTONARAKIS, E. S.; EMADI, A. Ruthenium-based chemotherapeutics: Are they ready for prime time? **Cancer Chemotherapy and Pharmacology**, v. 66, p. 1–9, 2010.

ANTONI, D. et al. Three-dimensional cell culture: a breakthrough *in vivo*. **International journal of molecular sciences**, v. 16, n. 3, p. 5517–27, 11 mar. 2015.

ARAÚJO, E. L.; ALENCAR, J. R. B.; ROLIM NETO, P. J. Lapachol: segurança e eficácia na terapêutica. **Revista Brasileira de Farmacognosia**, v. 12, n. 0102-695X, p. 57–59, 2002.

ARORA, S. et al. Downregulation of XPF–ERCC1 enhances cisplatin efficacy in cancer cells. **DNA Repair**, v. 9, n. 7, p. 745–753, 1 jul. 2010.

ASHKENAZI, R.; GENTRY, S. N.; JACKSON, T. L. Pathways to Tumorigenesis—Modeling Mutation Acquisition in Stem Cells and Their Progeny. **Neoplasia**, v. 10, n. 11, p. 1170-IN6, nov. 2008.

ASLANTÜRK, Ö. S. *In Vitro* Cytotoxicity and Cell Viability Assays: Principles, Advantages, and Disadvantages. **Genotoxicity - A Predictable Risk to Our Actual World**, p. 1–18, 2018.

AVENDAÑO, C.; MENÉNDEZ, J. C. **Medicinal Chemistry of Anticancer Drugs**. 2nd edition. Elsevier Science, 2008.

AVORN, J. The $2.6 Billion Pill — Methodologic and Policy Considerations. **New England Journal of Medicine**, v. 372, n. 20, p. 1877–1879, 14 maio 2015.

BADONI SEMWAL, R. et al. *Lawsonia inermis* L. (henna): Ethnobotanical, phytochemical and pharmacological aspects. **Journal of Ethnopharmacology**, v. 155, n. 1, p. 80–103, ago. 2014.

BAKA, E.; COMER, J. E. A.; TAKÁCS-NOVÁK, K. Study of equilibrium solubility measurement by saturation shake-flask method using hydrochlorothiazide as model compound. **Journal of Pharmaceutical and Biomedical Analysis**, v. 46, n. 2, p. 335–341, 2008.

BAKER, S. J.; REDDY, E. P. CDK4: A key player in the cell cycle, development, and cancer. **Genes and Cancer**, 2012.

BAL-PRICE, A.; COECKE, S. Guidance on Good Cell Culture Practice (GCCP). In: **Cell Culture Techniques**. v. 56, p. 1–25, 2011.

BALIZA, I. R. S. et al. Ruthenium Complexes With Piplartine Cause Apoptosis Through MAPK Signaling by a p53-Dependent Pathway in Human Colon Carcinoma Cells and Inhibit Tumor Development in a Xenograft Model. **Frontiers in Oncology**, v. 9, n. July, p. 1–11, 2019.

BARBOSA, I. R. et al. Cancer mortality in Brazil: Temporal Trends and Predictions for the Year 2030. **Medicine**, v. 94, n. 16, p. e746, abr. 2015.

BASU, A.; KRISHNAMURTHY, S. Cellular responses to cisplatin-induced DNA damage. **Journal of Nucleic Acids**, v. 20, n. 10, p. 1–16, 2010.

BERGAMO, A. et al. Preclinical combination therapy of the investigational drug NAMI-A with doxorubicin for mammary cancer. **Investigational New Drugs**, v. 33, n. 1, p. 53–63, 2015.

BEZERRA, D. P. et al. Overview of the therapeutic potential of piplartine (piperlongumine). **European Journal of Pharmaceutical Sciences**, v. 48, n. 3, p. 453–463, fev. 2013.

BIZARI, L.; SILVA, A. E.; TAJARA, E. H. Gene amplification in carcinogenesis. **Genetics and Molecular Biology**, 2006.

BLACKADAR, C. B. Historical review of the causes of cancer. **World Journal of Clinical Oncology**, v. 7, n. 1, p. 54–86, 2016.

BLOCK, J. et al. Early clinical studies with lapachol (NSC-11905). **Cancer chemotherapy reports. Part 2**, v. 4, n. 4, p. 27, 1974.

BO, S. et al. Chk1, but not Chk2, is responsible for G2/M phase arrest induced by diallyl disulfide in human gastric cancer BGC823 cells. **Food and Chemical Toxicology**, v. 68, p. 61–70, 2014.

BOMFIM, L. M. et al. Ruthenium(II) complexes with 6-methyl-2-thiouracil selectively reduce cell proliferation, cause DNA double-strand break and trigger caspase-mediated apoptosis through JNK/p38 pathways in human acute promyelocytic leukemia cells. **Scientific Reports**, v. 9, n. 1, p. 1–17, 2019.

BRABEC, V.; KASPARKOVA, J. Ruthenium coordination compounds of biological and biomedical significance. DNA binding agents. **Coordination Chemistry Reviews**, v. 376, p. 75–94, 2018.

BRANDÃO, G. C. et al. Antimalarial naphthoquinones. Synthesis via click chemistry, in vitro activity, docking to PfDHODH and SAR of lapachol-based compounds. **European Journal of Medicinal Chemistry**, v. 145, p. 191–205, 2018.

BRANDÃO, H. N. et al. Química e farmacologia de quimioterápicos antineoplásicos derivados de plantas. **Química Nova**, v. 33, n. 6, p. 1359–1369, 2010.

BRAY, F. et al. Global cancer statistics 2018: GLOBOCAN estimates of incidence and mortality worldwide for 36 cancers in 185 countries. **CA: A Cancer Journal for Clinicians**, v. 68, n. 6, p. 394–424, 2018.

BUSTIN, S. A. et al. The MIQE guidelines: Minimum information for publication of quantitative real-time PCR experiments. **Clinical Chemistry**, v. 55, n. 4, p. 611–622,

2009.

CADET, J.; WAGNER, J. R. DNA Base Damage by Reactive Oxygen Species, Oxidizing Agents, and UV Radiation. **Cold Spring Harbor Perspectives in Biology**, v. 5, n. 2, p. a012559–a012559, 1 fev. 2013.

ČANOVIĆ, P. et al. Impact of aromaticity on anticancer activity of polypyridyl ruthenium(II) complexes: synthesis, structure, DNA/protein binding, lipophilicity and anticancer activity. **Journal of Biological Inorganic Chemistry**, v. 22, n. 7, p. 1007–1028, 2017.

CARMENA, M. et al. The chromosomal passenger complex (CPC): from easy rider to the godfather of mitosis. **Nature Reviews Molecular Cell Biology**, v. 13, n. 12, p. 789–803, 23 dez. 2012.

CASTRO, F. A. V et al. Cytotoxicity mechanism of two naphthoquinones (menadione and plumbagin) in Saccharomyces cerevisiae. **PLoS ONE**, v. 3, n. 12, 2008.

CHAITANYA, G. V.; ALEXANDER, J. S.; BABU, P. P. PARP-1 cleavage fragments: Signatures of cell-death proteases in neurodegeneration. **Cell Communication and Signaling**, v. 8, n. 1, p. 31, 2010.

CHEN, J. et al. Synthesis, characterization, cellular uptake and apoptosis-inducing properties of two highly cytotoxic cyclometalated ruthenium(II) β-carboline complexes. **European Journal of Medicinal Chemistry**, v. 140, p. 104–117, nov. 2017.

CHIEFFI, P. et al. Aurora B expression directly correlates with prostate cancer malignancy and influence prostate cell proliferation. **Prostate**, v. 66, n. 3, p. 326–333, 2006.

CHIEFFI, P. Aurora B: A new promising therapeutic target in cancer. **Intractable and Rare Diseases Research**, v. 7, n. 2, p. 141–144, 2018.

COELHO-CERQUEIRA, E. et al. Beyond Topoisomerase Inhibition: Antitumor 1,4-Naphthoquinones as Potential Inhibitors of Human Monoamine Oxidase. **Chemical Biology & Drug Design**, v. 83, n. 4, p. 401–410, 2014.

CONKLIN, K. A. Chemotherapy-associated oxidative stress: Impact on chemotherapeutic effectiveness. **Integrative Cancer Therapies**, v. 3, n. 4, p. 294–300, 2004.

COOPER, G. The Development and Causes of Cancer. **The Cell: A Molecular Approach.** 2nd edition. Sunderland (MA): Sunderland (MA): Sinauer Associates; 2000.

The Development and Causes of Cancer. Disponível em: <https://www.ncbi.nlm.nih.gov/books/NBK9963/>.

CORREA, R. S. et al. Ru(II)-based complexes with N-(acyl)-N′,N′-(disubstituted)thiourea ligands: Synthesis, characterization, BSA- and DNA-binding studies of new cytotoxic agents against lung and prostate tumour cells. **Journal of Inorganic Biochemistry**, v. 150, p. 63–71, set. 2015.

CORTES, J. et al. Eribulin monotherapy versus treatment of physician's choice in patients with metastatic breast cancer (EMBRACE): A phase 3 open-label randomised study. **The Lancet**, v. 377, n. 9769, p. 914–923, 2011.

COSTA, E. V. S. et al. Antileishmanial Activity of *Handroanthus serratifolius* (Vahl) S. Grose (Bignoniaceae). **Evidence-Based Complementary and Alternative Medicine**, v. 2017, p. 1–6, 2017.

CUMMINGS, B. S.; WILLS, L. P.; SCHNELLMANN, R. G. Measurement of Cell Death in Mammalian Cells. **Curr Protoc Phamacol**, v. 1, n. Lemasters 1999, p. 1–30, 2004.

CUNHA, B. N. et al. Hydrolysis reaction promotes changes in coordination mode of Ru(II)/acylthiourea organometallic complexes with cytotoxicity against human lung tumor cell lines. **Journal of Inorganic Biochemistry**, v. 186, n. March, p. 147–156, 2018.

D'SOUSA, C. O. et al. Novel piplartine-containing ruthenium complexes: synthesis, cell growth inhibition, apoptosis induction and ROS production on HCT116 cells. **Oncotarget**, v. 8, n. 61, p. 104367–104392, 2017.

DASARI, S.; BERNARD TCHOUNWOU, P. Cisplatin in cancer therapy: Molecular mechanisms of action. **European Journal of Pharmacology**, v. 740, p. 364–378, 2014.

DASH, S. P. et al. Syntheses and structural investigation of some alkali metal ion-mediated LVVO2- (L2- = tridentate ONO ligands) species: DNA binding, photo-induced DNA cleavage and cytotoxic activities. **Dalton Transactions**, v. 43, n. 26, p. 10139–10156, 2014.

DE CAMARGO, M. S. et al. Inhibition of human DNA topoisomerase IB by nonmutagenic ruthenium(II)-based compounds with antitumoral activity. **Metallomics**, v. 8, n. 2, p. 179–192, 2016.

DE CARVALHO, N. C. et al. A novel ruthenium complex with xanthoxylin induces S-phase arrest and causes ERK1/2-mediated apoptosis in HepG2 cells through a p53-

independent pathway article. **Cell Death and Disease**, v. 9, n. 2, 2018.

DE GRANDIS, R. A. et al. Human topoisomerase inhibition and DNA/BSA binding of Ru(II)–SCAR complexes as potential anticancer candidates for oral application. **BioMetals**, v. 30, n. 3, p. 321–334, 16 jun. 2017.

DE GRANDIS, R. A. et al. Novel lawsone-containing ruthenium(II) complexes: Synthesis, characterization and anticancer activity on 2D and 3D spheroid models of prostate cancer cells. **Bioorganic Chemistry**, v. 85, n. January, p. 455–468, 2019.

DE SOUSA, I. H. et al. Ruthenium (II) complexes with N, O-chelating proline and threonine ligands cause selective cytotoxicity by the induction of genomic instability, cell cycle arrest and apoptosis in breast and prostate tumor cells. **Toxicology in Vitro**, v. 62, n. July 2019, p. 104679, 2020.

DENG, Z. et al. Ruthenium complexes with phenylterpyridine derivatives target cell membrane and trigger death receptors-mediated apoptosis in cancer cells. **Biomaterials**, v. 129, p. 111–126, 2017.

DERIANO, L.; ROTH, D. B. Modernizing the Nonhomologous End-Joining Repertoire: Alternative and Classical NHEJ Share the Stage. **Annual Review of Genetics**, v. 47, n. 1, p. 433–455, 2013.

DIMASI, J. A.; GRABOWSKI, H. G. Economics of New Oncology Drug Development. **Journal of Clinical Oncology**, v. 25, n. 2, p. 209–216, 10 jan. 2007.

DUVAL, K. et al. Modeling Physiological Events in 2D vs. 3D Cell Culture. **Physiology**, v. 32, n. 4, p. 266–277, jul. 2017.

EDMONDSON, R. et al. Three-dimensional cell culture systems and their applications in drug discovery and cell-based biosensors. **Assay and drug development technologies**, v. 12, n. 4, p. 207–18, 2014.

ELMORE, S. Apoptosis: A Review of Programmed Cell Death. **Toxicologic Pathology**, v. 35, n. 4, p. 495–516, 25 jun. 2007.

EPIFANO, F. et al. Lapachol and its congeners as anticancer agents: A review. **Phytochemistry Reviews**, v. 13, n. 1, p. 37–49, 2014.

ESPINOSA, E. et al. Classification of anticancer drugs - A new system based on therapeutic targets. **Cancer Treatment Reviews**, v. 29, n. 6, p. 515–523, 2003.

FAGUET, G. B. A brief history of cancer: Age-old milestones underlying our current

knowledge database. **International Journal of Cancer**, v. 136, n. 9, p. 2022–2036, 2015.

FANG, H. et al. RecQL4-Aurora B kinase axis is essential for cellular proliferation , cell cycle progression , and mitotic integrity. **Oncogenesis**, p. 0–11, 2018.

FANG, Y.; EGLEN, R. M. Three-Dimensional Cell Cultures in Drug Discovery and Development. **SLAS DISCOVERY: Advancing Life Sciences R&D**, v. 22, n. 5, p. 456–472, 18 jun. 2017.

FELL, V. L. et al. Ku70 Serine 155 mediates Aurora B inhibition and activation of the DNA damage response. **Scientific Reports**, v. 6, n. October, p. 1–17, 2016.

FENECH, M. The in vitro micronucleus technique. **Mutation Research - Fundamental and Molecular Mechanisms of Mutagenesis**, v. 455, n. 1–2, p. 81–95, 2000.

FORBES, S. A. et al. COSMIC: exploring the world's knowledge of somatic mutations in human cancer. **Nucleic Acids Research**, v. 43, n. D1, p. D805–D811, 28 jan. 2015.

FRANKEN, N. A P. et al. Clonogenic assay of cells in vitro. **Nature protocols**, v. 1, n. 5, p. 2315–2319, 2006.

FRIEDRICH, J. et al. Spheroid-based drug screen: considerations and practical approach. **Nat. Protocols**, v. 4, n. 3, p. 309–324, 2009.

FRIK, M. et al. Luminescent iminophosphorane gold, palladium and platinum complexes as potential anticancer agents. **Inorganic Chemistry Frontiers**, v. 1, n. 3, p. 231–241, 2014.

GALLUZZI, L. et al. Guidelines for the use and interpretation of assays for monitoring cell death in higher eukaryotes. **Cell Death and Differentiation**, v. 16, n. 8, p. 1093–1107, 2009.

GIANCOTTI, F. G. Deregulation of cell signaling in cancer. **FEBS Letters**, v. 588, n. 16, p. 2558–2570, 19 ago. 2014.

GOLAN, D. E. **Principles of Pharmacology: The Pathophysiologic Basis of Drug Therapy**. 4th ed. Lippincontt Willians & Wilkins, 2016.

GÓMEZ CASTELLANOS, J. R.; PRIETO, J. M.; HEINRICH, M. Red Lapacho (*Tabebuia impetiginosa)* - A global ethnopharmacological commodity? **Journal of Ethnopharmacology**, v. 121, n. 1, p. 1–13, jan. 2009.

GRIVICICH, I.; REGNER, A.; ROCHA, A. B. DA. Morte Celular por Apoptose (Apoptosis: Programmed Cell Death). **Revista Brasileira de Cancerologia**, v. 53, n. 3, p. 335–343, 2007.

GRONER, B.; WEISS, A. Targeting Survivin in cancer: Novel drug development approaches. **BioDrugs**, v. 28, n. 1, p. 27-39, 2014.

GUIDELINE FOR TESTING OS CHEMICALS, O. *In vitro* mammalian cell micronucleus test. No. 487. **OECD Guidelines**, n. September, p. 1–26, 2014.

GURDEN, M. D. et al. Aurora B prevents premature removal of spindle assembly checkpoint proteins from the kinetochore : A key role for Aurora B in mitosis. **Oncotarget**, v. 9, n. 28, p. 19525–19542, 2018.

HALASI, M. et al. ROS inhibitor *N* -acetyl-L-cysteine antagonizes the activity of proteasome inhibitors. **Biochemical Journal**, v. 454, n. 2, p. 201–208, 2013.

HAN, B. J. et al. DNA interaction, antioxidant activity, and bioactivity studies of two ruthenium(II) complexes. **Spectrochimica Acta - Part A: Molecular and Biomolecular Spectroscopy**, v. 135, p. 840–849, 2015.

HANAHAN, D.; WEINBERG, R. A. The hallmarks of cancer. **Cell**, v. 100, n. 1, p. 57–70, 7 jan. 2000.

HANAHAN, D.; WEINBERG, R. A. Hallmarks of Cancer: The Next Generation. **Cell**, v. 144, n. 5, p. 646–674, mar. 2011.

HE, X.; JIN, L.; TAN, L. DNA-binding, topoisomerases I and II inhibition and in vitro cytotoxicity of ruthenium(II) polypyridyl complexes: $[Ru(dppz)_2L](^{2+})$ (L=dppz-11-CO_2Me and dppz). **Spectrochimica acta. Part A, Molecular and biomolecular spectroscopy**, v. 135C, p. 101–109, 2014.

HERCEG, Z.; WANG, Z. Q. Functions of poly(ADP-ribose) polymerase (PARP) in DNA repair, genomic integrity and cell death. **Mutation Research - Fundamental and Molecular Mechanisms of Mutagenesis**, v. 477, n. 1–2, p. 97–110, 2001.

HOE, K. H.; VERMA, C. S.; LANE, D. P. Drugging the p53 pathway: understanding the route to clinical efficacy. **Nature Reviews Drug Discovery**, v. 13, n. 3, p. 217–236, 1 mar. 2014.

HURTADO, M. et al. Novel survivin inhibitor for suppressing pancreatic cancer cells growth via downregulating Sp1 and Sp3 transcription factors. **Cellular Physiology and Biochemistry**, v. 51, n. 4, p. 1894–1907, 2018.

HUSSAIN, H. et al. Lapachol: an overview. **Arkivoc**, v. 2007, n. ii, p. 145–171, 2007.

HUSSAIN, H.; GREEN, I. R. Lapachol and lapachone analogs: a journey of two decades of patent research (1997-2016). **Expert Opinion on Therapeutic Patents**, v. 27, n. 10, p. 1111–1121, 3 out. 2017.

IARC, I. A. FOR R. ON C. Latest global cancer data: Cancer burden rises to 18.1 million new cases and 9.6 million cancer deaths in 2018. **WHO - Word Health Organization**, n. September, p. 13–15, 2018.

INCA, INSTITUTO NACIONAL DO CÂNCER. **Incidência de Câncer no Brasil (Estimativa 2018)**. Disponivel em: <https://www.inca.gov.br/publicacoes/>. Acesso em 19 de dez de 2019.

INCA, INSTITUTO NACIONAL DO CÂNCER. **ESTIMATIVA 2016: Incidência de Câncer no Brasil**. Disponivel em: <https://www.inca.gov.br>. Acesso em 11 de jul de 2017.

JEMAL, A. et al. Global Patterns of Cancer Incidence and Mortality Rates and Trends. **Cancer Epidemiology Biomarkers & Prevention**, v. 19, n. 8, p. 1893–1907, 2010.

JIANG, B. et al. IDH1 Mutation Promotes Tumorigenesis by Inhibiting JNK Activation and Apoptosis Induced by Serum Starvation. **Cell Reports**, v. 19, n. 2, p. 389–400, abr. 2017.

KAUFMANN, S. H. et al. Specific Proteolytic Cleavage of Poly(ADP-ribose) Polymerase: An Early Marker of Chemotherapy-induced Apoptosis. **Cancer Research**, v. 53, n. 17, p. 3976–3985, 1993.

KELLAND, L. The resurgence of platinum-based cancer chemotherapy. **Nature reviews. Cancer**, v. 7, n. 7, p. 573–584, 2007.

KHARMATE, G. et al. Epidermal growth factor receptor in prostate cancer derived exosomes. **PLoS ONE**, v. 11, n. 5, p. 1–14, 2016.

KIRKLAND, D. et al. Updated recommended lists of genotoxic and non-genotoxic chemicals for assessment of the performance of new or improved genotoxicity tests. **Mutation Research/Genetic Toxicology and Environmental Mutagenesis**, v. 795, p. 7–30, 2016.

KOCEVA-CHYŁA, A. et al. Insights into the in vitro Anticancer Effects of Diruthenium-1. **ChemMedChem**, v. 2, p. 2171–2187, 2016.

KOPPENOL, W. H.; BOUNDS, P. L.; DANG, C. V. Otto Warburg's contributions to current concepts of cancer metabolism. **Nature Reviews Cancer**, v. 11, n. 5, p. 325–337, 2011.

KOSIHA, A. et al. Metal complexes of naphthoquinone based ligand: synthesis, characterization, protein binding, DNA binding/cleavage and cytotoxicity studies. **Journal of Biomolecular Structure and Dynamics**, v. 1102, n. 12, p. 1–12, 20 dez. 2017.

KRISHNAMOORTHY, P. et al. Copper(I) and nickel(II) complexes with 1:1 vs. 1:2 coordination of ferrocenyl hydrazone ligands: Do the geometry and composition of complexes affect DNA binding/cleavage, protein binding, antioxidant and cytotoxic activities? **Dalton Transactions**, v. 41, n. 15, p. 4423–4436, 2012.

KRUISWIJK, F.; LABUSCHAGNE, C. F.; VOUSDEN, K. H. p53 in survival, death and metabolic health: a lifeguard with a licence to kill. **Nature Reviews Molecular Cell Biology**, v. 16, n. 7, p. 393–405, 2015.

KUBANIK, M. et al. Towards targeting anticancer drugs: ruthenium(ii)-arene complexes with biologically active naphthoquinone-derived ligand systems. **Dalton transactions,** v. 45, n. 33, p. 13091–103, 2016.

KUMAR, B. et al. YM155 Reverses Cisplatin Resistance in Head and Neck Cancer by Decreasing Cytoplasmic Survivin Levels. **Molecular Cancer Therapeutics**, v. 11, n. 9, p. 1988–1998, 2012.

KUMARI, S. et al. Reactive Oxygen Species: A Key Constituent in Cancer Survival. **Biomarker Insights**, v. 13, p. 117727191875539, 6 jan. 2018.

LABARBERA, D. V; REID, B. G.; YOO, B. H. The multicellular tumor spheroid model for high-throughput cancer drug discovery. **Expert Opinion on Drug Discovery**, v. 7, n. 9, p. 819–830, 2012.

LACERDA, M. A. Chemotherapy and Anaesthesia. **Rev Bras Anestesiol**, v. 51, n. 3, p. 250–270, 2001.

LAI, S. H. et al. Protein binding and anticancer activity studies of ruthenium(II) polypyridyl complexes toward BEL-7402 cells. **Journal of Photochemistry and Photobiology B: Biology**, v. 158, p. 39–48, 2016.

LAMHAMEDI-CHERRADI, S. E. et al. 3D tissue-engineered model of Ewing's sarcoma. **Advanced Drug Delivery Reviews**, v. 79, p. 155–171, 2014.

LANE, D. P. p53 - Guardian of the Genome. **Nature**, v. 358, n. 2, p. 15–16, 1992.

LANGHANS, S. A. Three-dimensional in vitro cell culture models in drug discovery and drug repositioning. **Frontiers in Pharmacology**, v. 9, n. 1, p. 1–14, 2018.

LAWLEY, P. D. Mutagens as carcinogens: development of current concepts. **Mutation research**, v. 213, n. 1, p. 3–25, 1989.

LEE, E. C. Y. et al. Targeting aurora kinases for the treatment of prostate cancer. **Cancer Research**, v. 66, n. 10, p. 4996–5002, 2006.

LEE, R. et al. The Differential Distribution of RAPTA-T in Non-Invasive and Invasive Breast Cancer Cells Correlates with Its Anti-Invasive and Anti-Metastatic Effects. **International Journal of Molecular Sciences**, v. 18, n. 9, p. 1869, 2017.

LEE, S. W. et al. SUMOylation of hnRNP-K is required for p53-mediated cell-cycle arrest in response to DNA damage. **The EMBO Journal**, v. 31, n. 23, p. 4441–4452, 28,. 2012.

LEGESSE-MILLER, A. et al. Quiescent fibroblasts are protected from proteasome inhibition–mediated toxicity. **Molecular Biology of the Cell**, v. 23, n. 18, p. 3566–3581, 2012.

LEIJEN, S. et al. Phase I/II study with ruthenium compound NAMI-A and gemcitabine in patients with non-small cell lung cancer after first line therapy. **Investigational New Drugs**, v. 33, n. 1, p. 201–214, 2015.

LI, W. et al. Ruthenium(II) complexes: DNA-binding, cytotoxicity, apoptosis, cellular localization, cell cycle arrest, reactive oxygen species, mitochondrial membrane potential and western blot analysis. **Journal of photochemistry and photobiology. B, Biology**, v. 140, p. 94–104, 2014.

LI, Y. et al. Polypyridyl Ruthenium(II) complex-induced mitochondrial membrane potential dissipation activates DNA damage-mediated apoptosis to inhibit liver cancer. **European Journal of Medicinal Chemistry**, v. 164, p. 282–291, 2019.

LIBERTI, M. V.; LOCASALE, J. W. The Warburg Effect: How Does it Benefit Cancer Cells? **Trends in Biochemical Sciences**, v. 41, n. 3, p. 211–218, 2016.

LIMA, A. P. et al. Cytoxicity and apoptotic mechanism of ruthenium(II) amino acid complexes in sarcoma-180 tumor cells. **PLoS ONE**, v. 9, n. 10, 2014.

LIMA, A. R. et al. Discrimination between the human prostate normal and cancer cell

exometabolome by GC-MS. **Scientific Reports**, v. 8, n. 1, p. 5539, 2018.

LIMA, C. J.; RODRÍGUEZ, L. Phosphine-Gold (I) Compounds as Anticancer Agents : General Description and Mechanisms of Action. **Anti-Cancer Agents in Medicinal Chemistry**, v. 11, n. I, p. 921–928, 2011.

LIRA, A. A. M. et al. Development of Lapachol Topical Formulation: Anti-inflammatory Study of a Selected Formulation. **AAPS PharmSciTech**, v. 9, n. 1, p. 163–168, 25 mar. 2008.

LISS, M. A. et al. mTOR inhibitors for treatment of low-risk prostate cancer. **Medical Hypotheses**, v. 117, n. 1, p. 63–68, 2018.

LÓPEZ-LÓPEZ, L. I. et al. Naphthoquinones: Biological properties and synthesis of lawsone and derivatives - A structured review. **Vitae**, v. 21, n. 3, p. 248–258, 2014.

LOZANO-PÉREZ, A. A. et al. Antitumor properties of platinum(IV) prodrug-loaded silk fibroin nanoparticles. **Dalton transactions**, v. 44, n. 30, p. 13513–21, 2015.

LUCKERT, C. et al. Comparative analysis of 3D culture methods on human HepG2 cells. **Archives of toxicology**, v. 91, n. 1, p. 393-406, 2016.

LUNDQVIST, E. Å.; FUJIWARA, K.; SEOUD, M. Principles of chemotherapy. **International Journal of Gynecology & Obstetrics**, v. 131, n. 12, p. S146–S149, 2015.

LUO, G. et al. Design, synthesis and biological evaluation of novel 3-substituted 4-anilino-coumarin derivatives as antitumor agents. **Bioorganic & Medicinal Chemistry Letters**, v. 27, n. 4, p. 867–874, fev. 2017.

MACIP, S. et al. Oxidative stress induces a prolonged but reversible arrest in p53-null cancer cells, involving a Chk1-dependent G2 checkpoint. **Oncogene**, v. 25, n. 45, p. 6037–6047, 2006.

MARMUR, J. A procedure for the isolation of deoxyribonucleic acid from micro-organisms. **Journal of Molecular Biology**, v. 3, n. 2, p. 201-218, 1961.

MÁRQUEZ-JURADO, S. et al. Mitochondrial levels determine variability in cell death by modulating apoptotic gene expression. **Nature Communications**, v. 9, n. 1, 2018.

MARULLO, R. et al. Cisplatin induces a mitochondrial-ros response that contributes to cytotoxicity depending on mitochondrial redox status and bioenergetic functions. **PLoS ONE**, v. 8, n. 11, p. 1–15, 2013.

MARX, K. A. et al. Data Mining the NCI Cancer Cell Line Compound GI50 Values: Identifying Quinone Subtypes Effective Against Melanoma and Leukemia Cell Classes. **Journal of Chemical Information and Computer Sciences**, v. 43, n. 5, p. 1652–1667, 2003.

MC GEE, M. M. Targeting the Mitotic Catastrophe Signaling Pathway in Cancer. **Mediators of Inflammation**, v. 2015, 2015.

MCNEIL, E. M.; MELTON, D. W. DNA repair endonuclease ERCC1-XPF as a novel therapeutic target to overcome chemoresistance in cancer therapy. **Nucleic Acids Research**, v. 40, n. 20, p. 9990–10004, 2012.

MEDEIROS, C. S. et al. Antifungal activity of the naphthoquinone beta-lapachone against disseminated infection with *Cryptococcus neoformans* in dexamethasone-immunosuppressed Swiss mice. **Brazilian Journal of Medical and Biological Research**, v. 43, n. 4, p. 345–349, abr. 2010.

MEHTA, G. et al. Opportunities and challenges for use of tumor spheroids as models to test drug delivery and efficacy. **Journal of Controlled Release**, v. 164, n. 2, p. 192–204, dez. 2012.

MELLO-ANDRADE, F. et al. Antitumor effectiveness and mechanism of action of Ru(II)/amino acid/diphosphine complexes in the peritoneal carcinomatosis progression. **Tumor Biology**, v. 39, n. 10, p. 1–18, 2017.

MELLO-ANDRADE, F. et al. Acute toxic effects of ruthenium (II)/amino acid/diphosphine complexes on Swiss mice and zebrafish embryos. **Biomedicine & Pharmacotherapy**, v. 107, n. August, p. 1082–1092, nov. 2018.

MENYHÁRT, O. et al. Guidelines for the selection of functional assays to evaluate the hallmarks of cancer. **Biochimica et Biophysica Acta - Reviews on Cancer**, v. 1866, n. 2, p. 300–319, 2016.

MILUTINOVIĆ, M. M. et al. New 4′-(4-chlorophenyl)-2,2′:6′,2″-terpyridine ruthenium(II) complexes: Synthesis, characterization, interaction with DNA/BSA and cytotoxicity studies. **Journal of Inorganic Biochemistry**, v. 169, p. 1–12, 2017.

MIMEAULT, M.; BATRA, S. K. Recent advances on multiple tumorigenic cascades involved in prostatic cancer progression and targeting therapies. **Carcinogenesis**, v. 27, n. 1, p. 1–22, 2005.

MONACO, L. et al. Inhibition of Aurora-B kinase activity by poly(ADP-ribosyl)ation in

response to DNA damage. **Proceedings of the National Academy of Sciences of the United States of America**, v. 102, n. 40, p. 14244–14248, 2005.

MOTSWAINYANA, W. M.; AJIBADE, P. A. Anticancer Activities of Mononuclear Ruthenium(II) Coordination Complexes. **Advances in Chemistry**, v. 2015, p. 1–21, 2015.

MUHAMMAD, N.; GUO, Z. Metal-based anticancer chemotherapeutic agents. **Current Opinion in Chemical Biology**, v. 19, p. 144–153, 2014.

NAKAHARA, T. et al. YM155, a novel small-molecule survivin suppressant, induces regression of established human hormone-refractory prostate tumor xenografts. **Cancer Research**, v. 67, n. 17, p. 8014–8021, 2017.

NAVARRO-SERER, B. et al. Aurora A inhibition limits centrosome clustering and promotes mitotic catastrophe in cells with supernumerary centrosomes. **Oncotarget**, v. 10, n. 17, p. 1649–1659, 2019.

NCI, National Cancer Institute. **What Is Cancer? A Collection of Related Diseases**. Disponível em: < https://www.cancer.gov/about-cancer/understanding/what-is-cancer>. Acesso em 27 de set de 2018

NITA, M.; GRZYBOWSKI, A. The Role of the Reactive Oxygen Species and Oxidative Stress in the Pathomechanism of the Age-Related Ocular Diseases and Other Pathologies of the Anterior and Posterior Eye Segments in Adults. **Oxidative Medicine and Cellular Longevity**, v. 2016, p. 1–23, 2016.

NITSCHE, R. Cell fluorescence assays on the Agilent 2100 bioanalyzer – general use. **Agilent Technologies**, v. 1, n. 1, p. 1–8, 2002.

OCANA, A. et al. Preclinical development of molecular-targeted agents for cancer. **Nature Reviews Clinical Oncology**, v. 8, n. 4, p. 200–209, 2011.

OLIVEIRA, K. M. et al. Ruthenium (II)/ triphenylphosphine complexes : An effective way to improve the cytotoxicity of lapachol. **Polyhedron**, v. 130, p. 108–114, 2017a.

OLIVEIRA, K. M. et al. Selective Ru (II)/ lawsone complexes inhibiting tumor cell growth by apoptosis. **Journal of Inorganic Biochemistry**, v. 176, n. August, p. 66–76, 2017b.

OLIVEIRA, L. et al. Antileishmanial Activity of 2-Methoxy-4H-spiro-[naphthalene-1,2′-oxiran]-4-one (Epoxymethoxy-lawsone): A Promising New Drug Candidate for Leishmaniasis Treatment. **Molecules**, v. 23, n. 4, p. 864, 2018.

OLIVEIRA, M. DE S. et al. A novel platinum complex containing a piplartine derivative exhibits enhanced cytotoxicity, causes oxidative stress and triggers apoptotic cell death by ERK/p38 pathway in human acute promyelocytic leukemia HL-60 cells. **Redox Biology**, v. 20, n. 6, p. 182–194, 2019.

ORAMAS-ROYO, S. et al. Synthesis and cytotoxic activity of metallic complexes of lawsone. **Bioorganic and Medicinal Chemistry**, v. 21, n. 9, p. 2471–2477, 2013.

OTT, I.; GUST, R. Non platinum metal complexes as anti-cancer drugs. **Archiv der Pharmazie**, v. 340, n. 3, p. 117–126, 2007.

OUN, R.; MOUSSA, Y. E.; WHEATE, N. J. The side effects of platinum-based chemotherapy drugs: a review for chemists. **Dalton Transactions**, v. 47, n. 19, p. 6645–6653, 2018.

OURIQUE, F. et al. DNA damage and inhibition of akt pathway in MCF-7 cells and ehrlich tumor in mice treated with 1,4-naphthoquinones in combination with ascorbate. **Oxidative Medicine and Cellular Longevity**, v. 2015, Article ID 495305, 2015.

PAGE, B.; PAGE, M.; NOEL, C. A New Fluorometric Assay for Cytotoxicity Measurements in vitro. **International Journal of Oncology**, v. 3, n. 3, p. 473–476, 1993.

PAN, H. W. et al. Targeted TPX2 increases chromosome missegregation and suppresses tumor cell growth in human prostate cancer. **OncoTargets and Therapy**, v. 10, p. 3531–3543, 2017.

PETROS, A. M.; OLEJNICZAK, E. T.; FESIK, S. W. Structural biology of the Bcl-2 family of proteins. **Biochimica et Biophysica Acta (BBA) - Molecular Cell Research**, v. 1644, n. 2–3, p. 83–94, mar. 2004.

PFAFFL, M. W. A new mathematical model for relative quantification in real-time RT-PCR. **Nucleic acids research**, v. 29, n. 9, p. e45, 2001.

PINHO, B. R. et al. Naphthoquinones' biological activities and toxicological effects. **Bioactive Compounds: Types, Biological Activities and Health Effects**, n. March, p. 181–218, 2012.

PIRES, W. C. et al. Ru(II)/diphenylphosphine/pyridine-6-thiolate complexes induce S-180 cell apoptosis through intrinsic mitochondrial pathway involving inhibition of Bcl-2 and p53/Bax activation. **Molecular and Cellular Biochemistry**, v. 438, n. 1–2, p. 199–217, 2018.

PÓPULO, H.; LOPES, J. M.; SOARES, P. The mTOR signalling pathway in human cancer**. International Journal of Molecular Sciences**, v. 13, n. 2, p. 1886–1918, 2012.

PRADHAN, R. et al. From Body Art to Anticancer Activities: Perspectives on Medicinal Properties of Henna. **Current Drug Targets**, v. 13, n. 14, p. 1777–1798,. 2012.

PRESA, A. et al. Photoswitching the Cytotoxic Properties of Platinum(II) Compounds. **Angewandte Chemie - International Edition**, v. 54, n. 15, p. 4561–4565, 2015.

RADEMAKER-LAKHAI, J. M. et al. A phase I and pharmacological study with imidazolium-trans-DMSO-imidazole-tetrachlororuthenate, a novel ruthenium anticancer agent. **Clinical Cancer Research**, v. 10, n. 11, p. 3717–3727, 2004.

RAJA, W.; AGRAWAL, R. C.; OVAIS, M. Chemopreventive action of *Lawsonia inermis* leaf extract on DMBA-induced skin papilloma and B16F10 melanoma tumour. **Pharmacologyonline**, v. 2, p. 1243–1249, 2009.

RAJENDRAN, M. Quinones as photosensitizer for photodynamic therapy: ROS generation, mechanism and detection methods. **Photodiagnosis and photodynamic therapy**, v. 13, p. 175–187, 2015.

RAMADEVI, P. et al. Journal of Photochemistry and Photobiology A : Chemistry Ruthenium complexes of ferrocene mannich bases : DNA / BSA interactions and cytotoxicity against A549 cell line. **"Journal of Photochemistry & Photobiology, A: Chemistry"**, v. 305, p. 1–10, 2015.

RIEDL, S. J.; SHI, Y. Molecular mechanisms of caspase regulation during apoptosis. **Nature Reviews Molecular Cell Biology**, v. 5, n. 11, p. 897–907, 2004.

ROWE, L. A.; DEGTYAREVA, N.; DOETSCH, P. W. DNA damage-induced reactive oxygen species (ROS) stress response in Saccharomyces cerevisiae. **Free Radical Biology and Medicine**, v. 45, n. 8, p. 1167–1177, out. 2008.

SANT, S.; JOHNSTON, P. A. The production of 3D tumor spheroids for cancer drug discovery. **Drug Discovery Today: Technologies**, v. 23, p. 27–36, mar. 2017.

SARWAR, T. et al. Multi-spectroscopic and molecular modelling studies on the interaction of esculetin with calf thymus DNA. **Molecular BioSystems**, v. 11, n. 2, p. 522–531, 2015.

SATOH, T. et al. Phase I study of YM155, a novel survivin suppressant, in patients with advanced solid tumors. **Clinical Cancer Research**, v. 15, n. 11, p. 3872–3880, 2009.

MINISTÉRIO DA SAÚDE, Brasil. **Sistema de Informação Ambulatorial do SUS - ONCOLOGIA**. Disponível em: <http://bvsms.saude.gov.br/bvs/publicacoes/inca/manual>. Acesso em 21 de dez de 2019

SAVA, G. et al. Metal complexes of ruthenium: antineoplastic properties and perspectives. **Anticancer Drugs**, v. 1, n. 2, p. 99–108, 1990.

SAVA, G.; BERGAMO, A. Ruthenium-based compounds and tumour growth control (review). **International Jounal of Oncology**, v. 17, n. 2, p. 353–365, 2000.

SCHETTINI, F. et al. CDK 4/6 Inhibitors as Single Agent in Advanced Solid Tumors. **Frontiers in Oncology**, v. 8, n. 12, p. 1–12, 2018.

SCHNEIDER, C. D.; OLIVEIRA, A. R. Radicais libres de oxigênio e ecercício: mecanismos de formação e adpatação ao treinamento físico. **Revista Brasileira de Medicina do Esporte**, v. 10, n. 9, p. 308–313, 2004.

SCHULER, F. et al. Checkpoint kinase 1 is essential for normal B cell development and lymphomagenesis. **Nature Communications**, v. 8, n. 1, p. 1–12, 2017.

SEGURA, D. F. et al. Synthesis and biological evaluation of ternary silver compounds bearing N,N-chelating ligands and thiourea: X-ray structure of [{Ag(bpy)(μ-tu)}$_2$](NO_3)$_2$(bpy = 2,2′-bipyridine; Tu = thiourea). **Polyhedron**, v. 79, p. 197–206, 2014.

SHAH, R. B.; GHOSH, D.; ELDER, J. T. Epidermal Growth Factor Receptor (ErbB1) Expression in ProstateCancer Progression: Correlation With Androgen Independence. **The Prostate**, v. 66, n. 4, p. 129–138, 2008.

SHEPPARD, K. E.; MCARTHUR, G. A. The cell-cycle regulator CDK4: An emerging therapeutic target in melanoma. **Clinical Cancer Research**, v. 19, n. 19, p. 5320–5328, 2013.

SHIBAI-OGATA, A. et al. Evaluation of high-throughput screening for *in vitro* micronucleus test using fluorescence-based cell imaging. **Mutagenesis**, v. 26, n. 6, p. 709–719, 1 nov. 2011.

SHOEMAKER, R. H. The NCI60 human tumour cell line anticancer drug screen. **Nature reviews of Cancer**, v. 6, n. 10, p. 813–23, 2006.

SIEGEL, R. L.; MILLER, K. D.; JEMAL, A. Cancer Statistics, 2016. **CA Cancer J Clin**, v. 66, n. 1, p. 7–30, 2016.

SIEGEL, R. L.; MILLER, K. D.; JEMAL, A. Cancer statistics, 2017. **CA: A Cancer Journal for Clinicians**, v. 67, n. 1, p. 7–30, 2017.

SIKOV, W. M. Assessing the Role of Platinum Agents in Aggressive Breast Cancers. **Current Oncology Reports**, v. 17, n. 2, Article number: 3, 2015. Disponível em: <http://www.ncbi.nlm.nih.gov/pubmed/25665554>. Acesso em: 11 de mai de 2018.

SILVA, S. L. R. et al. Ru(II)-thymine complex causes DNA damage and apoptotic cell death in human colon carcinoma HCT116 cells mediated by JNK/p38/ERK1/2 via a p53-independent signaling. **Scientific Reports**, v. 9, n. 1, p. 1–11, 2019.

SIMPSON, P. V. et al. Defining the Anti-Cancer Activity of Tricarbonyl Rhenium Complexes: Induction of G2/M Cell Cycle Arrest and Blockade of Aurora-A Kinase Phosphorylation. **Chemistry - A European Journal**, v. 23, n. 27, p. 6518–6521, 2017.

SINGH, D. K.; LUQMAN, S. *Lawsonia inermis* (L.): A perspective on anticancer potential of Mehndi/Henna. **Biomedical Research and Therapy**, v. 1, n. 4, p. 112–120, 2014.

SINGH, S. et al. p53 regulates ERK activation in carboplatin induced apoptosis in cervical carcinoma: A novel target of p53 in apoptosis. **FEBS Letters**, v. 581, n. 2, p. 289–295, 23 jan. 2007.

SLADE, D. Mitotic functions of poly(ADP-ribose) polymerases. **Biochemical Pharmacology**, v. 167, n. March, p. 33–43, 2019.

SOUZA, M. A. et al. The antimicrobial activity of lapachol and its thiosemicarbazone and semicarbazone derivatives. **Memórias do Instituto Oswaldo Cruz**, v. 108, n. 3, p. 342–351, maio 2013.

SPOERLEIN-GUETTLER, C. et al. Ferrocene and (arene)ruthenium(II) complexes of the natural anticancer naphthoquinone plumbagin with enhanced efficacy against resistant cancer cells and a genuine mode of action. **Journal of Inorganic Biochemistry**, v. 138, p. 64–72, 2014.

SRISHAILAM, A. et al. Synthesis, characterization; DNA binding and antitumor activity of ruthenium(II) polypyridyl complexes. **Journal of Photochemistry and Photobiology B: Biology**, v. 141, p. 47–58, dez. 2014.

SU, Z. et al. Apoptosis, autophagy, necroptosis, and cancer metastasis. **Molecular Cancer**, v. 14, n. 1, p. 48, 2015.

SUROVA, O.; ZHIVOTOVSKY, B. Various modes of cell death induced by DNA

damage. **Oncogene**, v. 32, n. 33, p. 3789–3797, 2013.
TABRIZI, L.; CHINIFOROSHAN, H. Ruthenium(II) p-cymene complexes of naphthoquinone derivatives as antitumor agents: A structure−activity relationship study. **Journal of Organometallic Chemistry**, v. 822, p. 211–220, nov. 2016.

TABRIZI, L.; TALAIE, F.; CHINIFOROSHAN, H. Copper(II), cobalt(II) and nickel(II) complexes of lapachol: synthesis, DNA interaction, and cytotoxicity. **Journal of Biomolecular Structure and Dynamics**, v. 35, n. 15, p. 3330–3341, 18 nov. 2017.

TANG, A. et al. Aurora kinases: novel therapy targets in cancers. **Oncotarget**, v. 8, n. 14, p. 23937–23954, 2017.

TANG, D. et al. ERK Activation Mediates Cell Cycle Arrest and Apoptosis after DNA Damage Independently of p53. **Journal of Biological Chemistry**, v. 277, n. 15, p. 12710–12717, 12 abr. 2002.

THEODORAKI, M. A. et al. Spontaneously-forming spheroids as an *in vitro* cancer cell model for anticancer drug screening. **Oncotarget**, v. 6, n. 25, 2015.

TICE, R. R. et al. Single cell gel/comet assay: Guidelines for *in vitro* and *in vivo* genetic toxicology testing. **Environmental and Molecular Mutagenesis**, v. 35, n. 3, p. 206–221, 6 jun. 2000.

TORCHIA, E. C. et al. Aurora Kinase-A Deficiency during Skin Development Impairs Cell Division and Stratification. **Journal of Investigative Dermatology**, v. 133, n. 1, p. 78–86, 2013.

TORGOVNICK, A.; SCHUMACHER, B. DNA repair mechanisms in cancer development and therapy. **Frontiers in Genetics**, v. 6, n. 4, p. 1–15, 2015.

TOUFEKTCHAN, E.; TOLEDO, F. The Guardian of the Genome Revisited: p53 Downregulates Genes Required for Telomere Maintenance, DNA Repair, and Centromere Structure. **Cancers**, v. 10, n. 5, p. 135, 2018.

TUNG, Y.-C. et al. High-throughput 3D spheroid culture and drug testing using a 384 hanging drop array. **The Analyst**, v. 136, n. 3, p. 473–478, 2011.

VAN RIJT, S. H.; SADLER, P. J. Current applications and future potential for bioinorganic chemistry in the development of anticancer drugs**. Drug Discovery Today**, 2009.

VANTANGOLI, M. M. et al. Morphologic Effects of Estrogen Stimulation on 3D MCF-7 Microtissues. **Toxicology Letters**, v. 248, p. 1–8, 2016.

VAZ, C. A. V. **Effect of Regucalcin on the expression of oncogenes and tumor suppressor genes in prostate cell lines**. Thesis. Universidade da Beira Interior, Covilhã, Portugal, 2010.

VERJANS, E.-T. et al. Three-dimensional cell culture models for anticancer drug screening: Worth the effort? **Journal of Cellular Physiology**, v. 233, n. 4, p. 2993–3003, abr. 2018.

VERMES, I. et al. A novel assay for apoptosis Flow cytometric detection of phosphatidylserine early apoptotic cells using fluorescein labelled expression on Annexin V. **Journal of Immunological Methods**, v. 184, n. 95, p. 39–51, 1995.

VIJAYAN, P. et al. Dissymmetric thiosemicarbazone ligands containing substituted aldehyde arm and their ruthenium(II) carbonyl complexes with PPh3/AsPh3 as ancillary ligands: Synthesis, structural characterization, DNA/BSA interaction and in vitro anticancer activity. **Journal of Organometallic Chemistry**, v. 768, p. 163–177, 2014.

VIJAYARAGHAVAN, S. et al. Inhibiting CDK in Cancer Therapy: Current Evidence and Future DirectionsTargeted Oncology. **Targeted Oncology**, v. 13, n. 1, p. 21–38, 2018.

VINCI, M. et al. Advances in establishment and analysis of three-dimensional tumor spheroid-based functional assays for target validation and drug evaluation. **BMC Biology**, v. 10, n. 1, p. 29, 2012.

VITALE, I. et al. Mitotic catastrophe: a mechanism for avoiding genomic instability. **Nature reviews. Molecular cell biology**, v. 12, n. 6, p. 385–392, 2011.

WAN, D. et al. Synthesis and anticancer properties of ruthenium (II) complexes as potent apoptosis inducers through mitochondrial disruption. **European Journal of Medicinal Chemistry**, v. 139, p. 180–190, 2017.

WANG, F. et al. Protective effects of N-acetylcysteine on cisplatin-induced oxidative stress and DNA damage in HepG2 cells. **Experimental and Therapeutic Medicine**, v. 8, n. 6, p. 1939–1945, dez. 2014.

WANG, H.; JOSEPH, J. A. Quantifying cellular oxidative stress by dichlorofluorescein assay using microplate reader. **Free Radical Biology and Medicine**, v. 27, n. 5–6, p. 612–616, 1999.

WANG XIANG, J., YAN, M., ZHANG, Y., ZHAO, Y., YUE, C., XU, J., ZHENG, F., CHEN, J., KANG, Z., CHEN, T., XING, D., LIU, Q., L. et al. The Mitotic Kinase Aurora-A Induces Mammary Cell Migration and Breast Cancer Metastasis by Activating the

Cofilin-F-actin Pathway. **Cancer Research**, v. 70, n. 22, p. 9118–9128, 2010.

WANG, Y.; ZHU, W. G.; ZHAO, Y. Autophagy substrate SQSTM1/p62 regulates chromatin ubiquitination during the DNA damage response. **Autophagy**, v. 13, n. 1, p. 212–213, 2017.

WEISS, A. et al. In vivo anti-tumor activity of the organometallic ruthenium(II)-arene complex [Ru(η6-p-cymene)-Cl2(pta)] (RAPTA-C) in human ovarian and colorectal carcinomas. **Chem. Sci.**, v. 5, n. 12, p. 4742–4748, 2014.

WELLINGTON, K. W. Understanding cancer and the anticancer activities of naphthoquinones – a review. **RSC Adv.**, v. 5, n. 26, p. 20309–20338, 2015.

WILLEMS, E. et al. The functional diversity of Aurora kinases: A comprehensive review. **Cell Division**, v. 13, n. 1, p. 1–17, 2018.

XIAO, D. et al. Diallyl trisulfide-induced G2-M phase cell cycle arrest in human prostate cancer cells is caused by reactive oxygen species-dependent destruction and hyperphosphorylation of Cdc25C. **Oncogene**, v. 24, n. 41, p. 6256–6268, 2005.

XU, S.; WEIHUA, Z. Loss of EGFR induced autophagy sensitizes hormone refractory prostate cancer cells to adriamycin. **Prostate**, v. 71, n. 11, p. 1216–1224, 2011.

YAMANAKA, K. et al. Antitumor activity of YM155, a selective small-molecule survivin suppressant, alone and in combination with docetaxel in human malignant melanoma models. **Clinical Cancer Research**, v. 17, n. 16, p. 5423–5431, 2011.

YANG, C. et al. Aurora-B Mediated ATM Serine 1403 Phosphorylation Is Required for Mitotic ATM Activation and the Spindle Checkpoint. **Molecular Cell**, v. 44, n. 4, p. 597–608, 2011.

YOKOTA, J. Tumor progression and metastasis. **Carcinogenesis**, v. 21, n. 3, p. 497–503, 2000.

ZEKRI, A. et al. Inhibitor of Aurora Kinase B Induces Differentially Cell Death and Polyploidy via DNA Damage Response Pathways in Neurological Malignancy: Shedding New Light on the Challenge of Resistance to AZD1152-HQPA. **Molecular Neurobiology**, v. 53, n. 3, p. 1808–1823, 2016.

ZEKRIA, A. et al. Reactive oxygen species generation and increase in mitochondrial copy number: New insight into the potential mechanism of cytotoxicity induced by aurora kinase inhibitor, AZD1152-HQPA. **Anti-Cancer Drugs**, v. 28, n. 8, p. 841–851, 2017.

ZENG, C. C. et al. The induction of apoptosis in HepG-2 cells by ruthenium(II) complexes through an intrinsic ROS-mediated mitochondrial dysfunction pathway. **European Journal of Medicinal Chemistry**, v. 122, p. 118–126, 2016.

ZHANG, C. X.; LIPPARD, S. J. New metal complexes as potential therapeutics. **Current Opinion in Chemical Biology**, v. 7, n. 4, p. 481-489, 2003.

ZHANG, Y.; HUNTER, T. Roles of Chk1 in cell biology and cancer therapy. **International Journal of Cancer**, v. 134, n. 5, p. 1013–1023, 2014.

ZHAO, J. et al. Ruthenium arene complex induces cell cycle arrest and apoptosis through activation of P53-mediated signaling pathways. **Journal of Organometallic Chemistry**, v. 898, p. 120-139, 2019.

ZHENG, W. L. et al. ROS-mediated cell cycle arrest and apoptosis induced by zearalenone in mouse sertoli cells via ER stress and the ATP/AMPK pathway. **Toxins**, v. 10, n. 1, 2018.

ZORZET, S. et al. Lack of In vitro cytotoxicity, associated to increased G(2)-M cell fraction and inhibition of matrigel invasion, may predict In vivo-selective antimetastasis activity of ruthenium complexes. **The Journal of pharmacology and experimental therapeutics**, v. 295, n. 3, p. 927–933, 2000.

ZUMRUTDAL, E.; OZASLAN, M. A miracle plant for the herbal pharmacy; Henna (*Lawsonia inermis*). **International Journal of Pharmacology**, v. 8, n. 6, p. 483–489, 2012.

Capítulo 2

Bioorganic Chemistry 85 (2019) 455–468

Contents lists available at ScienceDirect

Bioorganic Chemistry

journal homepage: www.elsevier.com/locate/bioorg

Novel lawsone-containing ruthenium(II) complexes: Synthesis, characterization and anticancer activity on 2D and 3D spheroid models of prostate cancer cells

Rone Aparecido De Grandis[a,*], Patrick Wellington da Silva dos Santos[b], Katia Mara de Oliveira[c], Ana Rita Tomazela Machado[b], Alexandre Ferro Aissa[b], Alzir Azevedo Batista[c], Lusânia Maria Greggi Antunes[b], Fernando Rogério Pavan[a,*]

[a] School of Pharmaceutical Sciences, São Paulo State University, Araraquara, São Paulo 14800-903, Brazil
[b] School of Pharmaceutical Sciences of Ribeirão Preto, University of São Paulo, Ribeirão Preto, São Paulo 14040-903, Brazil
[c] Department of Chemistry, Federal University of São Carlos, São Carlos, São Paulo 13561-901, Brazil

ARTICLE INFO

Keywords:
Cancer
1,4-naphthoquinone
3D-cell culture
ROS
Apoptosis
BAX/BCL-2

ABSTRACT

This study describes a series of newly synthesized phosphine/diimine ruthenium complexes containing the lawsone as bioligand with enhanced cytotoxicity against different cancer cells, and apoptosis induction in prostatic cancer cells DU-145. The complexes $[Ru(law)(N\text{-}N)_2]PF_6$ where N-N is 2,2′-bipyridine (**1**) or 1,10-phenanthroline (**2**) and $[Ru(law)(dppm)(N\text{-}N)]PF_6$, where dppm means *bis*(diphenylphosphino)methane, N-N is 2,2′-bipyridine (**3**) or 1,10-phenanthroline (**4**), and law is lawsone, were synthesized and fully characterized by elemental analysis, molar conductivity, NMR, UV–vis, IR spectroscopies and cyclic voltammetry. The interaction of the complexes (**1**–**4**) with DNA was evaluated by circular dichroism, gel electrophoresis, and fluorescence, and the complexes presented interactions by the minor grooves DNA. The phosphinic series of complexes exhibited a remarkably broad spectrum of anticancer activity with approximately 34-fold higher than cisplatin and 5-fold higher than doxorubicin, inhibiting the growth of 3D tumor spheroids and the ability to retain the colony survival of DU-145 cells. Also, the complex (**4**) inhibits DU-145 cell adhesion and migration potential indicating antimetastatic properties. The mechanism of its anticancer activity was found to be related to increased reactive oxygen species (ROS) generation, increased the *BAX/BCL-2* ratio and subsequent apoptosis induction. Overall, these findings suggested that the complex (**4**) could be a promising candidate for further evaluation as a chemotherapeutic agent in the prostate cancer treatment.

1. Introduction

The research based on transition metals was strongly encouraged thanks to the quest for novel anticancer therapies [1]. So far, cisplatin is probably still the most essential chemotherapeutic based on metals complexes. However, platinum complexes have caused several side effects and cross drug resistance which limited their applications [2]. Therefore, the development of novel metallodrugs agents remains a significant challenge.

In this important field, ruthenium-based complexes are highlighted due to its unique properties as chemical stability, a variety of oxidation states, structural diversity, low toxicity and ability to mimic iron binding in the biological system [3–6]. Moreover, several ruthenium (Ru) complexes have been foreground reported due to its antimetastatic activities, low toxicity to non-cancer cells and high selectivity for tumor cells [7,8]. For instance, some Ru complexes as NAMI-A (*trans*-$[RuCl_4(1H\text{-imidazole})(DMSO\text{-}S)]$), NKP-1339 (sodium [*trans*-$RuCl_4(1H\text{-indazole})_2$]) and KP1019 (*trans*-$[RuCl_4(1H\text{-in-dazole})_2]$) have been evaluated in preclinical and phase I or II clinical trials, representing a novel class of less toxic antineoplastic chemotherapy [9,10]. Accumulative evidences suggest that Ru-based compounds could act as potential anticancer agents through molecular mechanisms providing an increase of reactive oxygen species (ROS) [11], DNA intercalation [12], DNA damage [13], induction of cell apoptosis and metastasis inhibition [14,15].

One rational approach to improve the efficacy of metal complexes consists of incorporating different chelating ligands with complementary biological activity to enhance the physiological targets of

* Corresponding authors.
E-mail addresses: degrandis.rone@fcfar.unesp.br (R.A. De Grandis), fernando.pavan@unesp.br (F.R. Pavan).

https://doi.org/10.1016/j.bioorg.2019.02.010
Received 11 September 2018; Received in revised form 29 January 2019; Accepted 3 February 2019
Available online 08 February 2019
0045-2068/ © 2019 Elsevier Inc. All rights reserved.

the metallodrug. In this context, active ligands with quinone moiety represent an unquestioned tool in bioinorganic medicinal chemistry for improving the anticancer activity of metal complexes. Undoubtedly, some quinone based drugs such as doxorubicin, mitomycin C, and mitoxantrone are recognized as FDA-approved compounds with excellent anticancer properties [16,17]. A representative class of quinone compounds, known as naphthoquinones, widely distributed in nature, have been recognized to own an extensive range of biological activities such as antimicrobial [18], antiparasitic [19], antiviral [20] and anticancer activity [21].

Mainly, 1,4-naphthoquinone, or lawsone, is an example of a natural compound that contains two ketone groups as suitable chromophore responsible for its biological activity due to their ability to accept electrons [22,23]. Recently, lawsone compounds have shown promising pharmacological effects presenting antiproliferative activity in a large number of cancer cell lines and inhibition of tumor burden *in vivo* [24,25].

Furthermore, findings indicated that anticancer activity also might be related to the inhibition of the enzyme DNA-topoisomerase II [26]. Lawsone can bind potentially to metal ions in different oxidations states coordinating metals in a bidentate way which allows them to play an essential role in biological systems [27]. Indeed, some metal complexes containing lawsone ligands have been exhibited higher biological activity than free lawsone [28]. Therefore, as part of our ongoing effort to design multi-target bioactive metallodrug candidates, in the last years our research group has synthesized several Ru-complexes containing phosphine and diimines ligands with promising pharmacological activities for anticancer proposes [29–35]. In light of these considerations and of some previous results, herein we have investigated the anticancer properties of the newly synthesized phosphine/diimine Ru-complexes containing lawsone as bioligand. The corresponding complexes **1–4** (showed in Fig. 1) were synthesized and characterized, and their potential as anticancer agents was investigated for the first time towards a comprehensive panel of human cancer cell lines cultured in conventional and 3D models. Besides, we analyzed the antimetastatic effects on human prostate carcinoma DU-145 cells and their ability to interact with CT-DNA. Finally, for elucidating the anti-cancer functions and molecular mechanisms, reactive oxygen species (ROS) production and apoptosis-inducing ability were also investigated.

2. Results and discussion

2.1. Synthesis of novel lawsone-containing ruthenium complexes

The complexes (**1–4**) containing lawsone (law), phosphines and diimines as ligands were obtained according to the procedure illustrated in Fig. 1.

The synthetic route obtained pure complexes with high-yield according to spectroscopic data, as well as elemental analyses, molar conductivity and 31P{1H}, 1H and 13C NMR spectrum. All complexes are dark purple air-stable solids, soluble in dichloromethane, acetone, methanol, dimethyl sulfoxide and water insoluble.

In the IR spectra of the free law is observed the intense band of the stretching modes of the phenolic ν(O–H) around 3200 cm^{-1}, this band disappear from the spectra of all complexes, indicating the ligand deprotonation and the coordination by oxygen. The band relative to the carbonyl group (C_1=O) at 1640 cm^{-1} in the free law were shifted to lower frequencies, around 1603 cm^{-1} in the complexes, denoting the bidentate coordination. Also, the band at 1679 cm^{-1} of the group (C_4=O) also presented a small displacement to lower frequencies, 1614 cm^{-1}. The band C_2–O presented displacement from 982 cm^{-1} to 1098 cm^{-1}, approximately, in the complexes, which are in concordance with the coordination by the oxygen. The same behavior was observed for others ruthenium complexes containing the lawsone as ligand [28].

The complexes (**1–4**) were characterized by $^{31}P\{1H\}$, ^{1}H and ^{13}C NMR spectroscopy. In the $^{31}P\{1H\}$ of complexes (**3**) and (**4**) was

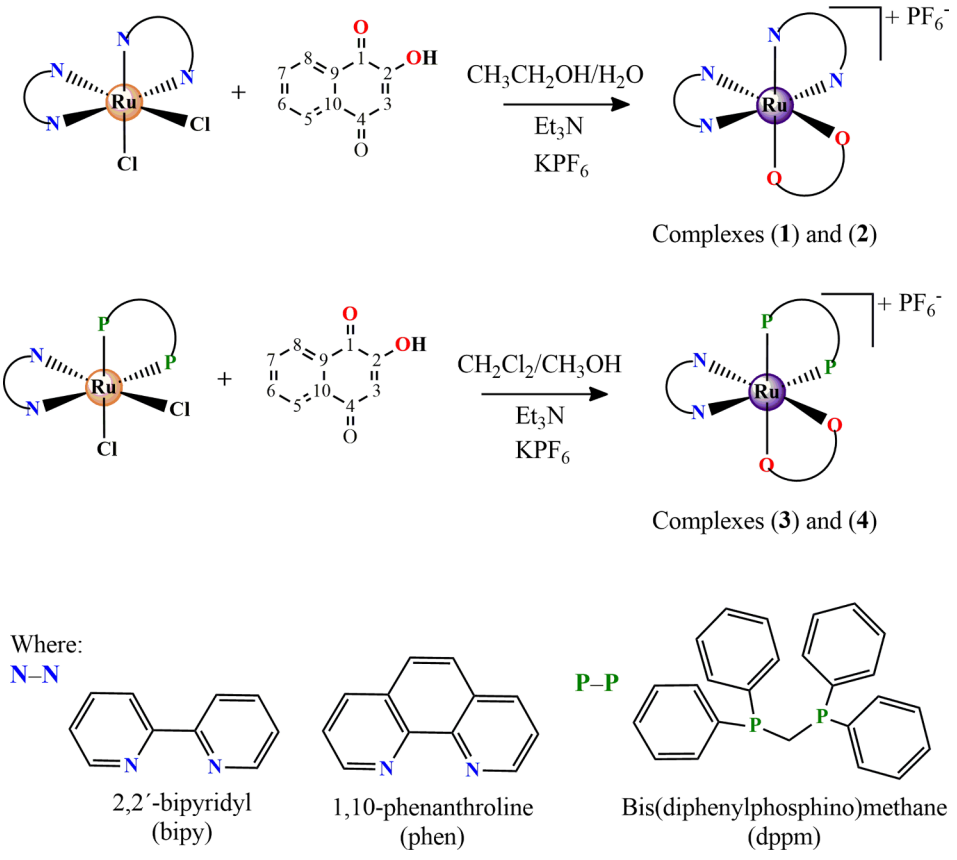


Fig. 1. Synthetic route to the preparation of the new ruthenium complexes containing the naphthoquinone lawsone.

observed four pairs of signals (17.9/6.7 ppm and 15.2/5.9 ppm for complex (**3**) and 18.2/6.6 ppm and 15.4/6.2 ppm for complex (**4**)) for the two phosphorus atoms of biphosphine dppm, indicating the non-equivalence of phosphorus. The duplication of the signals is due to the formation of isomers, where there is an isomer with the phosphorus atom of dppm trans to the oxygen of the carbonyl of lawsone, and in the other, the oxygen atom of the carbonyl is trans to the nitrogen of bipy or phen (see Supplementary Information, Figs. S2–S3). In the ^{1}H spectra of all complexes were observed the presence of the singlet at ca. 5.8 ppm belonging to the hydrogen of bonded to carbon 3 of lawsone. In the case of complex (**4**) was observed in the region of 9.2–6.3 multiplets referring to 32 hydrogen atoms from the dppm, phen and law, and in 5.5 ppm was observed the multiplet attributed to the CH_2 of aliphatic chain of dppm. All complexes presented the same behavior.

Characteristic NMR ^{13}C signals belonging to the carbon of carbonyl groups of lawsone were observed for complex (**4**) at 200.3 ppm (C_1═O), 182.5 ppm (C4═O) and 172.6 ppm (C_2−O). These signals are observed in 184.5 ppm (C_1═O), 181.2 ppm (C4═O) and 159.5 ppm (C_2−O) in free lawsone. The most significant displacements are found for the carbons atoms of the groups C_1═O and C_2−O, indicating the coordination of these oxygen atoms. More recently, our research group developed *trans*-[Ru(law)(PPh_3)$_2$(N-N)]PF_6 complexes and were observed the same behavior in NMR experiments [31].

The electrochemical behavior of the complexes was evaluated by cyclic voltammetry and the redox process Ru(II)/Ru(III) for all complexes were observed in the region of 1–1.1 V. The values are higher than those for complexes precursors, which occur around 0.1–0.6 V. This difference can be explained by the higher stability of the complexes after coordination of lawsone, due the replacement of two chlorides σ and π donor by a negative monocharged chelating lawsone.

2.2. Partition coefficient (log P) study

Determining the lipophilicity is an important physicochemical property that figures out the possible pharmacokinetic and pharmacodynamic profile of new drugs candidates in the discovery development phase [36]. The well-known shake-flask has been widely recommended as a reference method to determine a partition coefficient experimentally [37]. The log *P*(o/w) values, calculated by the shake-flask method, were positive and ranged from 0.228 ± 0.012 to complex (**1**), 0.573 ± 0.023 to complex (**2**), 0.437 ± 0.025 to complex (**3**) and 0.793 ± 0.031 to complex (**4**). As demonstrates, the higher lipophilicity of complexes (**2**) and (**4**) can be attributed to the presence of phen ligand. Other studies established that the presence of 1,10-Phenanthroline acts improving the lipophilicity of silver complexes when compared to bipyridine analogs [38]. Our finding also suggests that the use of diphosphines as ligands can adjust the lipophilic/hydrophilic balance in metal complexes, where in general, its biological activity is found to increase thanks to an increase in the lipophilicity [39]. Thus, the log *P* indicates that the coordination of phen and dppm chelating ligands in one single molecular structure improve the lipophilicity and, as a consequence, may contribute to enhance the cell membrane permeability and its biological activity.

2.3. The complexes display enhanced cytotoxicity against a panel of cancer cell lines

The cytotoxicity of the ruthenium complexes was evaluated in a panel of different histological types of cancer cell lines (A549, Caco-2, DU-145, HepG2, PC-3 and MDA-MB-231) and against two non-cancer cells (FGH and HUVEC) in two-dimensional (2D) culture by Alamar Blue assay 24 h after incubation, as shown in Table 1. All of the complexes presented enhanced cytotoxicity to different cancer cells and more potent activity than metal-free lawsone. The synthesized Ru(II) phosphine complexes investigated exhibited remarkable cytotoxic properties displaying better anticancer activity than cisplatin (Fauldcispla®) and doxorubicin (Fauldoxo®). As expected, the phosphine-coordinating ligand improved not only the lipophilicity of ruthenium compounds but also their biological activity. Metal complexes with different phosphine ligands had antitumor profiles characterized by high cytotoxic potency and selectivity between different cancer cells [40,41]. Compared to the other complexes and metal-free lawsone, the phosphine complexes (**3**) and (**4**) had low IC_{50} values, where complex (3) presented IC_{50} values ranging from to 1.9 to 4.8 μM for cancer cell lines DU-145 and A549, respectively and (**4**) presented IC_{50} values ranging from 1.3 to 3.0 μM for cancer cell lines DU-145 and MDA-MB-231, respectively.

In addition, complex (**3**) was more potent than cisplatin in A549 (3-fold), Caco-2 (7-fold), DU-145 (12-fold), HepG2 (6-fold), PC-3 (6-fold) and MDA-MB-231 (10-fold). Complex (**4**) was more potent than doxorubicin on DU-145 (4-fold), HepG2 (2-fold), PC-3 (2-fold) and cisplatin on A549 (4-fold), Caco-2 (8-fold), DU-145 (18-fold), HepG2 (6-fold), PC-3 (9-fold) and MDA-MB-231 (12-fold). The precursors of types [$RuCl_2$(N-N)$_2$]PF_6) and [$RuCl_2$(dppm)(N-N)]PF_6 (N-N = 2,2′-bipyridine or 1,10-phenanthroline) exhibited weak cytotoxicity (IC_{50} > 100 μM). The IC_{50} value for non-cancer cells was 4.3 and 8.1 μM for the complex (**3**), 3.2 and 6.9 μM for the complex (**4**) and 1.9 and 4.6 μM for doxorubicin on FGH and HUVEC cells, respectively.

Table 2 shows the calculated selectivity index (SI) of each compound. The SI was calculated using the following formula: SI = IC_{50} [non-cancer cells]/IC_{50} [cancer cells]. The SI is a clear manner to estimate the therapeutic range of a drug and to identify drug candidates for further studies [11]. Complexes (**3**) and (**4**) were more cytotoxic and selective to prostate cancer cells DU-145. Furthermore, both complexes exhibit selectivity index greater than displayed by the drug controls cisplatin and doxorubicin, which are clinically useful drugs in the treatment of cancer. Probably, the presence of the dppm ligand in the complexes (**3**) and (**4**) may contribute to increasing cytotoxic activity, as previously observed for other ruthenium complexes, where the increase of phosphine ligands is directly related to the increase of biological activity [30,42].

The promising cytotoxic activity of the complexes (**3**) and (**4**) towards prostate cancer cells encouraged us to study their effects at the cellular level. In a new set of experiment, DU-145 cell line was used as a cellular model, since it was among the most sensitive cell line to the complexes tested. Therefore, the cytotoxicity of phosphine complexes was confirmed by clonogenic survival assay that is extremely sensitive to determine the effects on cell proliferation after treatments. Clonogenic assays represent the gold-standard method to study the cytotoxic and constitute a traditional technique of choice to determine the long-term effect of proliferating cells [43]. The results revealed that both complexes inhibited cell colony formation of DU-145 cells in a dose-dependent manner as shown in Fig. 2A. The plating efficiency of untreated DU-145 cells was higher than 70% for all replicates. Moreover, following seven days of culture, the inhibitory effect of the complex (**4**) was greater than that of the complex (**3**) at the same concentration. At concentrations of 0.125, 0.25, 0.5 and 1 μM, the complex (**3**) reduced the colony-forming presenting survival fractions (SF) of 79.1, 68.2, 31.1 and 13.4%, respectively. Complex (**4**), at same concentrations, presented SF of 68.1, 39.5, 22.4 and 5.1%, respectively. No significant (p > 0.05) decrease in the number of colonies was observed in control (DMSO 0.1% v/v). Few colonies of DU-145 cells were visible after incubation with 1 μM of (**4**) which indicates that the substitution of diimine ligand increases the activity of the compound (Fig. 2B).

The higher cytotoxicity, exhibited by complexes (**3**) and (**4**), indicated that the coordination of phosphine and lawsone chelating ligands in one single molecule made it possible to create a compound with increased antitumor activity. Furthermore, these findings predicted the loss of clonogenicity of DU-145 cells after the exposure with (**3**) and (**4**) which is an effective parameter to distinguish the cytostatic of the cytotoxic effects of drug treatments [44]. Cisplatin did not

Table 1
Cytotoxic activity of Ru complexes in human cell lines.

	IC_{50} in μM							
	FGH	HUVEC	A549	Caco-2	DU-145	HepG2	PC-3	MDA-MB-231
BB	> 100	> 100	> 100	> 100	> 100	> 100	> 100	> 100
BP	> 100	> 100	> 100	> 100	> 100	> 100	> 100	> 100
DB	> 100	> 100	> 100	> 100	> 100	> 100	> 100	> 100
DP	> 100	> 100	> 100	> 100	> 100	> 100	> 100	> 100
LAW	> 100	> 100	> 100	> 100	> 100	> 100	> 100	> 100
(1)	74.3 ± 1.4	93.1 ± 7.4	99.1 ± 0.2	60.3 ± 5.3	41.4 ± 4.5	53.9 ± 3.8	61.9 ± 2.3	63.1 ± 5.7
(2)	80.7 ± 6.6	78.7 ± 2.2	69.1 ± 5.2	58.1 ± 2.9	37.2 ± 2.1	49.0 ± 3.6	52.1 ± 1.0	69.4 ± 4.5
(3)	4.3 ± 0.6	8.1 ± 1.6	4.8 ± 0.4	2.6 ± 0.2	1.9 ± 0.6	1.8 ± 0.3	3.3 ± 0.9	3.6 ± 0.5
(4)	3.2 ± 0.4	6.9 ± 0.8	4.2 ± 0.2	2.4 ± 0.3	1.3 ± 0.2	1.8 ± 0.3	2.2 ± 1.8	3.0 ± 0.3
CIS	11.2 ± 0.5	11.0 ± 0.5	16.5 ± 1.0	19.9 ± 0.9	24.5 ± 2.8	11.4 ± 1.6	21.3 ± 0.1	37.4 ± 6.2
DXR	1.9 ± 0.2	4.6 ± 0.2	2.3 ± 1.8	1.8 ± 0.3	2.5 ± 1.3	3.8 ± 1.6	4.5 ± 0.1	2.5 ± 0.3

Data are presented as the means ± S.E.M. of IC_{50} values in μM obtained by nonlinear regression from at the least three independent experiments performed in triplicate, measured by Alamar blue assay after 24 h incubation. Cancer cells: A549 (human lung carcinoma); Caco-2 (human colorectal adenocarcinoma); DU-145 (human prostate carcinoma); HepG2 (human hepatocellular carcinoma); PC-3 (human prostate adenocarcinoma) and MDA-MB-231 (human breast adenocarcinoma). Non-cancer cells: FGH (human mouth fibroblast) and HUVEC (human umbilical vein endothelial cells). The precursor complexes *bis*-bipyridine (BB), *bis*-phenanthroline (BP), *bis*-diphenylphosphinomethane:bipyridine (DB), diphenylphosphinomethane:phenanthroline (DP) and the ligand lawsone (LAW) were used as controls. Cisplatin (CIS, Fauldcispla®) and doxorubicin (DXR, Fauldoxo®) were used as positive controls.

Table 2
Selectivity index of the Ru complexes.

		Cancer cells					
Non-cancer cells		A549	Caco-2	DU-145	HepG2	PC-3	MDA-MB-231
FGH	(1)	0.7	1.2	1.8	1.4	1.2	1.2
	(2)	1.1	1.4	2.2	1.6	1.5	1.2
	(3)	0.9	1.6	2.3	2.4	1.3	0.8
	(4)	0.8	1.3	2.5	1.8	1.4	1.0
	CIS	0.7	0.6	0.4	1.0	0.5	0.3
	DXR	0.8	1.0	0.7	0.5	0.4	0.7
HUVEC	(1)	0.9	1.5	2.2	1.7	1.5	1.4
	(2)	1.1	1.3	2.1	1.6	1.5	1.1
	(3)	1.6	3.1	4.2	4.5	2.4	2.2
	(4)	1.6	2.8	5.3	3.8	3.1	2.3
	CIS	0.6	0.5	0.4	0.9	0.5	0.2
	DXR	2.0	2.5	1.8	1.2	1.0	1.8

Data are presented with the selectivity index (SI) calculated using the following formula: SI = IC_{50}[non-cancer cells]/IC_{50}[cancer cells]. Cancer cells: A549 (human lung carcinoma); Caco-2 (human colorectal adenocarcinoma); DU-145 (human prostate carcinoma); HepG2 (human hepatocellular carcinoma); PC-3 (human prostate adenocarcinoma) and MDA-MB-231 (human breast adenocarcinoma). Non-cancer cells: FGH (human mouth fibroblast) and HUVEC (human umbilical vein endothelial cells). Cisplatin (CIS – Fauldcispla®) and doxorubicin (DXR – Fauldoxo®) were used as positive controls.

significantly reduce the colony-forming at the same concentrations analyzed ($p > 0.05$).

In complementary to conventional cell monolayer cytotoxic assays performed, we also established 3D multicellular tumor spheroids (MCTS) based on DU-145 cells and used this model for investigating the activity of the ruthenium phosphine complexes toward prostate carcinoma spheroids. The MCTS is a well-established 3D *in vitro* model system that closely reflects the *in vivo* tumor environment concerning nutrient and oxygen gradients, hypoxic/necrotic regions, cell-cell matrix interactions, and gene expression profiles [45]. Therefore, the MCTS was introduced to mimic solid tumors *in vitro* and to study the viability of DU-145 cancer cells treated with the Ru(II) complexes once this model represents a great tool for drug discovery [46,47]. Spheroids grown in ultra-low attachment 96-well plates for 5 days were treated with complexes (**3**) and (**4**) for a period of 24 h to determinate the MCTS viability and were examined for morphological changes until 12 days. The Alamar Blue assay showed that complexes (**3**) and (**4**) reduced the viability of DU-145 MCTS after treatment (Fig. 3A). In general, DU-145 MCTS showed more considerable resistance to both complexes compared to the 2D-cultured cells. Indeed, the MCTS are typically more resistant to antiproliferative compounds because of the differences in the drugs penetration and varying microenvironments (such as pH, hypoxia, extracellular matrix) within spheroids [48]. Similar to *in vivo* tumors, the hypoxic regions inside the spheroids reduces the rate of cell division impairs the effects of anti-proliferative drugs such as cisplatin [49].

Interestingly, the cells in the spheroids showed morphological changes, indicating an effective permeability into spheroid and, therefore, cytotoxicity. The treatment with complex (**4**) disrupted the cell aggregations, resulting in the presence of cell debris after 9 days, suggesting disturbance in cell-matrix interactions (Fig. 3B). The IC_{50} of the complexes (**3**) and (**4**) was 4.1 and 3.4 μM, respectively, while cisplatin presented IC_{50} of 62.6 μM. The complex (**4**) was more potent than cisplatin at the least 18-fold, demonstrating that its cytotoxic activity is effective in the tumor microenvironment, independent of hypoxia. Therefore, (**4**) was selected for detailed studies of the mechanism of cell death.

2.4. The complexes reduce DU-145 cell adhesive and migratory potential

Afterward, cell adhesion and migration assays were performed to evaluate the antimetastatic capability of the complex (**4**). Cancer metastasis mainly occurs due to the migration and adhesion of neoplastic cells from a primary tumor to distant sites following angiogenesis and tumor growth [50]. Therefore, in this research, the anti-migratory and anti-adhesive effects of the complex (**4**) were investigated by wound healing and extracellular matrix adhesion assay on DU-145 cells. For this assays, the cells were treated with concentrations below the IC_{50} values of (**4**) (1.3 ± 0.2 μM, in 24 h). As seen in Fig. 4, untreated DU-145 monolayers were wounded at 0 h and images were registered at different time points after the treatment. The wound space was reduced severely in size in the absence of compounds because of cell proliferation and migration. Complex (**4**) inhibits the cell migration of DU-145 cells, exhibiting deeply reduced wound healing patterns after 48 h were the cells exposed to 0.5 μM presents inhibition of 80% of wound closure, compared to control at the same time. Indeed, the complex (**4**) as expectedly showed an antimetastatic feature, in accordance with the previously reported studies of anti-migratory and anti-angiogenic effects of others ruthenium complexes containing phosphines and diimines as ligands [28,51]. These data demonstrate that low concentrations of (**4**) impaired the androgen-metastatic prostate cancer DU-145 cells migratory potential.

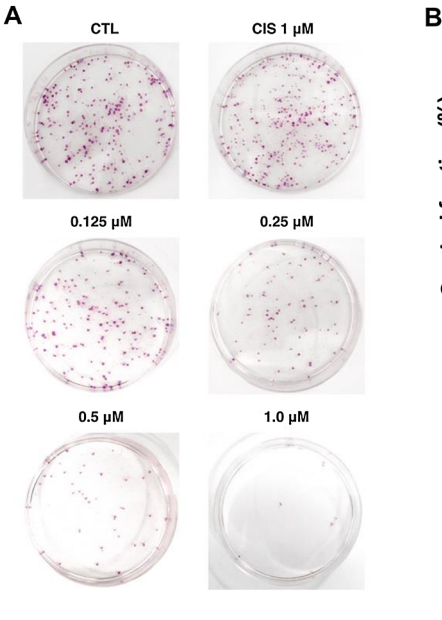
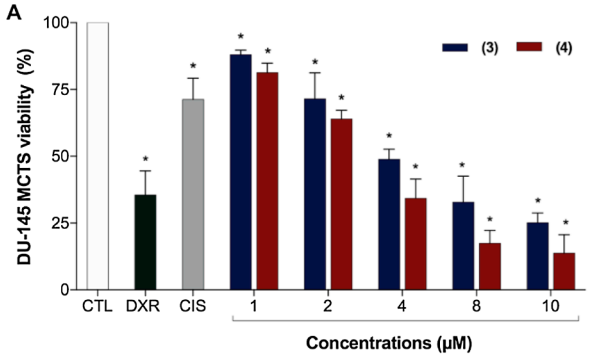


Fig. 2. Assessment of colony survival by clonogenic assay. (A) Representative colony formation images of DU-145 cells after treatment with complex (4). (B) The survival fractions after 24 h treatment with 0.125; 0.25; 0.5 and 1 μM of (3), (4) and cisplatin against DU-145 cells. The negative control (CTL) was treated with the vehicle (0.1% DMSO) used for diluting the tested compound. Data are presented as the means ± S.E.M. of three independent experiments performed in triplicate. $^{*}p < 0.05$ compared with the control by ANOVA followed by Dunnet's test.

Next, we assessed the cell adhesion inhibition of complex (**4**) using mimic extracellular matrix (ECM) adhesion assay. The *in vivo* binding of cells to the extracellular matrix (ECM) is fundamental for cell survival and cell-to-cell communication but is also essential for the metastatic potential of cancer cells [52]. DU-145 cells were incubated to adhere to either collagen or Matrigel® in the presence of different concentrations of the complex (**4**) and assessing the relative numbers of attached cells. As measured by colorimetric assay, untreated and vehicle-treated (CTL) cells exhibited similar adhesion to collagen (Fig. 5A) or Matrigel® (Fig. 5B). The treatments of DU-145 cells with different concentrations of the complex (**4**) significantly inhibited the cell adhesion in a concentration-dependent manner. At 0.5 μM the maximum inhibition of



Spheroids	IC_{50} in μM		
	(3)	(4)	CIS
DU-145	4.1 ± 0.1	3.4 ± 0.5	62.6 ± 3.2

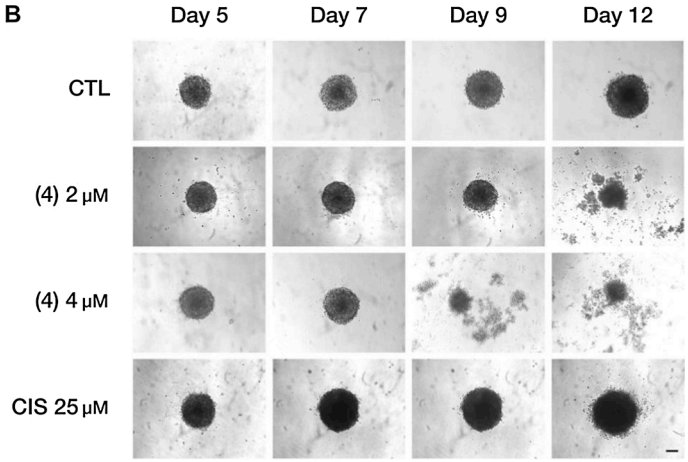


Fig. 3. Effects of the complex (3) and (4) in 3D *in vitro* model of multicellular tumor spheroids of DU-145 cells. (A) The MCTS viability determined by Alamar Blue assay after 24 h treatment and IC_{50} values in μM obtained by nonlinear regression from at the least three independent experiments performed in triplicate. The negative control (CTL) was treated with the vehicle (0.1% DMSO) used for diluting the compounds tested. Doxorubicin (DOX, Fauldoxo® 5 μM), Cisplatin (CIS, Fauldcispla® 25 μM) were used as the positive controls. (B) DU-145 MCTS were examined using inverted microscope (amplification 200×), scale bar = 100 μm. Data are presented as the mean ± S.E.M. of three independent experiments performed in triplicate. $^{*}p < 0.05$ compared with the control by ANOVA followed by Dunnet's test.

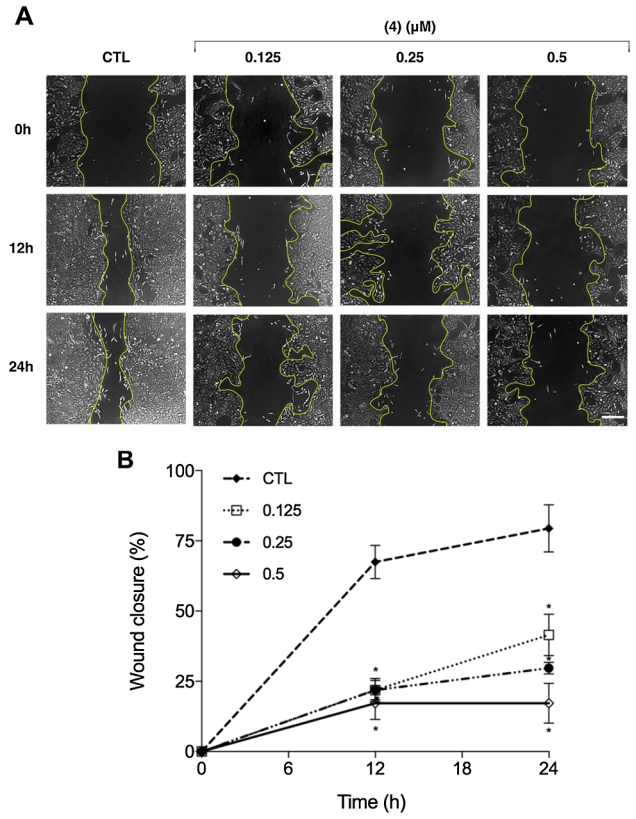


Fig. 4. Inhibitory effects of the complex (4) on DU-145 cells migration *in vitro*. (A) Representative photographs taken at 0, 24 and 48 h post-wound using inverted microscope (amplification 100×), scale bar = 200 μm. The cell monolayer was wounded by a 100 μL pipette tip followed by treatment with different concentrations (0.125, 0.25, and 0.5 μM) of (4) for 24 h. The distance of the wound edge was measured before and after the treatments. (B) Quantification of the relative migration by wound closure. Wound closure (%) were identified from measurements of the migration distance of DU-145 cells from the control group and with complex (4) treatment. Data are presented as the mean ± S.E.M. of three independent experiments performed in triplicate. $^{*}p < 0.05$ compared with the control by ANOVA followed by Dunnet's test.

DU-145 adhesion was calculated by more than 70% on Matrigel® matrix. The anti-metastatic activity of ruthenium compounds is well-recognized by NAMI-A studies [53]. Furthermore, current studies suggest Ru-based complexes inhibits the formation of tube-like structures, an essential step in angiogenesis and metastasis [54]. Our findings indicate that complex (**4**) reduce the ability of DU-145 cells to adhere to ECMs which may impact on their metastatic capacity.

2.5. DNA interactions

The DNA is the most studied targets when it comes to the development of compounds with antitumor properties. It occurs because the interaction between DNA and compounds can cause irreversible damage and prevent cell replication, leading to cell death [55]. In this context, we investigated the ability of the ruthenium complexes to interact with DNA by Circular Dichroism (CD), fluorescence and gel electrophoresis.

The CD technique can be used to analyze the conformation changes in the secondary structure of the calf-thymus DNA (CT-DNA) by monitoring the two bands in the UV region, a positive band at 275 nm and a negative band at 245 nm, due to base stacking and right-handed helicity, respectively. Thus, the CT-DNA was incubated with ruthenium complexes in different molar ratios (0.1–0.4), and the bands were analyzed, and the effects are shown in Fig. 6 for complex (**4**). The intensities of negative and positive bands of the CT-DNA did not show any significant change in intensity upon addition of the ruthenium complex, and the same behavior was observed for all complexes (**1**–**4**).

The ability of the complexes to change the tertiary structure of DNA was investigated by electrophoresis in agarose gel employing the pBR322 plasmid DNA, upon incubation with ruthenium complexes in different molar ratios. Alterations in the electrophoretic mobility of plasmid DNA on agarose gel is commonly considered as evidence for direct DNA–metal interactions. Modification of the DNA structure causes hindrance in the migration of supercoiled DNA and a slight improvement in the mobility of open circular DNA to a feature where both forms comigrate. The pBR322 presents three forms, OC (open circular), L (linear) and CC (supercoiled), which show different electrophoretic mobility. Fig. 7 shows the effect of ruthenium complexes on the mobility of pBR322 after incubation at 37 °C for 18 h. The control in lane 2 refers only to pBR322, and the lines 3–11 correspond to the pBR322 in the presence of complexes (3) and (4). The complexes were capable of affecting the mobility of the bands of pBR322, mainly to OC

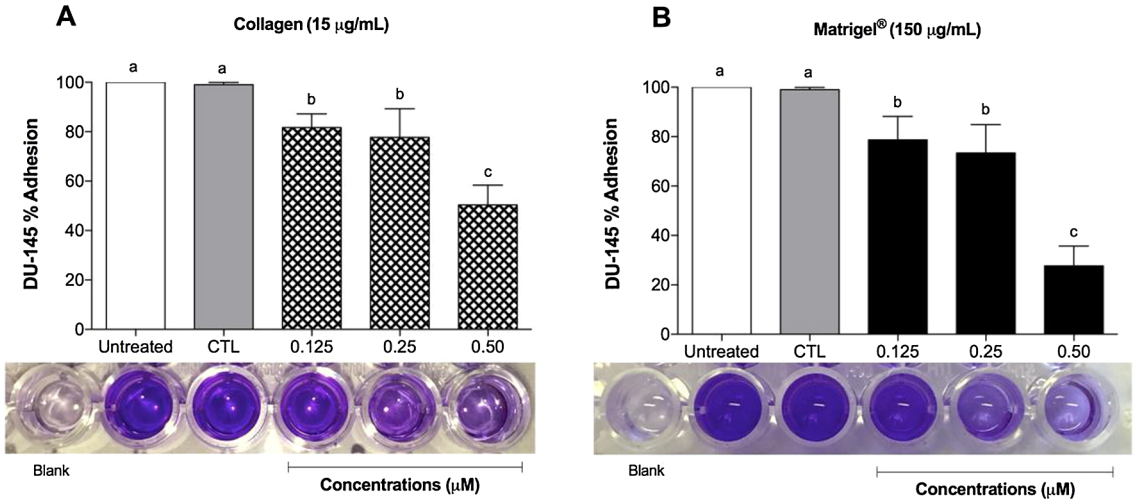


Fig. 5. Complex (4) significantly decreased DU-145 cells adhesive rate on collagen and Matrigel® matrixes. DU-145 cells in the presence of 0.125, 0.25 and 0.5 μM were seeded into 96 well plates coated with collagen (A) and Matrigel® (B) and allowed adhere for 24 h after which supernatants were removed and adhered cells washed and stained with crystal violet. Plates were assayed on a plate reader at 590 nm. Data are presented as the mean ± S.E.M. of three independent experiments performed in triplicate. Values not sharing the same letter are significantly different from each other ($p < 0.05$; ANOVA followed by the Tukey's test).

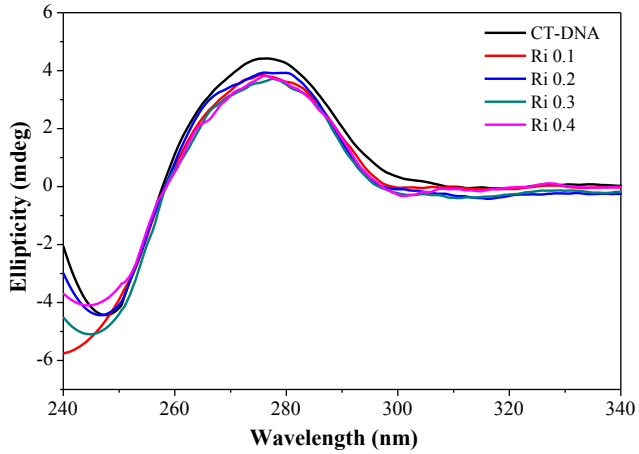


Fig. 6. Fluorescence emission spectra of complex (4) in the presence of increasing amounts of CT-DNA. CD spectra of CT-DNA (50 μM) in the absence and presence of complex (1) in different molar ratio (Ri = [complex (4)]/[DNA], after 18 h of incubation at 37 °C.

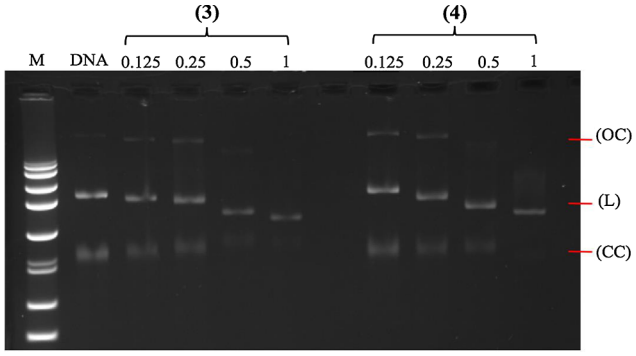


Fig. 7. Electrophoresis mobility of pBR322 plasmid DNA with increasing amounts of complexes (3) and (4) after 18 h of incubation at 37 °C.

and CC bands at Ri 0.5 and 1. The complex (4) was found to exhibit nuclease activity followed by conversion of CC into L, proposing single strand DNA cleavage and the amount of nicked DNA increased at 1 μM showing complete disappearance of CC.

To gain more information about the interaction of complexes with DNA the competition assay using the Hoechst 33258, the fluorescent dye that interacts with DNA through the minor groove, was performed. DNA binding dyes are extensively used to study the mode of drug-DNA interaction. Hoechst 33258 produce a weak fluorescence, but when it binds to DNA a significant increase in fluorescence at 455 nm is observed when excited at 343 nm, thus, it is used as a probe to monitor compounds that interact with DNA [56–58]. Fig. 8 shows the fluorescence spectra of the Hoechst-CT-DNA upon successive addition of complex (**4**). The complex (**4**) was able to decrease the fluorescence of the Hoechst-CT-DNA system with increasing of the concentration, indicating that the complex (**4**) interact with DNA by the minor groove and compete with Hoechst, removing it from DNA structure and consequently, decrease the fluorescence of the system. The same behavior was observed to all ruthenium complexes (Figs. S3–S6 of Supplementary Information). Taken together all the assays employed to investigate the interaction with DNA, we can conclude that ruthenium complexes interact with DNA via the minor groove.

2.6. The complexes induce apoptosis via the BAX/BCL-2 pathway in DU-145 cells

Apoptosis is acknowledged as an essential physiological process in tissue homeostasis. Nevertheless, some cancer cells may adapt to high

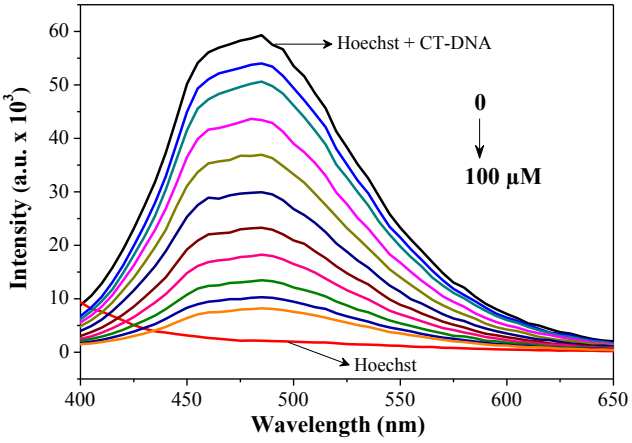


Fig. 8. Emission spectra of Hoechst (2.7 μM, λ_{ex} = 343 nm), CT-DNA (125 μM) in presence of the complex (4) in different concentrations (0–100 μM), at 37 °C.

levels of oncogenic signaling by disabling their senescence- or apoptosis-inducing circuitry. This acquired resistance is appreciated as a hallmark of almost all types of cancer [58,59]. To evaluate whether the complex (**4**) presents the ability to induce apoptosis or necrosis, we selected its concentrations that have shown cytotoxic activity. Therefore, nuclear morphology was assessed by Hoechst 33342/propidium iodide (PI) staining technique for fluorescence microscopy. The results clearly showed that complex (**4**) might induce apoptosis of DU-145 cells based on its staining and morphological characterization after treatments (Fig. 9A).

To determine the percentage of apoptosis and necrosis, the DU-145 cells were treated with 0.25–2.0 μM of the complex (**4**) for 24 h followed by annexin V-FITC/PI staining, and the results were analyzed by using flow cytometry. In live cells, phosphatidylserine (Ptd-L-Ser) is located on the cytoplasmic surface of the cell membrane. The exposure of Ptd-L-Ser on the outer leaflet of the plasma membrane is the final event of apoptosis and can be detected by the binding of fluorescently labeled annexin V [60]. Therefore, annexin V-FITC/PI dual staining can be used to quantify the different cell phenotypes that occur during apoptosis. The percentages of early apoptotic, late apoptotic, necrotic and living cells of DU-145 are shown in Fig. 9B. The incubation of DU-145 cells with increasing concentrations of the complex (**4**) produced a considerable increase in the percentage of apoptotic cells (Q2 and Q4 quadrants) (Fig. 9C). The population of apoptotic cells treated with complex (**4**) had increased remarkably with dose-dependent relation (6.30% for control group, 19.1% for 0.25 μM, 30.9% for 0.50 μM, 45.1% for 1.0 μM and 66.8% for 2.0 μM). Cisplatin treatment at the fixed concentration of 25 μM (IC_{50}) showed 19.5% of apoptotic cells. Therefore, a 100-fold lower concentration of (4) was required for the same effect of cisplatin on DU-145 cells. None of the concentrations induced a significant increase in necrotic cells. Indeed, ruthenium complexes with different ligands have been lead to the apoptosis through the mitochondria, death receptor and oxidative stress pathways [34,61,62]. The molecular mechanism underlying the apoptotic effect of the complex (**4**) was assessed at the level of mRNA expression of pro-apoptotic and anti-apoptotic genes. The 24 h treatment with complex (**4**) at 1.5 μM (IC_{50}) upregulated *BAX* expression by 2.73-fold and downregulated the expression of the gene *BCL-2* by 2.40-fold (Fig. 9D). *BAX* and *BCL-2* are two members of a gene family involved in the regulation of cellular apoptosis. Gene expression analysis revealed that complex (**4**) induced an increase of the expression of the pro-apoptotic *BAX* gene and a decrease of the expression of the anti-apoptotic *BCL-2*. Cells with a high *BAX/BCL-2* ratio will be more sensitive to given apoptotic stimuli when compared to a similar cell type with a comparatively low *BAX/BCL-2* ratio [63]. Therefore, the altered ratio might be an essential key question to understand the sensitizing effect

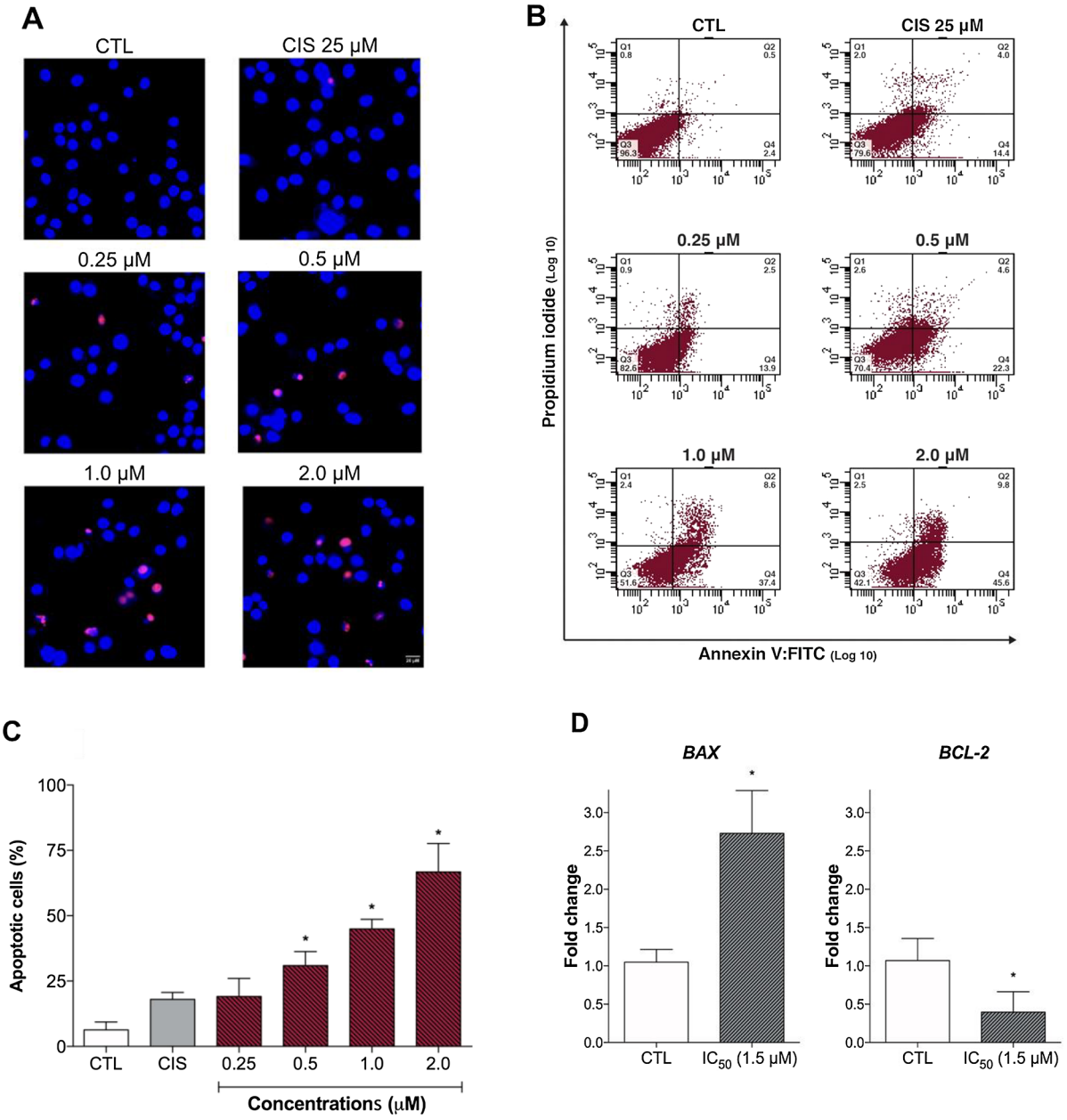


Fig. 9. Effect of the ruthenium complex (4) on the induction of apoptosis in DU-145 cells. (A) Representative images of DU-145 cells double-stained with Hoechst 33342 and PI captured with ImageXpress micro, scale bar = 20 μm. (B) Representative flow cytometry dot plots show the percent cells in the viable (Q3), early apoptotic (Q4), late apoptotic (Q2) and necrotic (Q1) stages as determined by flow cytometry using annexin V-FITC/PI staining. (C) Quantification of apoptotic DU-145 cells. (D) Relative expression of the genes *BAX* and *BCL-2* in DU-145 cells treated with complex (4) for 24 h. *ACTB* was used as reference gene for normalization. The negative control (CTL) was treated with the vehicle (0.1% DMSO) used for diluting the tested compound and cisplatin (CIS, 25 μM) was used as drug control. Data are presented as the means ± S.E.M. of three independent experiments performed in triplicate. Ten thousand events were evaluated per experiment, and cellular debris was omitted from the analysis. *$p < 0.05$ compared with the control by ANOVA followed by Dunnet's test.

of the complex (**4**) in DU-145 cells. Thus, our results demonstrated that complex (**4**) induced cell death by up-regulation of *BAX* and down-regulation of *BCL-2* in DU-145 cancer cells.

2.7. Scavenging intracellular ROS abolishes the cytotoxic effects of the complex (4)

It has been reported that ROS play an important role in cancer cell death and apoptosis. This activity is widely induced by several chemotherapeutic drugs to kill the cancer cells [64]. To investigate whether ROS production is underlying the cytotoxic activities of the complex (**4**), we used the Cellular ROS/Superoxide Detection Assay (ab139476) to detect the production of reactive species of oxygen and nitrogen (ROS/RNS) in DU-145 cells. Previously, the total ROS levels were assessed after a 1, 6, 12 and 24 h of incubation with the complex (**4**) using 2′,7′-dichlorodihydrofluorescein diacetate (H_2DCFDA) as a fluorescent dye to determine which time would be more appropriate for a ROS/Superoxide analysis.

As shown in Fig. 10A, upon treatment of DU-145 cells for different times with a single dose of the complex (**4**) (IC_{50}), a higher increase of ROS generation was observed at 24 h of exposure. Due to this result, the ROS/Superoxide production was assessed after 24 h of treatment with

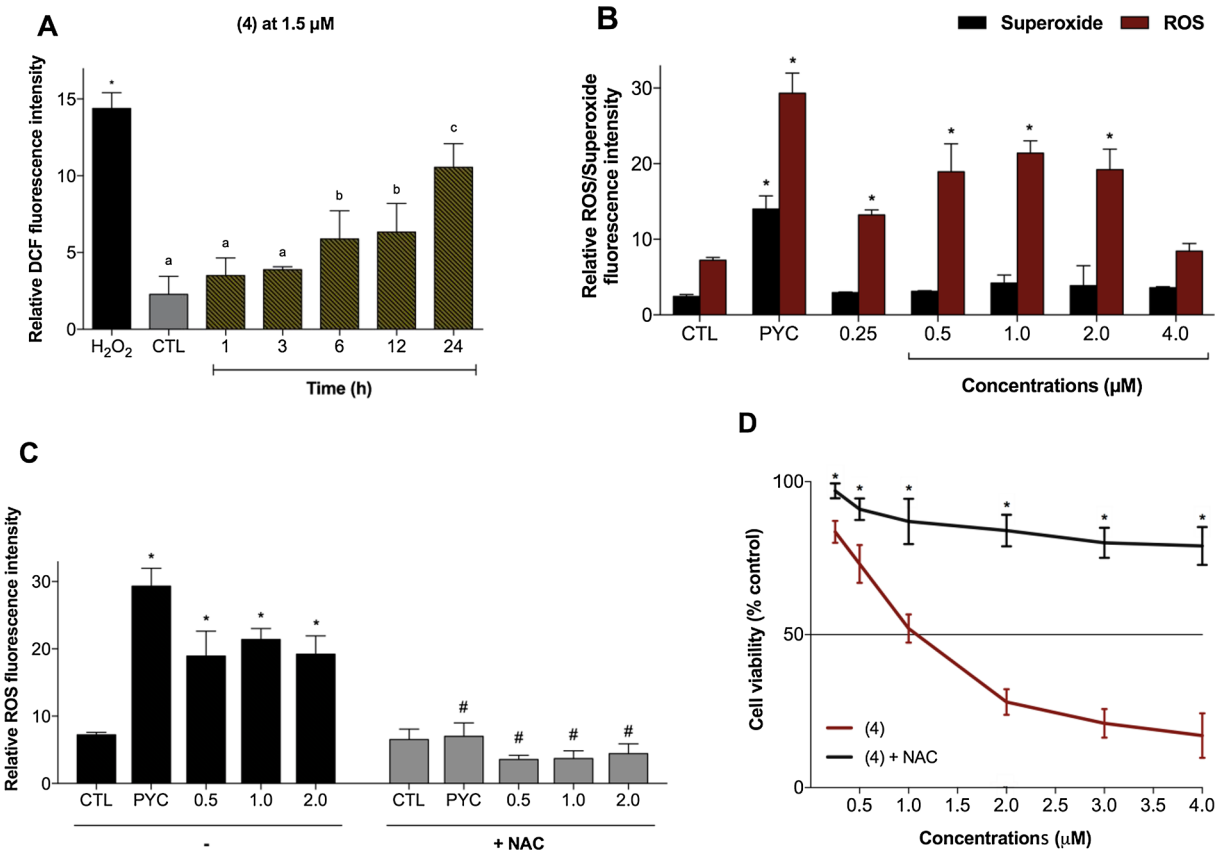


Fig. 10. Effect of the ruthenium complex (4) in the levels of reactive oxygen species (ROS) of DU-145 cells and protection by NAC. (A) ROS levels of DU-145 cells after 1, 3, 6, 12 and 24 h of incubation with complex (4) at IC_{50} (1.5 µM). (B) Assessment of total intracellular ROS/Superoxide levels 24 h after incubation with different concentrations of (4). (C) ROS levels of DU-145 cells after 24 h treatment with complex (4) at 0.5, 1 and 2 µM with or without the antioxidant NAC (5 mM). (D) Cell viability of DU-145 cells assessed by Alamar Blue assay after 24 h incubation with different concentrations of (4) with or without the antioxidant NAC (5 mM). The negative control (CTL) was treated with the vehicle (0.1% DMSO) used for diluting the tested compounds. Hydrogen peroxide (H_2O_2, 200 µM) and pyocyanin (PYC, 250 µM) were used as the positive controls. Data are presented as the mean ± S.E.M. of three independent experiments performed in triplicate or quadruplicate. $^{*}p < 0.05$ compared with the control by ANOVA followed Dunnet's test. # $p < 0.05$ compared with the respective treatment without NAC by ANOVA followed Dunnet's test. Values not sharing the same letter are significantly different from each other ($p < 0.05$; ANOVA followed by the Tukey's test).

different concentrations of the complex (**4**). After the complex (**4**) treatment, DU-145 cells exhibited an increase of reactive species, yielding a fluorescent product indicative of cellular production of different ROS/RNS types (Fig. 10B). Moreover, at 4 µM was observed a decrease of ROS/RNS levels, probably because increasing concentrations promotes cell death. These results indicate that complex (**4**) can enhance intracellular oxidative stress suggesting that apoptosis may be the principal mechanism of cell death triggered by ROS. This effect can be guaranteed by the use of lawsone that has a mechanism of action closely related with their electron accepting capability producing semiquinone radicals that can induce ROS production in the intracellular environment [65]. On the other hand, the production of superoxide did not appear in any treatment of the complex (**4**), except in inducer control (pyocyanin).

Besides, to verify whether or not ROS/RNS generation increase is related to the complex (**4**)-induced cytotoxicity, the cells were treated with the ROS-scavenger *N*-acetyl-L-cysteine (NAC), an antioxidant that has been demonstrated to present cytoprotective effects against ROS-induced cell death [66]. The results displayed that co-treatment with NAC suppressed the generation of intracellular ROS induced by complex (**4**) (Fig. 10C) and prevented the reduction of cell viability, as assessed by Alamar Blue assay (Fig. 10D). These findings suggest that the complex (**4**) played an essential role in inducing apoptosis, just as other naphthoquinones derivatives compounds do [67], by induced increasing oxidative stress, which was prevented by co-treatment with NAC.

3. Conclusions

In this paper, novel lawsone-containing ruthenium(II) complexes were synthesized and assessed for its cellular response in human prostate carcinoma DU-145 cells in 2D and 3D culture systems for the first time. As discussed, other studies have shown that ruthenium complexes have been extensively reported as anticancer candidates *in vitro* and *in vivo* [6,68,69]. Herein we proposed lawsone as a bioactive natural compound that forms ruthenium complexes with potent cytotoxic activity in cancer cells. Overall, the phosphine complexes studied in this work showed promising values of IC_{50} against DU-145 prostate cancer cells. Complexes (**3**) and (**4**) displayed more potent cytotoxicity than metal-free lawsone against different cancer cell lines and can decrease the survival of DU-145 cells at lower concentrations better than cisplatin. Several studies shown the addition of phosphine ligand increase the lipophilicity of the complex, which in turn enhances the cytotoxic effect against several cancer cell lines [70–73]. This effect is related with the enhanced lipophilicity which considerably affecting the uptake by tumor cells and proteins binding [41,74]. Our ruthenium complexes, especially the complex (**4**), exhibited considerable cytotoxic effects against 3D multicellular DU-145 spheroids that simulate the prostate tumor microenvironment. The compound also exhibited cytotoxic potency over 18-fold orders of magnitude higher than cisplatin in monolayers of DU-145 cancer cells and for 3D multicellular DU-145 tumor spheroids. Even under a low non-cytotoxic concentration of 0.125–0.5 µM, (**4**) was able to effectively inhibit the cell adhesion and

migration of DU-145 cells indicating antimetastatic potential *in vitro*. Taken together, all the complexes (**1–4**) showed an effective DNA interactive abilities via DNA minor groove intercalation, which can be considered very valuable taking into account the importance of the history and development of DNA intercalators as anticancer agents. Additionally, complex (**4**) induced DU-145 cell apoptosis through elevated intracellular ROS levels. Moreover, we also showed that ROS scavenger NAC reduced cytotoxicity induced by ROS production caused by the complex (**4**). In summary, this study describes a series of newly synthesized phosphine/diimine ruthenium complexes containing the 1,4-naphthoquinone that have been identified as a potent antiproliferative and antimetastatic agents towards DU-145 cells. By our data, we suggest the coordination with naphthoquinone bioligand enhance ROS-induced apoptotic cell death via upregulation of *BAX/BCL-2* ratio. Therefore, the 1,4-naphthoquinone-containing ruthenium complexes showed a promising anticancer activity better than cisplatin toward prostate cancer cells, target the intracellular oxidative stress.

4. Experimental

4.1. Materials

4.1.1. Chemical and equipments

All chemicals used to prepare the ruthenium complexes were of analytical grade or chemically pure grade. The synthesis of the complexes were carried under argon atmosphere. The $RuCl_3{\cdot}3H_2O$ (CAS 13815-94-6), KPF_6 (CAS 17084-13-8), triphenylphosphine (PPh_3, CAS 603-35-0), *bis*(diphenylphosphino)methane (dppm, CAS 2071-20-7), N-N = 2,2′-bipyridine (bipy, CAS 366-18-7), 1,10-phenanthroline (phen, CAS 66-71-7), resazurin sodium salt (CAS 62758-13-8), calf-thymus DNA (CT-DNA, CAS 73049-39-5), dimethylsulfoxide (DMSO, CAS 67-68-5), dimethylformamide (DMF, CAS 68-12-2), methanol (CAS 67-56-1), acetic acid (CAS 64-19-7), Triton™ X-100 (CAS 9002-93-1), 2′,7′-dichlorofluorescein diacetate (H_2DCFDA; CAS 4091-99-0), hydrogen peroxide solution 30% (w/w) (H_2O_2; CAS 7722-84-1) agarose (CAS 9012-36- 6), collagen (CAS 9007-34-5), trypan blue (CAS 72-57-1), crystal violet (CAS 548-62-9), *N*-acetyl-L-cysteine (NAC, CAS 616-91-1) and pBR322 plasmid DNA from *E. coli* (CAS 93384-17-9) were obtained from Sigma-Aldrich® MERCK (St. Louis, MO, USA). Fetal bovine serum (FBS), Dulbecco's Modified Eagle's Medium (DMEM), Roswell Park Memorial Institute Medium (RPMI 1640), trypsin-EDTA 5X, accutase, L-glutamine, antibiotic-antimycotic mix 100X, Hoechst 33342 (CAS 23491-52-3) and propidium iodide (PI; CAS 25535-16-4) were acquired from Gibco-Invitrogen® Thermo Fisher Scientific (Waltham, MA, USA). Matrigel® matrix was obtained from Corning (New York, NY, USA). Fauldcispla® (cisplatin) and Fauldoxo® (doxorubicin hydrochloride) were purchased from Libbs Pharmaceutical Ltda. (São Paulo, SP, Brazil). All the other chemicals were of analytical grade.

Elemental analyses (C, H, and N) were performed using a FISIONS CHNS, model EA 1108 Thermo Fisher Scientific (Waltham, MA, USA) equipment. The IR spectra were recorded on an FT-IR Bomem-Michelson 102 spectrometer in the 4000–250 cm^{-1} region using KBr pellets. Conductivity measures were obtained in a Meter Lab CDM2300 using 10^{-3} M solutions of the complexes in CH_2Cl_2, at room temperature. All the NMR experiments were recorded on a Bruker DRX 400 MHz using tetramethylsilane as reference and DMSO-d_6 to solubilize the complexes. UV–visible (UV–vis) was recorded on a Hewlett Packard diode array − 8452A spectrophotometer. Fluorescence spectra were performed using a Synergy H1 Fluorescence Spectrophotometer (BioTek®). The electrochemical experiments were carried using a BAS, model 100B at room temperature in CH_2Cl_2 containing 0.10 M tetrabutylammonium perchlorate (TBAP) (Fluka Purum®) as a supporting electrolyte. The working and auxiliary electrodes were stationary Pt foils, and the reference electrode was Ag/AgCl, 0.10 M TBAP in CH_2Cl_2, in a Luggin capillary probe.

4.1.2. Cell lines and culture conditions

Human lung carcinoma (A549, ATCC® CCL-185™), human prostate carcinoma (DU-145, ATCC® HTB-81™), human hepatocellular carcinoma (HepG2, ATCC® HB-8065™), human prostate adenocarcinoma (PC-3, ATCC® CRL-1435™), human breast adenocarcinoma (MDA-MB-231, ATCC® HTB-26™) and human umbilical vein endothelial cells (HUVEC, ATCC® CRL-1730™) were obtained from American Type Cell Collection (ATCC). Human colorectal adenocarcinoma (Caco-2, BCRJ 0059) and human gingival normal fibroblasts (FGH BCRJ 0089) were obtained from Rio de Janeiro Cells Bank (BCRJ). The cells A549, Caco-2, DU-145, HepG2, MDA-MB-231, and FGH, were cultured in Dulbecco's Modified Eagle's Medium (DMEM), PC-3 and HUVEC cells were grown in Roswell Park Memorial Institute Medium (RPMI 1640). Both mediums were supplemented according to the needs of each lineage, as recommended by its cell banks with 2 mM L-glutamine, 10% or 20% FBS, 1% antibiotic–antimycotic solution (5 mg/mL penicillin, 5 mg/mL streptomycin, and 10 mg/mL neomycin), 4.5 g/L of glucose and 3.7 g/L of $NaHCO_3$. All cell lines were cultured in flasks at 37 °C in 5% CO_2 and 96% of relative humidity according to the procedures proposed by [75]. The experiments were conducted between the third and the eight-cell passage with sub-cultures every 3–4 days to maintain exponential growth. The cell viability was examined using the trypan blue exclusion assay for all experiments where over 90% of the cells were viable at the beginning of the culture.

4.2. Methods

4.2.1. Synthesis and characterization of the ruthenium complexes

4.2.1.1. [Ru(law)(N-N)$_2$]PF$_6$. The complexes [Ru(law)(N-N)$_2$]PF_6 where N-N = bipy or phen were obtained from the reaction between the complex precursor *cis*-[$RuCl_2$(N-N)$_2$] prepared how described by [76] and the ligand lawsone (law). The ligand law (0.054 g; 0.31 mmol) was added to the solution of ethanol and water (2:1 v/v) (30 mL) with the complex precursor (0.21 mmol), 80 μL of triethylamine and KPF_6 (0.076 g; 0.41 mmol). The mixture was maintained in argon atmosphere and reflux for 12 h. The dark solution was concentrated to ca. 5 mL and the solid formed was filtered, washed with distilled water and ethyl ether and dried under vacuum.

[Ru(law)(bipy)$_2$]PF_6 (**1**): Yield: 0.113 g (75%). Anal. Calc. For $C_{30}H_{21}F_6N_4O_3PRu$ exp. (calc.) C, 49.03 (49.25); H, 3.29 (2.89); N, 7.73 (7.66) %. Λ_M = 49.81 Ω^{-1} cm^2 mol^{-1}, in 1.0 mM CH_2Cl_2 solution. IR (Selected bands, cm^{-1}): ν(C_1=O) 1590, ν(C_4=O) 1609, ν(C_2–O) 1027; ^{1}H NMR (400 MHz, DMSO-d_6, 25 °C): δ(ppm): 10.3–7.3 (m, 20H, an overlap of aromatic protons of bipy (16H) and Law (4H), 5.7 (s, 1H, Law); ^{13}C NMR (400 MHz, DMSO-d_6, 25 °C): δ(ppm) 196.9 (C_1=O), 182.7 (C_4=O) and 172.7 (C_2–O).

[Ru(law)(phen)$_2$]PF_6 (**2**): Yield: 0.102 g (70%). Anal. Calc. For $C_{34}H_{21}F_6N_4O_3PRu$ exp. (calc.) C, 52.09 (52.38); H, 2.81 (2.72); N, 6.93 (7.19) %. Λ_M = 44.74 Ω^{-1} cm^2 mol^{-1}, in 1.0 mM CH_2Cl_2 solution. IR (Selected bands, cm^{-1}): ν(C_1=O) 1593, ν(C_4=O) 1612, ν(C_2–O) 1098; ^{1}H NMR (400 MHz, DMSO-d_6, 25 °C): δ(ppm): 10.8–7.4 (m, 20H, an overlap of aromatic protons of phen (16H) and Law (4H), 5.6 (s, 1H, Law); ^{13}C NMR (400 MHz, DMSO-d_6, 25 °C): δ(ppm) 197.3 (C_1=O), 182.5 (C_4=O) and 172.9 (C_2–O).

4.2.1.2. [Ru(law)(dppm)(N-N)]PF$_6$. Firstly, the precursor complexes *cis*-[$RuCl_2$(dppm)(bipy)] and *cis*-[$RuCl_2$(dppm)(phen)] were obtained from the reaction of the *cis,trans*-[$RuCl_2(PPh_3)_2$(N-N)], where N-N = bipy or phen [77] (0.12 mmol) with the dppm (0.14 mmol) in 50 mL of toluene. The reaction was kept in reflux under argon atmosphere for 48 h. The red solid formed was filtered, washed with ethyl ether and dried under vacuum.

The complexes [Ru(law)(dppm)(N-N)]PF_6, where N-N = bipy or phen were obtained from the precursor *cis*-[$RuCl_2$(dppm)(N-N)]. For this, the ligand law (0.04 g; 0.22 mol) was added to the solution of *cis*-[$RuCl_2$(dppm)(N-N)] (0.14 mmol) in 30 mL of CH_2Cl_2:CH_3OH (1:1, v/

v). 80 μL of triethylamine and KPF_6 (0.28 mmol) were added and the reaction kept in reflux under argon atmosphere for 12 h. The volume was reduced to ca. 5 mL and water was added to precipitate a dark solid.

[Ru(law)(dppm)(bipy)]PF_6 (**3**): Yield: 0.129 g (82%). Anal. Calc. for $C_{45}H_{35}F_6N_2O_3P_3Ru$ exp. (calc.) C, 56.26 (56.31); H 3.85 (3.68); N 2.65 (2.92) %. Λ_M = 48.0 Ω^{-1} cm^2 mol^{-1}, in 1.0 mM CH_2Cl_2 solution. IR (Selected bands, cm^{-1}): $\nu(C_1{=}O)$ 1603, $\nu(C_4{=}O)$ 1614, $\nu(C_2{-}O)$ 1097. $^{31}P\{^1H\}$ NMR (162 MHz, CH_2Cl_2, 25 °C) δ(ppm): (d, 17.9; 6.7/15.2; 5.75/^2J = 73/68 Hz); ^1H NMR (400 MHz, DMSO-d_6, 25 °C): δ(ppm): 8.8–6.7 (m, 32H, an overlap of aromatic protons of phenyl groups of dppm (20H), bipy (8H) and Law (4H), 5.8 (s, 1H, Law), 5.4 (m, 2H, chain aliphatic of dppm); ^{13}C NMR (400 MHz, DMSO-d_6, 25 °C): δ(ppm) 200.2/196.8 ($C_1{=}O$), 182.4/181.9 ($C_4{=}O$) and 172.4/171.2 ($C_2{-}O$).

[Ru(law)(dppm)(phen)]PF_6 (**4**): Yield: 0.104 g (78%). Anal. Calc. for $C_{47}H_{35}F_6N_2O_3P_3Ru$ exp. (calc.) C, 57.67 (57.38); H, 3.71 (3.59); N, 2.48 (2.85) %. Λ_M = 50.3 Ω^{-1} cm^2 mol^{-1}, in 1.0 mM CH_2Cl_2 solution. IR (Selected bands, cm^{-1}): $\nu(C_1{=}O)$ 1599, $\nu(C_4{=}O)$ 1614, $\nu(C_2{-}O)$ 1101. $^{31}P\{^1H\}$ NMR (162 MHz, CH_2Cl_2, 25 °C) δ(ppm): (d, 18.2; 6.6/15.4; 6.2/^2J = 74/68 Hz); ^1H NMR (400 MHz, DMSO-d_6, 25 °C): δ(ppm): 9.2–6.3 (m, 32H, an overlap of aromatic protons of phenyl groups of dppm (20H), phen (8H) and Law (4H), 5.8 (s, 1H, Law), 5.5 (m, 2H, chain aliphatic of dppm); ^{13}C NMR (400 MHz, DMSO-d_6, 25 °C): δ(ppm) 200.3/196.8 ($C_1{=}O$), 182.5/181.9 ($C_4{=}O$) and 172.6/171.4 ($C_2{-}O$).

4.2.2. Partition coefficient (n-octanol/water) determination

The octanol-water partition coefficient (log *P*) were determined using the shake-flask method [78]. Each complex was tested in a mixture of equal volumes of water and *n*-octanol with continuous shaking for 24 h at 112*g* and 37 °C. Then the samples were centrifuged for 5 min at 10*g*, and the organic and aqueous phases were separated. The concentration of drug in each phase was measured spectrophotometrically to determine values of log *P* = [compound] (in *n*-octanol)/[compound] (in water). The experiments were carried out in triplicate.

4.2.3. Cytotoxicity activity assay

The *in vitro* antiproliferative activity was quantified using the Alamar Blue assay, according to the method reported by [79]. Cells were inserted in 96-well plates for all experiments (1.5 × 10^4 cells/well). After 24 h, the complexes were dissolved in DMSO and added to each well and incubated for 24 h. Dilutions of the complexes were prepared to obtain concentrations ranging from 0.3 to 100 μM. Cisplatin (Fauldcispla®) and doxorubicin hydrochloride (Fauldoxo®) were used as the reference cytotoxic drugs. DMSO (0.1% (v/v)) was used as the vehicle control. Following 24 h of incubation, 50 μL of Alamar Blue (resazurin at 0.01% w/v) was added to each well, and the plates were incubated for 2 h, at 37 °C, in the dark. The fluorescence reading was performed in a CaryEclipse Fluorescence Spectrophotometer (Agilent Technologies, Santa Clara, CA, USA) reader using excitation and emission filters at wavelengths of 560 and 590 nm, respectively. The potency of cell growth inhibition for each complex was expressed as half-maximal (50%) inhibitory concentration (IC_{50}).

4.2.4. Clonogenic assay

The clonogenic assay was performed in accordance by the guidelines of [43]. The DU-145 cells (1 × 10^6 cells/well) were inserted in 6-well plate and treated with different concentrations varying of 0.125 to 1 μM of the complexes and cisplatin for 24 h. Negative control received the vehicle (DMSO 0.1% (v/v)) that was used for diluting the compounds tested. At the end of the treatments, the cells were washed with PBS and harvested by trypsinization. The cells were counted using a Neubauer chamber and re-plated then on Nunclon® cell culture dishes of 21.5 cm^2 in a density of two hundred cells per culture dish for each treatment in triplicate. After 7 days cells were washed with PBS and fixed in ice-cold methanol: acetic acid: distilled water (1:1:8) for 20 min, air-dried and stained with crystal violet (0.5% (w/v)) in PBS for 20 min. Colonies with at least 50 cells were counted. The plating efficiency (PE) of DU-145 cells was calculated by the ratio of the number of colonies observed after 7 days of incubation to the number of cells seeded (two hundred). The average of colonies in control was regarded as 100% and the number of colonies that arise after treatment of cells, expressed regarding PE, is called the surviving fraction (SF), obtained by:

$$SF = \frac{Number\ of\ colonies\ counted\ in\ eacht\ treatment}{Number\ of\ colonies\ counted\ in\ control\ x\ PE} \times 100$$

4.2.5. 3D multicellular tumor spheroids culture

The multicellular tumor spheroids (MCTS) were obtained according to the method reported by [80]. Briefly, 200 μL of a solution of DU-145 cells (2.0 × 10^3 cells/well) were inserted in agarose-coated 96-well plates (1.5% (w/v)) and cultured in complete medium plus 3% Matrigel®. DU-145-MCTS with stable structures had formed after five days. Then, the spheroids were exposed to the complexes in a range of five different concentrations varying from 1 to 10 μM and incubated for 24 h. Cisplatin (Fauldcispla®) at 25 μM was used as the reference cytotoxic drug. Negative control received the vehicle (DMSO 0.1% v/v) that was used for diluting the compounds tested. At the end of the experiment, the cell viability was determined by Alamar Blue assay as described above. To investigate the morphological changes after treatment, other MCTSs were examined for 12 days by light microscopy (Inverted Trinocular Microscope Opton TNB-O5T-PL) using AxioVision LE software (Carl Zeiss, Jena, Germany).

4.2.6. Wound healing migration assay

DU-145 cells were seeded at a density of 1 × 10^5 cells per well in 12-well plates and grown for 48 h in 5% CO_2 in a humidified atmosphere at 37 °C in serum-free media. Once confluent, a "wound" was created across the cell monolayer using a sterile pipette. The culture medium containing cells in suspension was removed and replaced with new media containing different concentrations of the complex (**4**). Negative control received the vehicle (DMSO 0.1% (v/v)) that was used for diluting the compounds tested. Images of each wound were recorded using an inverted trinocular microscope (Opton TNB-O5T-PL) coupled to a camera (AxioVision) with amplification of 10×, at different times (0–24 h). The wound closure was analyzed by the recorded images using Image J software.

4.2.7. Cell adhesion

DU-145 cells were seeded at a density of 1.5 × 10^4 cells per well in the presence or absence of different concentrations of the complex (**4**) in pre-coated 96-well plates with either 15 μg/mL collagen or Matrigel® 150 μg/mL and left for 24 h at 5% CO_2 in a humidified atmosphere to adhere. Negative control received the vehicle (DMSO 0.1% (v/v)) that was used for diluting the compounds tested and, cell-free coated wells acted as blank controls. Following adhesion, cells were washed 3x with PBS and fixed with 100 μL methanol at −20 °C for 5 min. Once removed, cells were stained for 15 min with crystal violet (0.1% (w/v)) after which they were rinsed with tap water. Following 10 min air-drying, 50 μL of 0.5% Triton™ X-100 was added to wells and left 2 h at room temperature with gentle agitation. Finally, the absorbance was measured in a spectrophotometer (Biotek Elx800–Winooski, VT, USA) set at 590 nm.

4.2.8. DNA interactions assays

The CT-DNA solution was prepared by dilution of 2 mg of the CT-DNA in 1 mL of Tris-HCl buffer (4.5 mM Tris-HCl, 0.5 mM Tris-base, 50 mM NaCl, pH 7.4), and the concentration was determined by absorption spectrophotometric using the molar absorption coefficient 6600 mol^{-1} dm^3 cm^{-1} at 260 nm [81].

4.2.8.1. Interaction with CT-DNA (Calf Thymus) by circular dichroism (CD). The interaction of the ruthenium complexes (**1**–**4**) with CT-DNA by CD was investigated using a spectropolarimeter JASCO J720 from 240 to 350 nm at 298 K, in a continuous scanning mode (200 nm min^{-1}), under constant nitrogen flush. The complexes were incubated with CT-DNA (50 μM) at 37 °C for 18 h in Tris-HCl buffer containing 10% of DMSO for solubilization of the complexes, in molar ratios ([complex]/[DNA]) ranging from 0.1 to 0.5.

4.2.8.2. pBR322 plasmid. Plasmid pBR322 (38 μM) was mixed with different concentrations (4.84–38 μM) of ruthenium complexes and incubated at 37 °C for 18 h. Then the loading buffer was added and the samples and analyzed by agarose gel electrophoresis for 90 min in 1% agarose gel using a Tris-acetate-EDTA (TAE) buffer (0.45 M Tris-HCl, 0.45 M acetic acid, 10 mM EDTA, pH 7.4) and employing ethidium bromide for staining. The bands were visualized with a ChemiDoc MP imager (BioRad Laboratories, Hercules, CA, USA).

4.2.8.3. Competitive displacement with Hoechst 33258 by fluorescence. The competitive displacement assay was carried out using as probe the Hoechst 33258 by the fluorescence quenching experiment [57]. Thus, the CT-DNA (125 μM) was incubated with Hoechst (2.7 μM), and the extinction of the fluorescence intensity was monitored by the addition of different concentrations of ruthenium complexes in Tris-HCl containing 10% of DMSO. The fluorescence emission spectra were recorded from 300 to 500 nm after excitation wavelength of 343 nm, using an opaque 96-well plate, in a Synergy/H1-Biotek fluorimeter, at 37 °C.

4.2.9. Apoptosis analyses

The measurement of cell death was performed by the guidelines of [82]. Previously, the nuclear morphology of DU-145 cells was assessed by Hoechst-propidium iodide (PI) dual-staining assay. Briefly, the cells were seeded (5×10^3 cells/well) into black 96-well plates and maintained to attach at 37 °C in 5% CO_2. After 24 h, the cells were treated with complex (**4**) (0.25, 0.50, 1.0 and 2.0 μM) for 24 h. Negative control received the vehicle (DMSO 0.1% (v/v)) and, positive controls received cisplatin (25 μM) and doxorubicin (5 μM). The cells were incubated with Hoechst 33342 (10 μM) and PI (10 μM) diluted in PBS for 10 min at room temperature. The cells were then observed by ImageXpress Micro XLS system (Molecular Devices, CA, USA). The detection of apoptotic/necrotic cells was determined by flow cytometry using the Alexa Fluor® 488 Annexin V/PI (Molecular Probes™) and the analysis were performed according to the manufacturer's instructions. Briefly, DU-145 cells were seeded (5.5×10^4 cells/well) in 12-well plates and maintained to attach at 37 °C in 5% CO_2. After 24 h, the cells were treated as described above. Then, the cells were collected with accutase, washed with PBS and resuspended in 200 μL of cold annexin-binding buffer. Next, it was added 10 μL of Alexa Fluor® 488 Annexin V (50 μL/mL) staining buffer, and the mixture was incubated in the dark at 4 °C for 15 min. Previously the analyses, 100 μL of PI (2 μg/mL) was added, and then, the fluorescence was measured by flow cytometry in a FACSCanto flow cytometer (Becton Dickison, Franklin Lakes, NJ, USA) using the Diva software. Ten thousand events were evaluated per experiment, and cellular debris was omitted from the analysis.

4.2.10. Gene expression analysis by qPCR array

DU-145 cells were plated in bottles tissue culture ($1x10^5$ cells/mL). After 24 h of incubation with complex (**4**) at IC_{50}, total RNA was isolated from the cells using the RNeasy Plus mini kit (Qiagen, Hilden, Germany) according to the manufacturer's instructions. Total RNA was quantified using a spectrophotometer at an absorbance of 260 nm in NanoDrop ND-2000 (Thermo-Fisher Scientific, USA) and the quality of each RNA sample was verified by gel electrophoresis in a Bioanalyzer (Agilent Inc). RNA purity was calculated from the ratio of absorbance $A_{260/280}$ and the integrity by RIN (RNA Integrity Number). Complementary DNA (cDNA) strands were synthesized using the RT^2 First Strand kit (Qiagen, Germany), following the manufacturer's instructions. Quantitative PCR was carried out with the Power SYBR® Green Master Mix in a Step One Plus system (Applied Biosystems, Carlsbad, CA, USA), using KiCqStart® SYBR® Green Primers predesigned for gene expression for mRNA analysis (Sigma-Aldrich), as follows: H_ACTB_1 (NM_001101), H_BAX_1 (NM_004324) and H_BCL2_1 (NM_000633). Quantification of relative fold change of each gene was calculated by $2^{\Delta\Delta Ct}$ method [83] using the reference gene *ACTB* (actin beta) for normalization. All experiments were performed in triplicate in DNase/RNase free conditions.

4.2.11. Detection of intracellular ROS and RNS

The total intracellular ROS generation was measured using H2DCFDA, as reported by [84]. Briefly, DU-145 cells were seeded (1.5×10^4 cells/well) into black 96-well plates and maintained to attach at 37 °C in 5% CO_2. After 24 h, the cells were treated with 1.5 μM (IC_{50}) of the complex (**4**) for 1, 6, 12 and 24 h. After that, the cells were labeled with H2DCFDA solution at 5 μM in DMF. After that, the fluorescence intensity was measured in a Synergy H1 Fluorescence Spectrophotometer (BioTek®), at the excitation and emission wavelengths of 495 and 527 nm, respectively. After that, the ROS/RNS levels were measured using Cellular ROS/Superoxide Detection Assay Kit (Abcam). The cells were seeded (1.5×10^4 cells/well) into black 96-well plates and maintained to attach at 37 °C in 5% CO_2. After 24 h, the cells were treated with complex (**4**) (0.25, 0.50, 1.0 and 2.0 μM) for 24 h. Negative control received the vehicle (DMSO 0.1% v/v), and positive control received pyocyanin (250 μM) as ROS inducer. Following this, the cells were labeled with Oxidative Stress Detection Reagent (Green) for ROS detection and Superoxide Detection Reagent (Orange) according to the manufacturer's instruction. Fluorescence was then measured in quadruplicates using a fluorescent microplate reader Synergy H1 (BioTek®) with standard fluorescein (Ex = 488 nm, Em = 520 nm) and rhodamine (Ex = 550 nm, Em = 610 nm) filter sets for ROS and superoxide determination, respectively.

The protection assays using the antioxidant NAC were also performed. In brief, the cells were treated with 5 mM NAC in association with complex (**4**) (0.25, 0.50, 1.0 and 2.0 μM) for 24 h. The cells were then labeled with H2DCFDA solution, and the ROS levels were measured as described above. In a new set of experiments, the cells were treated with 5 mM NAC in association with cytotoxic concentrations of (**4**). After 24 h of treatment, the cell viability was determined by Alamar Blue assay as described above.

4.3. Statistical analysis

Data are presented as mean ± S.E.M. or as IC_{50} values with 95% confidence intervals (CI 95%) obtained by nonlinear regression. Differences between experimental groups were compared using analysis of variance (ANOVA) followed by the Dunnet's or Tukey's test ($p < 0.05$). All statistical analyses were performed using GraphPad Prism 7 for Mac OS X (Intuitive Software for Science, San Diego, CA, USA).

Acknowledgments

The authors gratefully acknowledge the financial support from the São Paulo Research Foundation (FAPESP, Grants 2016/22429-7, 2016/16312-0 and 2018/00163-0), Coordinating Committee for Advancement of Higher Education Staff in Brazil (CAPES) and National Council for Scientific and Technological Development (CNPq). The authors also thank Mrs. Joana D'Arc Castania Darin from the Department of Clinical Analysis, Toxicology and Food Sciences at FCFRP-USP for her technical assistance.

Appendix A. Supplementary material

Supplementary data to this article can be found online at https://doi.org/10.1016/j.bioorg.2019.02.010.

References

[1] M. Frezza, S. Hindo, D. Chen, A. Davenport, S. Schmitt, D. Tomco, et al., Novel metals and metal complexes as platforms for cancer therapy, Curr. Pharm. Des. 16 (2010) 1813–1825, https://doi.org/10.2174/138161210791209009.

[2] A.M. Florea, D. Büsselberg, Cisplatin as an anti-tumor drug: cellular mechanisms of activity, drug resistance and induced side effects, Cancers (Basel) 3 (2011) 1351–1371, https://doi.org/10.3390/cancers3011351.

[3] G. Sava, S. Pacor, G. Mestroni, E. Alessio, Na[*trans*-RuCl$_4$(DMSO)Im], a metal complex of ruthenium with antimetastatic properties, Clin. Exp. Metastasis. 10 (1992) 273–280, https://doi.org/10.1007/BF00133563.

[4] C.S. Allardyce, P.J. Dyson, Metal-based drugs that break the rules, Dalt. Trans. 45 (2016) 3201–3209, https://doi.org/10.1039/C5DT03919C.

[5] J.K. Barton, E.D. Olmon, P.A. Sontz, Metal complexes for DNA-mediated charge transport, Coord. Chem. Rev. 255 (2011) 619–634.

[6] M. Pal, U. Nandi, D. Mukherjee, Detailed account on activation mechanisms of ruthenium coordination complexes and their role as antineoplastic agents, Eur. J. Med. Chem. 150 (2018) 419–445, https://doi.org/10.1016/j.ejmech.2018.03.015.

[7] S. Zorzet, A. Bergamo, M. Cocchietto, A. Sorc, B. Gava, E. Alessio, et al., Lack of *In vitro* cytotoxicity, associated to increased G(2)-M cell fraction and inhibition of matrigel invasion, may predict *In vivo*-selective antimetastasis activity of ruthenium complexes, J. Pharmacol. Exp. Ther. 295 (2000) 927–933.

[8] C.S. Allardyce, P.J. Dyson, Ruthenium in medicine: Current clinical uses and future prospects, Platin. Met. Rev. 45 (2001) 62–69.

[9] F. Lentz, A. Drescher, A. Lindauer, M. Henke, R.A. Hilger, C.G. Hartinger, et al., Pharmacokinetics of a novel anticancer ruthenium complex (KP1019, FFC14A) in a phase I dose-escalation study, Anticancer. Drugs 20 (2009) 97–103, https://doi.org/10.1097/CAD.0b013e328322fbc5.

[10] S. Leijen, S.A. Burgers, P. Baas, D. Pluim, M. Tibben, E. Van Werkhoven, et al., Phase I/II study with ruthenium compound NAMI-A and gemcitabine in patients with non-small cell lung cancer after first line therapy, Invest. New Drugs. 33 (2015) 201–214, https://doi.org/10.1007/s10637-014-0179-1.

[11] C.O. D'Sousa, J.H. Araujo, I.R.S. Baliza, R.B. Dias, F. Valverde, M.T.A. Vidal, et al., Novel piplartine-containing ruthenium complexes: synthesis, cell growth inhibition, apoptosis induction and ROS production on HCT116 cells, Oncotarget 8 (2017) 104367–104392, https://doi.org/10.18632/oncotarget.22248.

[12] H. Chen, J.A. Parkinson, S. Parsons, R.A. Coxall, R.O. Gould, P.J. Sadler, Organometallic ruthenium(II) diamine anticancer complexes: Arene-nucleobase stacking and stereospecific hydrogen-bonding in guanine adducts, J. Am. Chem. Soc. 124 (2002) 3064–3082, https://doi.org/10.1021/ja017482e.

[13] R.A. De Grandis, F.A. Resende, M.M. Da Silva, F.R. Pavan, A.A. Batista, E.A. Varanda, *In vitro* evaluation of cyto-genotoxic potential of ruthenium(II) SCAR complexes: a promissing class of antituberculosis agents, Mutat. Res. Genet. Toxicol. Environ. Mutagen. 798 (2016) 11–18, https://doi.org/10.1016/j.actamat.2015.02.029.

[14] C. Tan, S. Hu, J. Liu, L. Ji, Synthesis, characterization, antiproliferative and anti-metastatic properties of two ruthenium-DMSO complexes containing 2,2′-biimidazole, Eur. J. Med. Chem. 46 (2011) 1555–1563, https://doi.org/10.1016/j.ejmech.2011.01.074.

[15] V.R. Silva, R.S. Corrêa, L.D.S. Santos, M.B.P. Soares, A.A. Batista, D.P. Bezerra, A ruthenium-based 5-fluorouracil complex with enhanced cytotoxicity and apoptosis induction action in HCT116 cells, Sci. Rep. 8 (2018) 1–13, https://doi.org/10.1038/s41598-017-18639-6.

[16] C. Avendaño, J.C. Menéndez, Medicinal Chemistry of Anticancer Drugs, Elsevier Science, 2008. http://doi.org/10.1016/B978-0-444-52824-7.00001-9.

[17] A.K. McClendon, N. Osheroff, DNA topoisomerase II, genotoxicity, and cancer, Mutat. Res. Fundam. Mol. Mech. Mutagen. 623 (2007) 83–97, https://doi.org/10.1016/j.mrfmmm.2007.06.009.

[18] J.S. Novais, C.S. Moreira, A.C.J.A. Silva, R.S. Loureiro, A.M. Sá Figueiredo, V.F. Ferreira, et al., Antibacterial naphthoquinone derivatives targeting resistant strain Gram-negative bacteria in biofilms, Microb. Pathog. 118 (2018) 105–114, https://doi.org/10.1016/j.micpath.2018.03.024.

[19] G.C. Brandão, F.C. Rocha Missias, L.M. Arantes, L.F. Soares, K.K. Roy, R.J. Doerksen, et al., Antimalarial naphthoquinones. Synthesis via click chemistry, *in vitro* activity, docking to PfDHODH and SAR of lapachol-based compounds, Eur. J. Med. Chem. 145 (2018) 191–205, https://doi.org/10.1016/j.ejmech.2017.12.051.

[20] E.C.B. Da Costa, R. Amorim, F.C. Da Silva, D.R. Rocha, M.P. Papa, L.B. De Arruda, et al., Synthetic 1,4-pyran naphthoquinones are potent inhibitors of dengue virus replication, PLoS One 8 (2013) 1–11, https://doi.org/10.1371/journal.pone.0082504.

[21] V. Prachayasittikul, R. Pingaew, A. Worachartcheewan, C. Nantasenamat, S. Prachayasittikul, S. Ruchirawat, et al., Synthesis, anticancer activity and QSAR study of 1,4-naphthoquinone derivatives, Eur. J. Med. Chem. 84 (2014) 247–263, https://doi.org/10.1016/j.ejmech.2014.07.024.

[22] R. Verma, Anti-cancer activities of 1,4-naphthoquinones: a QSAR Study, Anticancer. Agents Med. Chem. 6 (2006) 489–499, https://doi.org/10.2174/187152006778226512.

[23] J. Benites, J.A. Valderrama, K. Bettega, R.C. Pedrosa, P.B. Calderon, J. Verrax, Biological evaluation of donor-acceptor aminonaphthoquinones as antitumor agents, Eur. J. Med. Chem. 45 (2010) 6052–6057, https://doi.org/10.1016/j.ejmech.2010.10.006.

[24] L.I. López-López, D.S. Nery-Flores, Y.S. Silva-Belmares, A. Sáenz-Galindo, Naphthoquinones: Biological properties and synthesis of lawsone and derivatives - a structured review, Vitae 21 (2014) 248–258.

[25] D.K. Singh, S. Luqman, Lawsonia inermis (L.): a perspective on anticancer potential of Mehndi/Henna, Biomed. Res. Ther. 1 (2014) 112–120, https://doi.org/10.7603/s40730-014-0018-1.

[26] E. Coelho-Cerqueira, P.A. Netz, V.P. Do Canto, A.C. Pinto, C. Follmer, Beyond topoisomerase inhibition: antitumor 1,4-naphthoquinones as potential inhibitors of human monoamine oxidase, Chem. Biol. Drug Des. 83 (2014) 401–410, https://doi.org/10.1111/cbdd.12255.

[27] S. Oramas-Royo, C. Torrejón, I. Cuadrado, R. Hernández-Molina, S. Hortelano, A. Estévez-Braun, et al., Synthesis and cytotoxic activity of metallic complexes of lawsone, Bioorganic Med. Chem. 21 (2013) 2471–2477, https://doi.org/10.1016/j.bmc.2013.03.002.

[28] K.M. Oliveira, L. Liany, R.S. Corrêa, V.M. De, M.R. Cominetti, A.A. Batista, Selective Ru (II)/lawsone complexes inhibiting tumor cell growth by apoptosis, J. Inorg. Biochem. 176 (2017) 66–76, https://doi.org/10.1016/j.jinorgbio.2017.08.019.

[29] T.A. Heinrich, G. Von Poelhsitz, R.I. Reis, E.E. Castellano, A. Neves, M. Lanznaster, et al., A new nitrosyl ruthenium complex: synthesis, chemical characterization, *in vitro* and *in vivo* antitumor activities and probable mechanism of action, Eur. J. Med. Chem. 46 (2011) 3616–3622, https://doi.org/10.1016/j.ejmech.2011.04.064.

[30] R.A. De Grandis, M.S. de Camargo, M.M. da Silva, É.O. Lopes, E.C. Padilha, F.A. Resende, et al., Human topoisomerase inhibition and DNA/BSA binding of Ru (II)–SCAR complexes as potential anticancer candidates for oral application, BioMetals 30 (2017) 321–334, https://doi.org/10.1007/s10534-017-0008-z.

[31] K.M. Oliveira, R.S. Corrêa, M.I.F. Barbosa, J. Ellena, M.R. Cominetti, A.A. Batista, Ruthenium (II)/triphenylphosphine complexes: an effective way to improve the cytotoxicity of lapachol, Polyhedron 130 (2017) 108–114, https://doi.org/10.1016/j.poly.2017.04.005.

[32] L. Colina-Vegas, J.L. Dutra, W. Villarreal, J.H. João, M.R. Cominetti, F. Pavan, et al., Ru(II)/clotrimazole/diphenylphosphine/bipyridine complexes: Interaction with DNA, BSA and biological potential against tumor cell lines and *Mycobacterium tuberculosis*, J. Inorg. Biochem. 162 (2016) 135–145, https://doi.org/10.1016/j.jinorgbio.2016.06.023.

[33] M.S. de Camargo, M.M. da Silva, R.S. Correa, S.D. Vieira, S. Castelli, I. D'Anessa, et al., Inhibition of human DNA topoisomerase IB by nonmutagenic ruthenium(II)-based compounds with antitumoral activity, Metallomics 8 (2016) 179–192, https://doi.org/10.1039/C5MT00227C.

[34] N.C. De Carvalho, S.P. Neves, R.B. Dias, L.D.F. Valverde, C.B.S. Sales, C.A.G. Rocha, et al., A novel ruthenium complex with xanthoxylin induces S-phase arrest and causes ERK1/2-mediated apoptosis in HepG2 cells through a p53-independent pathway article, Cell Death Dis. 9 (2018), https://doi.org/10.1038/s41419-017-0104-6.

[35] W.C. Pires, B.A.V. Lima, F. de Castro Pereira, A.P. Lima, F. Mello-Andrade, H.D. Silva, et al., Ru(II)/diphenylphosphine/pyridine-6-thiolate complexes induce S-180 cell apoptosis through intrinsic mitochondrial pathway involving inhibition of Bcl-2 and p53/Bax activation, Mol. Cell. Biochem. 438 (2018) 199–217, https://doi.org/10.1007/s11010-017-3129-3.

[36] E. Rutkowska, K. Pająk, K. Jóźwiak, Lipophilicity - Methods of determination and its role in medicinal chemistry, Acta Pol. Pharm. Drug Res. 70 (2013) 3–18.

[37] O. Guideline, for testing os chemicals, Partition coefficient (*n*-octanol/water): shake flask method, OECD Guidel. 107 (1995) 1–4, https://doi.org/10.1787/9789264069626-en.

[38] D.F. Segura, A.V.G. Netto, R.C.G. Frem, A.E. Mauro, P.B. Da Silva, J.A. Fernandes, et al., Synthesis and biological evaluation of ternary silver compounds bearing N, N-chelating ligands and thiourea: X-ray structure of [{Ag(bpy)(μ-tu)$_3$2](N$_O$3)2(bpy = 2,2′-bipyridine; Tu = thiourea), Polyhedron 79 (2014) 197–206, https://doi.org/10.1016/j.poly.2014.05.004.

[39] C.J. Lima, L. Rodríguez, Phosphine-gold (I) compounds as anticancer agents: general description and mechanisms of action, Anticancer. Agents Med. Chem. 11 (2011) 921–928.

[40] W. Villarreal, L. Colina-Vegas, G. Visbal, O. Corona, R.S. Corrêa, J. Ellena, et al., Copper(I)-phosphine polypyridyl complexes: synthesis, characterization, DNA/HSA binding study, and antiproliferative activity, Inorg. Chem. 56 (2017) 3781–3793, https://doi.org/10.1021/acs.inorgchem.6b02419.

[41] J.J. Liu, P. Galettis, A. Farr, L. Maharaj, H. Samarasinha, A.C. McGechan, et al., *In vitro* antitumour and hepatotoxicity profiles of Au(I) and Ag(I) bidentate pyridyl phosphine complexes and relationships to cellular uptake, J. Inorg. Biochem. 102 (2008) 303–310, https://doi.org/10.1016/j.jinorgbio.2007.09.003.

[42] L. Biancalana, S. Zacchini, N. Ferri, M.G. Lupo, G. Pampaloni, F. Marchetti, Tuning the cytotoxicity of ruthenium(II) para-cymene complexes by mono-substitution at a triphenylphosphine/phenoxydiphenylphosphine ligand, Dalt. Trans. 46 (2017) 16589–16604, https://doi.org/10.1039/C7DT03385K.

[43] N.A.P. Franken, H.M. Rodermond, J. Stap, J. Haveman, C. van Bree, Clonogenic assay of cells in vitro, Nat. Protoc. 1 (2006) 2315–2319, https://doi.org/10.1038/nprot.2006.339.

[44] L. Galluzzi, S.A. Aaronson, J. Abrams, E.S. Alnemri, D.W. Andrews, E.H. Baehrecke, et al., Guidelines for the use and interpretation of assays for monitoring cell death in higher eukaryotes, Cell Death Differ. 16 (2009) 1093–1107, https://doi.org/10.1038/cdd.2009.44.

[45] L.C. Kimlin, G. Casagrande, V.M. Virador, *In vitro* three-dimensional (3D) models in cancer research: an update, Mol. Carcinog. 52 (2013) 167–182, https://doi.org/10.1002/mc.21844.

[46] S.A. Langhans, Three-dimensional *in vitro* cell culture models in drug discovery and drug repositioning, Front. Pharmacol. 9 (2018) 1–14, https://doi.org/10.3389/fphar.2018.00006.

[47] W.N. Hait, Anticancer drug development: the grand challenges, Nat. Rev. Drug Discov. 9 (2010) 253–254, https://doi.org/10.1038/nrd3144.

[48] E.T.9.J. Doijen, W. Luyten, B. Landuyt, L. Schoofs, Three-dimensional cell culture models for anticancer drug screening: Worth the effort? J. Cell. Physiol. (2017) 2993–3003, https://doi.org/10.1002/jcp.26052.

[49] G. Mehta, A.Y. Hsiao, M. Ingram, G.D. Luker, S. Takayama, Opportunities and challenges for use of tumor spheroids as models to test drug delivery and efficacy, J. Control. Release. 164 (2012) 192–204, https://doi.org/10.1016/j.jconrel.2012.04.045.

[50] P. Parhi, S. Suklabaidya, S.K. Sahoo, Enhanced anti-metastatic and anti-tumorigenic efficacy of Berbamine loaded lipid nanoparticles *in vivo*, Sci. Rep. (2017) 1–13, https://doi.org/10.1038/s41598-017-05296-y.

[51] L.F. Magalhães, F. Mello-Andrade, W.C. Pires, H.D. Silva, P.F.F. da Silva, L.M. Macedo, et al., *cis*-[RuCl(BzCN)(bipy)(dppe)]PF_6 induces anti-angiogenesis and apoptosis by a mechanism of caspase-dependent involving DNA damage, PARP activation, and Tp53 induction in Ehrlich tumor cells, Chem. Biol. Interact. 278 (2017) 101–113, https://doi.org/10.1016/j.cbi.2017.09.013.

[52] P. Lu, V.M. Weaver, Z. Werb, The extracellular matrix: A dynamic niche in cancer progression, J. Cell Biol. 196 (2012) 395–406, https://doi.org/10.1083/jcb.201102147.

[53] A. Vacca, M. Bruno, A. Boccarelli, M. Coluccia, D. Ribatti, A. Bergamo, et al., Inhibition of endothelial cell functions and of angiogenesis by the metastasis inhibitor NAMI-A, Br. J. Cancer. 4 (2002) 993–998, https://doi.org/10.1038/sj/bjc/6600176.

[54] L. Gu, X. Li, Q. Ran, C. Kang, C. Lee, J. Shen, Antimetastatic activity of novel ruthenium (III) pyridine complexes, Cancer Med. 5 (2016) 2850–2860, https://doi.org/10.1002/cam4.826.

[55] G. Barone, A. Terenzi, A. Lauria, A.M. Almerico, J.M. Leal, N. Busto, et al., DNA-binding of nickel(II), copper(II) and zinc(II) complexes: structure-affinity relationships, Coord. Chem. Rev. 257 (2013) 2848–2862, https://doi.org/10.1016/j.ccr.2013.02.023.

[56] N. Narayanaswamy, M. Kumar, S. Das, R. Sharma, P.K. Samanta, S.K. Pati, et al., A thiazole coumarin (TC) turn-on fluorescence probe for AT-base pair detection and multipurpose applications in different biological systems, Sci. Rep. 4 (2014) 1–10, https://doi.org/10.1038/srep06476.

[57] T. Sarwar, M.A. Husain, S.U. Rehman, H.M. Ishqi, M. Tabish, Multi-spectroscopic and molecular modelling studies on the interaction of esculetin with calf thymus DNA, Mol. Biosyst. 11 (2015) 522–531, https://doi.org/10.1039/c4mb00636d.

[58] D. Hanahan, R. Weinberg, The hallmarks of cancer, Cell 100 (2000) 57–70, https://doi.org/10.1007/s00262-010-0968-0.

[59] D. Hanahan, R. Weinberg, Hallmarks of cancer: the next generation, Cell 144 (2011) 646–674, https://doi.org/10.1016/j.cell.2011.02.013.

[60] I. Vermes, C. Haanen, H. Steffens-Nakken, C. Reutelingsperger, A novel assay for apoptosis Flow cytometric detection of phosphatidylserine early apoptotic cells using fluorescein labelled expression on Annexin V, J. Immunol. Methods 184 (1995) 39–51.

[61] F. Mello-Andrade, W.L. da Costa, W.C. Pires, F.de.C. Pereira, C.G. Cardoso, R.de.S. Lino-Junior, et al., Antitumor effectiveness and mechanism of action of Ru (II)/amino acid/diphosphine complexes in the peritoneal carcinomatosis progression, Tumor Biol. 39 (2017) 1–18, https://doi.org/10.1177/1010428317695933.

[62] Z. Deng, P. Gao, L. Yu, B. Ma, Y. You, L. Chan, et al., Ruthenium complexes with phenylterpyridine derivatives target cell membrane and trigger death receptors-mediated apoptosis in cancer cells, Biomaterials 129 (2017) 111–126, https://doi.org/10.1016/j.biomaterials.2017.03.017.

[63] H. Perlman, X. Zhang, M.W. Chen, K. Walsh, R. Buttyan, An elevated *BAX/BCL-2* ratio corresponds with the onset of prostate epithelial cell apoptosis, Cell Death Differ. 6 (1999) 48–54, https://doi.org/10.1038/sj.cdd.4400453.

[64] R. Kasiappan, S. Safe, ROS-inducing agents for cancer chemotherapy, React. Oxyg. Species 1 (2016) 22–37, https://doi.org/10.20455/ros.2016.805.

[65] K.W. Wellington, Understanding cancer and the anticancer activities of naphthoquinones – a review, RSC Adv. 5 (2015) 20309–20338, https://doi.org/10.1039/C4RA13547D.

[66] M. Halasi, M. Wang, T.S. Chavan, V. Gaponenko, N. Hay, A.L. Gartel, ROS inhibitor *N* -acetyl-L-cysteine antagonizes the activity of proteasome inhibitors, Biochem. J. 454 (2013) 201–208, https://doi.org/10.1042/BJ20130282.

[67] L.O. Klotz, X. Hou, C. Jacob, 1,4-naphthoquinones: From oxidative damage to cellular and inter-cellular signaling, Molecules 19 (2014) 14902–14918, https://doi.org/10.3390/molecules190914902.

[68] A. Bergamo, G. Sava, Linking the future of anticancer metal-complexes to the therapy of tumour metastases, Chem. Soc. Rev. 44 (2015) 8818–8835, https://doi.org/10.1039/C5CS00134J.

[69] J.X. Liang, H.J. Zhong, G. Yang, K. Vellaisamy, D.L. Ma, C.H. Leung, Recent development of transition metal complexes with *in vivo* antitumor activity, J. Inorg. Biochem. 177 (2017) 276–286, https://doi.org/10.1016/j.jinorgbio.2017.06.002.

[70] W.M. Motswainyana, P.A. Ajibade, Anticancer activities of mononuclear ruthenium (II) coordination complexes, Adv. Chem. 2015 (2015) 1–21, https://doi.org/10.1155/2015/859730.

[71] A.M. Al-Majid, S. Yousuf, M.I. Choudhary, F. Nahra, S.P. Nolan, Gold-NHC complexes as potent bioactive compounds, ChemistrySelect 1 (2016) 76–80, https://doi.org/10.1002/slct.201600009.

[72] M. Porchia, F. Tisato, M. Zancato, V. Gandin, C. Marzano, *In vitro* antitumor activity of water-soluble copper(I) complexes with diimine and monodentate phosphine ligands, Arab. J. Chem. (2017), https://doi.org/10.1016/j.arabjc.2017.09.003.

[73] M. Echeverri, A. Alvarez-Valdés, F. Navas, J. Perles, I. Sánchez-Pérez, A.G. Quiroga, Using phosphine ligands with a biological role to modulate reactivity in novel platinum complexes, R. Soc. Open Sci. 5 (2018), https://doi.org/10.1098/rsos.171340.

[74] M.J. McKeage, S.J. Berners-Price, P. Galettis, R.J. Bowen, W. Brouwer, L. Ding, et al., Role of lipophilicity in determining cellular uptake and antitumour activity of gold phosphine complexes, Cancer Chemother. Pharmacol. 46 (2000) 343–350, https://doi.org/10.1007/s002800000166.

[75] A. Bal-Price, S. Coecke, Guidance on good cell culture practice (GCCP), Cell Cult Tech. (2011) 1–25, https://doi.org/10.1007/978-1-61779-077-5_1.

[76] B.P. Sullivan, D.J. Salmon, T.J. Meyer, Mixed phosphine 2,2'-bipyridine complexes of ruthenium, Inorg. Chem. 17 (1978) 3334–3341, https://doi.org/10.1021/ic50190a006.

[77] A.A. Batista, M.O. Santiago, C.L. Donnici, I.S. Moreira, P.C. Healy, S.J. Berners-Price, et al., Electrochemical and spectroscopic studies on RuCl2(PPh3)2(N)2 and RuCl2(PPh3)2(N–N) complexes (N = pyridine derivatives and N-N = phenanthroline or bipyridine derivatives). X-ray structure of RuCl2(PPh3)2(phen), Polyhedron 20 (2001) 2123–2128, https://doi.org/10.1016/S0277-5387(01)00744-6.

[78] E. Baka, J.E.A. Comer, K. Takács-Novák, Study of equilibrium solubility measurement by saturation shake-flask method using hydrochlorothiazide as model compound, J. Pharm. Biomed. Anal. 46 (2008) 335–341, https://doi.org/10.1016/j.jpba.2007.10.030.

[79] S. Page, Ruthenium compounds as anticancer agents, Educ. Chem. 26–29 (2012).

[80] J. Friedrich, C. Seidel, R. Ebner, L.A. Kunz-Schughart, Spheroid-based drug screen: considerations and practical approach, Nat. Protoc. 4 (2009) 309–324, https://doi.org/10.1038/nprot.2008.226.

[81] J. Marmur, A procedure for the isolation of deoxyribonucleic acid from micro-organisms, J. Mol. Biol. 3 (1961) IN1-218, https://doi.org/10.1016/S0022-2836(61)80047-8.

[82] B.S. Cummings, L.P. Wills, R.G. Schnellmann, Measurement of cell death in mammalian cells, Curr. Protoc. Phamacol. 1 (2004) 1–30, https://doi.org/10.1002/0471141755.ph1208s25.

[83] T.D. Schmittgen, K.J. Livak, Analyzing real-time PCR data by the comparative C(T) method, Nat. Protoc. 3 (2008) 1101–1108, https://doi.org/10.1038/nprot.2008.73.

[84] H. Wang, J.A. Joseph, Quantifying cellular oxidative stress by dichlorofluorescein assay using microplate reader, Free Radic. Biol. Med. 27 (1999) 612–616, https://doi.org/10.1016/S0891-5849(99)00107-0.

Author's personal copy

Biometals (2017) 30:321–334
DOI 10.1007/s10534-017-0008-z

Human topoisomerase inhibition and DNA/BSA binding of Ru(II)–SCAR complexes as potential anticancer candidates for oral application

Rone A. De Grandis · Mariana S. de Camargo · Monize M. da Silva · Érica O. Lopes · Elias C. Padilha · Flávia A. Resende · Rosângela G. Peccinini · Fernando R. Pavan · Alessandro Desideri · Alzir A. Batista · Eliana A. Varanda

Received: 18 January 2017 / Accepted: 7 March 2017 / Published online: 16 March 2017
© Springer Science+Business Media New York 2017

Abstract Three ruthenium(II) phosphine/diimine/picolinate complexes were selected aimed at investigating anticancer activity against several cancer cell lines and the capacity of inhibiting the supercoiled DNA relaxation mediated by human topoisomerase IB (Top 1). The structure–lipophilicity relationship in membrane permeability using the Caco-2 cells have also been evaluated in this study. **SCAR 5** was found to present 45 times more cytotoxicity against breast cancer cell when compared to cisplatin. **SCAR 4** and **5** were both found to be capable of inhibiting the supercoiled DNA relaxation mediated by Top 1. Interaction studies showed that **SCAR 4** and **5** can bind to DNA through electrostatic interactions while **SCAR 6** is able to bind covalently to DNA. The complexes **SCAR** were found to interact differently with bovine serum albumin (BSA) suggesting hydrophobic interactions with albumin. The permeability of all complexes was seen to be dependent on their lipophilicity. **SCAR 4** and **5** exhibited high membrane permeability ($P_{app} > 10 \times 10^{-6}$ cm·s^{-1}) in the presence of BSA. The complexes may pass through Caco-2 monolayer via passive diffusion mechanism and our results suggest that lipophilicity and interaction with BSA may influence the complexes permeation. In conclusion, we demonstrated that complexes have powerful pharmacological activity, with different results for each complex depending on the combination of their ligands.

R. A. De Grandis (✉) · É. O. Lopes · E. C. Padilha · R. G. Peccinini · F. R. Pavan · E. A. Varanda
School of Pharmaceutical Sciences, São Paulo State University, Araraquara 14800-903, Brazil
e-mail: degrandis.rone@usp.br

M. S. de Camargo · M. M. da Silva · A. A. Batista
Center of Exact Sciences and Technology, Federal University of São Carlos, São Carlos 13565-905, Brazil

F. A. Resende (✉)
Department of Health and Biological Sciences, University of Araraquara, Araraquara 14801-340, Brazil
e-mail: flaviabiomed@yahoo.com.br

A. Desideri
Department of Biology, University of Rome Tor Vergata, Rome 173, Italy

Biometals
https://doi.org/10.1007/s10534-018-0160-0

Determination of in vitro absorption in Caco-2 monolayers of anticancer Ru(II)-based complexes acting as dual human topoisomerase and *PARP* inhibitors

Mariana S. de Camargo · Rone A. De Grandis · Monize M. da Silva · Patricia B. da Silva · Mariana M. Santoni · Carlos E. Eismann · Amauri A. Menegário · Marcia R. Cominetti · Cleslei F. Zanelli · Fernando R. Pavan · Alzir A. Batista

Received: 4 September 2018 / Accepted: 28 November 2018
© Springer Nature B.V. 2018

Abstract Due to their unique and versatile biochemical properties, ruthenium-based compounds have emerged as promising anticancer agents. Previous studies showed that three ruthenium(II) compounds: [Ru(pySH)(bipy)(dppb)]PF_6 (**1**), [Ru(HSpym)(bipy)(dppb)]PF_6 (**2**) and Ru[(SpymMe$_2$)(bipy)(dppb)]PF_6 (**3**) presented anticancer properties higher than doxorubicin and cisplatin and acted as human topoisomerase IB (Topo I) inhibitors. Here, we focused our studies on in vitro intestinal permeability and anticancer mechanisms of these three complexes. Caco-2 permeation studies showed that **1** did not permeate the monolayer of intestinal cells, suggesting a lack of absorption on oral administration, while **2** and **3** permeated the cells after 60 and 120 min, respectively. Complexes **2** and **3** fully inhibited Topo II relaxation activity at 125 μM. In previously studies, **3** was the most potent inhibitor of Topo I, here, we concluded that it is a dual topoisomerase inhibitor. Moreover, it presented selectivity to cancer cells when evaluated by clonogenic assay. Thus, **3** was selected to gene expression assay front MDA-MB-231 cells from triple-negative breast cancer (TNBC), which represents the highly aggressive subgroup of breast cancers with poor prognosis. The analyses revealed changes of 27 out of 84 sought target genes. *PARP1* and *PARP2* were 5.29 and 1.83 times down-regulated after treatment with **3**, respectively. *PARP*s have been attractive antitumor drug targets, considering *PARP* inhibition could suppress DNA damage repair and sensitize tumor cells to DNA damage agents. Recent advances in DNA repair studies have shown that an approach that causes cell lethality using synthetic PARP-inhibiting drugs has produced promising results in TNBC.

Keywords Ruthenium compounds · Triple negative breast cancer · Topoisomerase · *PARP* inhibitor

M. S. de Camargo (✉) · M. M. da Silva · A. A. Batista
Center of Exact Sciences and Technology, Federal University of São Carlos, São Carlos, SP 13565-905, Brazil
e-mail: marianasantoro@gmail.com

R. A. De Grandis · M. M. Santoni · C. F. Zanelli · F. R. Pavan
School of Pharmaceutical Sciences, São Paulo State University, Araraquara, SP 14800-903, Brazil

P. B. da Silva
Department of Genetics and Morphology, University of Brasilia, Federal District, DF 70910-970, Brazil

C. E. Eismann · A. A. Menegário
Center of Environmental Studies, São Paulo State University, Rio Claro, SP 13506-900, Brazil

M. R. Cominetti
Department of Gerontology, Federal University of São Carlos, São Carlos, SP 13565-905, Brazil

Published online: 30 November 2018

Dalton Transactions

PAPER

View Article Online
View Journal | View Issue

Published on 04 September 2019. Downloaded by UNIVERSIDADE FEDERAL SAO CARLOS on 11/11/2019 2:02:54 PM.

Check for updates

Cite this: *Dalton Trans.*, 2019, **48**, 14885

Non-mutagenic Ru(II) complexes: cytotoxicity, topoisomerase IB inhibition, DNA and HSA binding†

Monize M. da Silva, [a] Mariana S. de Camargo, [b] Rodrigo S. Correa, [c] Silvia Castelli,[a] Rone A. De Grandis, [d] Jessica E. Takarada, [a] Eliana A. Varanda, [d] Eduardo E. Castellano, [e] Victor M. Deflon, [f] Marcia R. Cominetti, [g] Alessandro Desideri [a] and Alzir A. Batista *[b]

Herein we discuss five ruthenium(II) complexes with good cytotoxicity against cancer cells. These complexes are named [Ru(tzdt)(bipy)(dppb)]PF_6 (**1**), [Ru(mmi)(bipy)(dppb)]PF_6 (**2**), [Ru(dmp)(bipy)(dppb)]PF_6 (**3**), [Ru(mpca)(bipy)(dppb)]PF_6 (**4**) and [Ru(2mq)(bipy)(dppb)]PF_6 (**5**), where tzdt = 1,3-thiazolidine-2-thione, mmi = mercapto-1-methyl-imidazole, dmp = 4,6-diamino-2-mercaptopyrimidine, mpca = 6-mercapto-pyridine-3-carboxylic acid, 2mq = 2-mercapto-4(3*H*)-quinazolinone, bipy = 2,2′-bipyridine and dppb = 1,4-bis(diphenylphosphino)butane. *In vitro* cell culture experiments revealed significant cytotoxic activity for **1–5** against MDA-MB-231, MCF-7, A549, DU-145 and HepG2 tumor cells, higher than that for the standard anticancer drug cisplatin. Compound/DNA interaction studies were carried out showing that **1–5** interact with DNA by electrostatic force of attraction or by hydrogen bonding. Moreover, the complexes interact, moderately and spontaneously, with human serum albumin (HSA) through the hydrophobic region. The five complexes are able to inhibit the DNA supercoiled relaxation mediated by human topoisomerase IB (TopIB), and complex **1** is found to be the most efficient TopIB inhibitor among the five compounds. The inhibitory effect and analysis of different steps of the TopIB catalytic cycle indicate that complex **1** inhibits the cleavage reaction impeding the binding of the enzyme to DNA and has no effect on the religation step. Complexes **1**, **2** and **3** did not show mutagenic activity when they were evaluated by the cytokinesis-block micronucleus cytome assay in HepG2 cells and the Ames test in the presence and absence of mouse liver S9 metabolic activation. Therefore, it is necessary to perform further in-depth analysis of the therapeutic potential of these promising ruthenium complexes as anticancer drugs.

Received 7th May 2019,
Accepted 4th September 2019

DOI: 10.1039/c9dt01905g

rsc.li/dalton

Introduction

Cisplatin is one of the most widely used anticancer drugs. The clinical drawbacks of this metallodrug are apparent, including limited applicability, acquired resistance, and serious side effects, which have limited its application.[1] Therefore, developing new metal-based compounds cytotoxic for cancer cells, which are less toxic than cisplatin has been increasing over the last few year, and one of the most promising metals in cancer therapy is ruthenium.[2–5] Thus, ruthenium complexes have attracted attention not only as anticancer candidates, but also as antibacterial and antifungal drug candidates.[6] The mechanism by which metal complexes exert anticancer activity has been widely investigated and several possibilities have been suggested to underlie the anticancer activities of metal complexes, including their interaction with DNA[7–9] and proteins[10,11] and inhibition of topoisomerase enzyme activity,[12,13] among others. Topoisomerases are involved in

[a]*Dipartimentodi Biologia, UniversitàTorVergatadi Roma, 00133 Rome, Italy. E-mail: monizemsilva@gmail.com*
[b]*Departamento de Química, Universidade Federal de São Carlos, CP 676, CEP 13565-905 São Carlos, SP, Brazil. E-mail: daab@ufscar.br; Tel: +55 16 33518285; Fax: +55 16 33518350*
[c]*Departamento de Química, Universidade Federal de Ouro Preto, CEP 35400-000 Ouro Preto, MG, Brazil*
[d]*Departamento de Ciências Biológicas, Faculdade de Ciências Farmacêuticas, UNESP, CEP 14801-902 Araraquara, SP, Brazil*
[e]*Instituto de Física, Universidade deSão Paulo, CP 369, CEP 13560-970 São Carlos, SP, Brazil*
[f]*Instituto de Química de São Carlos, Universidade de São Paulo, CP 780, CEP 13560-970 São Carlos, SP, Brazil*
[g]*Departamento de Gerontologia, Universidade Federal de São Carlos, CP 676, CEP 13565-905 São Carlos, SP, Brazil*

†Electronic supplementary information (ESI). CCDC 1483972 (**1**), 1484618 (**3**), and 1485378 (**5**). For ESI and crystallographic data in CIF or other electronic format see DOI: 10.1039/C9DT01905G

http://dx.doi.org/10.21577/0103-5053.20190214

J. Braz. Chem. Soc., Vol. 00, No. 00, 1-14, 2019
Printed in Brazil - ©2019 Sociedade Brasileira de Química

Article

Ruthenium(II)-mercapto Complexes with Anticancer Activity Interact with Topoisomerase IB

Monize M. da Silva,*,[a] Mariana S. de Camargo,[a] Silvia Castelli,[b] Rone A. de Grandis,[c] Eduardo E. Castellano,[d] Victor M. Deflon,[e] Marcia R. Cominetti,[f] Alessandro Desideri[b] and Alzir A. Batista*,[a]

[a]*Departamento de Química, Universidade Federal de São Carlos, CP 676, 13565-905 São Carlos-SP, Brazil*

[b]*Dipartimento di Biologia, Università Tor Vergata di Roma, 00133 Rome, Italy*

[c]*Departamento de Ciências Biológicas, Faculdade de Ciências Farmacêuticas, Universidade Estadual Paulista (Unesp), 14801-902 Araraquara-SP, Brazil*

[d]*Instituto de Física de São Carlos, Universidade de São Paulo, CP 369, 13560-970 São Carlos-SP, Brazil*

[e]*Instituto de Química de São Carlos, Universidade de São Paulo, CP 780, 13560-970 São Carlos-SP, Brazil*

[f]*Departamento de Gerontologia, Universidade Federal de São Carlos, CP 676, 13565-905 São Carlos-SP, Brazil*

Herein we present four new ruthenium(II) complexes: $[Ru(mtz)_2(dppb)]$ (**1**), $[Ru(mmi)_2(dppb)]$ (**2**), $[Ru(dmp)_2(dppb)]$ (**3**), and $[Ru(mpca)_2(dppb)]$ (**4**), where mtz = 2-mercaptothiazoline; mmi = 2-mercapto-1-methyl-imidazole; dmp = 4,6-diamino-2-mercaptopyrimidine; mpca = 6-mercaptopyridine-3-carboxylic acid; dppb = 1,4-bis(diphenylphosphino)butane. *In vitro* cell culture experiments revealed cytotoxic activity for complexes **2**, **3** and **4** against MCF-7 (breast, non-invasive), MDA-MB-231 (breast, invasive), A549 (lung), DU-145 (prostate) and HepG2 (liver) tumor cells, in some cases lower than the half maximal inhibitory concentration (IC_{50}) for the reference drug (cisplatin). The deoxyribonucleic acid (DNA) interactions studied by viscosity measurements, gel electrophoresis and square-wave voltammetry indicated that the DNA binding affinity primarily occurs through non-covalent interactions. Only complex **2** was able to fully inhibit the DNA supercoiled relaxation mediated by human topoisomerase IB (Top IB). The analysis indicates that complex **2** inhibits the cleavage and the reconnection steps of the catalytic cycle, being both a poison and a catalytic inhibitor.

Keywords: ruthenium(II) complexes, mercapto ligands, cytotoxicity, topoisomerase IB

Introduction

Mercapto molecules have been used as ligands to prepare compounds with different biological activities, mainly because they already have some antitumor and antiviral activities and may have synergistic effects when coordinated to the metal.[1-4] These characteristics make the interaction of mercapto ligands with heavy metals of particular interest for the synthesis of complexes that could be potential metalodrugs.[3]

Metal complexes, which efficiently bind and cleave deoxyribonucleic acid (DNA) under physiological conditions stopping the reconnection of the biomolecule, can be considered as potential candidates for use as therapeutic agents against cancer, and thus should be considered as an issue deserving further scrutiny.[5-8]

Ruthenium compounds with bidentate ligands are not very toxic and some of them have shown to be quite selective for cancer cells. Thus, this class of complexes has advantages compared to platinum drugs, showing greater selectivity for cancer cells, leading to reduced side effects. These complexes have also demonstrated cytotoxic activity

*e-mail: monize_martins@yahoo.com.br; daab@ufscar.br

Journal of Ethnopharmacology 235 (2019) 183–189

Contents lists available at ScienceDirect

Journal of Ethnopharmacology

journal homepage: www.elsevier.com/locate/jethpharm

Acid diterpenes from *Copaiba oleoresin (Copaifera langsdorffii)*: Chemical and plasma stability and intestinal permeability using Caco-2 cells

M. Mauro[a], R.A. De Grandis[a], M.L. Campos[b], A. Bauermeister[c], R.G. Peccinini[a], F.R. Pavan[a], N.P. Lopes[c], N.V. De Moraes[a,*]

[a] São Paulo State University (UNESP), School of Pharmaceutical Sciences, Araraquara, SP ZIP 14801-902, Brazil
[b] Federal University of Mato Grosso, Sinop, MT, Brazil
[c] University of Sao Paulo (USP), NPPNS, School of Pharmaceutical Sciences of Ribeirao Preto, Ribeirao Preto, SP ZIP 14040-903, Brazil

ARTICLE INFO

Keywords:
Copalic acid
Kaurenoic acid
Caco-2
Intestinal absorption
Viability

ABSTRACT

Ethnopharmacological relevance: Copaiba oleoresin has been used in folk medicine in the treatment of bronchitis, syphilis, skin diseases and ulcers due to its anti-inflammatory and antiseptic activities, but there is no information about major compounds oral absorption to support the traditional use.
Aim of study: Considering the potential of copalic (CA) and kaurenoic acid (KA) – major biological activity (in vitro) diterpenes found in the oleoresin, this study aimed to evaluate the intestinal permeability of CA and KA using Caco-2 cells model as predictive test for oral drug absorption.
Materials and methods: Chemical stability at pH 1.2 and 7.4 and plasma stability were evaluated to mimic physiological conditions of the gastrointestinal tract. The intestinal permeability of CA and KA was evaluated in Caco-2 cells in the presence and absence of the P-glycoprotein inhibitor verapamil.
Results: CA and KA were rapidly degraded at pH 1.2 (0.2 M Clark-Lubs buffer). At pH 7.4 (0.1 M phosphate buffer), CA was stable for up to 24 h and KA for up to 6 h. In human plasma, CA and KA can be considered stable for 24 h and 12 h at 37 °C, respectively. Caco-2 cells were considered viable when incubated with CA or KA in the range of 3.9–250 μM for 24 h. CA and KA exhibited moderate apparent permeability (P_{app}) of 4.67 (± 0.08) × 10^{-6} cm/s and 4.66 (± 0.04) × 10^{-6} cm/s, respectively. Simultaneous incubation with verapamil showed that P-glycoprotein does not play a relevant role on CA and KA oral absorption, with P_{app} of 4.48 (± 0.26) × 10^{-6} cm/s and 5.37 (± 0.72) × 10^{-6} cm/s observed for CA and KA, respectively.
Conclusion: The oral absorption of both CA and KA is driven by mainly passive permeability, is not limited by p-glycoprotein, but enteric-coated dosage forms should be used to avoid chemical instability in the gastric pH.

1. Introduction

Copaifera species, popularly known as "copaibeiras" or "copaíba", are of great economic and ecological interest in Amazon forest. It is estimated that Copaiba oleoresin has been used in popular medicine for more than 500 years (Pieri et al., 2009). Gaspar Barléu observed that animals rubbed themselves in the trunk of Copaifera to heal their wounds (Barléu, 1974). It is assumed that by observing this behaviour, natives began to use the oleoresin with the same intention of healing (Pieri et al., 2009; Veiga Junior and Pinto, 2002). Beyond the use for healing several skin wounds such as ulcers scarring and leishmania skin lesions, copaiba oleoresin has also been used orally in folk medicine in the treatment of bronchitis and syphilis due to anti-inflammatory and antiseptic activities (Albuquerque et al., 2017; Vargas et al., 2015; Tincusi et al., 2002). Natives also apply the oleoresin as mosquito repellent, and currently investigations allowed the development patented formulations for the use based on the traditional knowledge (Pohlit et al., 2011a, 2011b).

Copalic acid (CA) and kaurenoic acid (KA) (Fig. 1) are two major diterpenes of copaiba oleoresin (Veiga Junior et al., 2007, 2005). CA presents in vitro antibacterial activity (da Trindade et al., 2018; Souza et al., 2018), antifungal activity against dermatophytes, (Nakamura

* Correspondence to: São Paulo State University (UNESP), School of Pharmaceutical Sciences, Rodovia Araraquara-Jaú, km 01, Araraquara, SP ZIP 14801-902, Brazil.
E-mail addresses: mariana.mauro@unesp.br (M. Mauro), r.grandis@unesp.br (R.A. De Grandis), michelcampos@ufmt.br (M.L. Campos), ane.meister@usp.br (A. Bauermeister), rosangela.peccinini@unesp.br (R.G. Peccinini), fernando.pavan@unesp.br (F.R. Pavan), npelopes@fcfrp.usp.br (N.P. Lopes), natalia.v.moraes@unesp.br (N.V. De Moraes).

https://doi.org/10.1016/j.jep.2019.02.017
Received 30 November 2018; Received in revised form 4 February 2019; Accepted 10 February 2019
Available online 11 February 2019
0378-8741/ © 2019 Elsevier B.V. All rights reserved.

NATURAL PRODUCT RESEARCH
https://doi.org/10.1080/14786419.2018.1543673

Taylor & Francis
Taylor & Francis Group

Check for updates

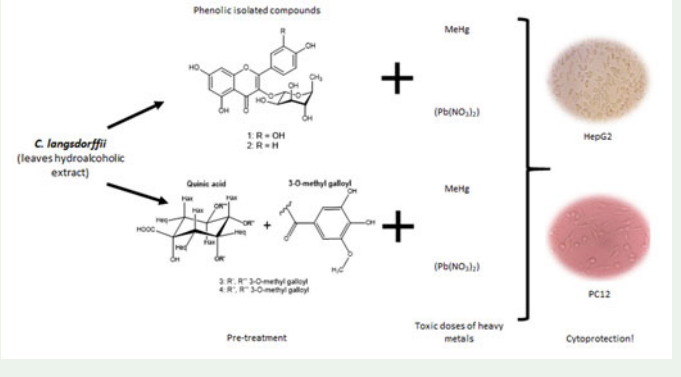
Evaluation of cytoprotective effects of compounds isolated from *Copaifera langsdorffii* Desf. against induced cytotoxicity by exposure to methylmercury and lead

Jennyfer Andrea Aldana[a], Rone Aparecido De Grandis[b], Heloiza Nicolella[d], Ana Paula Prado Guissoni[d], Iara Squarisi[d], Caroline Arruda[a], Victor Pena Ribeiro[a], Denise Crispim Tavares[d], Gustavo Rafael Mazzaron Barcelos[c], Lusânia Maria Greggi Antunes[c] and Jairo Kenupp Bastos[a]

[a]Department of Pharmaceutical Sciences, University of São Paulo, Ribeirão Preto, Brazil; [b]Department of Biological Sciences, São Paulo State University, Araraquara, Brazil; [c]Department of Clinical Toxicological and Bromatological Analyses, University of São Paulo, Ribeirão Preto, Brazil; [d]Nucleus of Research in Sciences and Technology, University of Franca, Franca, Brazil

ABSTRACT

Copaifera langsdorffii L. is one of the most known medicinal species in Brazil. Its leaves are rich in phenolic compounds with potential biological activities as an antioxidant and chelating agent. This paper reports the isolation of four compounds from the hydroalcoholic extract of the leaves of *C. langsdorffii* and the investigation of their possible cytoprotective effects against heavy metal poisoning. Quercitrin (1), afzelin (2), 3,5-di-O-(3-O-methyl galloyl) quinic acid (3) and 4,5-di-O-(3-O-methyl galloyl) quinic acid (4), were associated with toxic doses of methylmercury and lead and evaluated by Alamar blue cell viability assays in HepG2 and PC12. The compounds displayed significant cytoprotective effect for the HepG2 cell line against both metals. Compounds 1–4 did not protect PC12 cells against methylmercury induced-cytotoxicity, but at lower concentrations, they protected against lead induced-cytotoxicity. The evaluated compounds showed a promising cytoprotection effect against exposure to heavy metals and should be further investigated as protective agents.



ARTICLE HISTORY

Received 12 July 2018
Accepted 29 October 2018

KEYWORDS

Copaifera langsdorffii; Caesalpinaceae; cytoprotection; heavy metals; flavonoids; galloylquinic compounds

CONTACT Jairo Kenupp Bastos jkbastos@fcfrp.usp.br

Supplemental data for this article can be accessed at https://doi.org/10.1080/14786419.2018.1543673.

© 2018 Informa UK Limited, trading as Taylor & Francis Group

Food and Chemical Toxicology 136 (2020) 111047

Contents lists available at ScienceDirect

Food and Chemical Toxicology

journal homepage: www.elsevier.com/locate/foodchemtox

Transcriptome and DNA methylation changes modulated by sulforaphane induce cell cycle arrest, apoptosis, DNA damage, and suppression of proliferation in human liver cancer cells

Patrick Wellington da Silva dos Santos[a], Ana Rita Thomazela Machado[a], Rone Aparecido De Grandis[b], Diego Luis Ribeiro[b], Katiuska Tuttis[b], Marco Morselli[c], Alexandre Ferro Aissa[a], Matteo Pellegrini[c], Lusânia Maria Greggi Antunes[a,*]

[a] Department of Clinical Analysis, Toxicology and Food Sciences, School of Pharmaceutical Sciences of Ribeirão Preto, University of São Paulo, Av. do Café - Vila Monte Alegre, Ribeirão Preto, SP, 14040-903, Brazil
[b] Department of Genetics, Ribeirão Preto Medical School, University of São Paulo, Av. Bandeirantes, 3900 - Vila Monte Alegre, Ribeirão Preto, SP, 14049-900, Brazil
[c] Department of Molecular, Cell, and Developmental Biology, University of California at Los Angeles, 610 Charles E Young Dr S, Los Angeles, CA, 90095, USA

ARTICLE INFO

Keywords:
Isothiocyanate
Active compound
Sequencing
Epigenetics
Chemoprevention

ABSTRACT

Abnormal epigenetic alterations are one of the keystones of cancer development. Epigenetic targeting drugs have become a promising and effective cancer therapy strategy. However, due to the high toxicity and unclear mechanisms of action of these drugs, natural compounds that cause epigenetic modulation have also been studied. Sulforaphane (SFN) is a promising bioactive compound for epigenetic targeting therapy. In this study, we investigate the effects of SFN on gene expression and DNA methylation in human hepatocellular carcinoma cells (HepG2). Using high throughput technologies in combination with cell-based assays, we find SFN is a potent anticancer agent, as it induces DNA damage, mitotic spindle abnormalities followed by apoptosis and proliferation inhibition in HepG2 cells. Our results show the upregulation of DNA damage response and cell cycle checkpoint genes. Also, we find the downregulation of cellular pathways frequently overexpressed in human cancer. As expected, SFN exerts epigenetic modulation effects by inhibiting histone deacetylases (HDACs). SFN might affect the activity of oncogenic transcription factors through methylation of its binding sites motifs. Our findings offer insights into SFN chemopreventive molecular effects in HepG2 cells and highlight SFN as a valuable natural approach to cancer therapy for future investigation.

1. Introduction

Hepatocellular carcinoma (HCC) is the most aggressive and lethal malignancy of primary liver cancer (Hlady and Robertson, 2018). Unsatisfactory results with conventional treatments due to the high recurrence rate underscore the need for novel approaches to treat liver cancer (Zeidler et al., 2017). In addition to genetic mutations, epigenetic modulation is associated with the initiation and development of HCC (Ma et al., 2014). Silencing of tumor suppressors and activation of oncogenes by epigenetic mechanisms such as aberrant DNA methylation pattern and histone modifications plays an essential role in promoting cancer (Kelly and Issa, 2017). Global DNA methylation changes and abnormal expression of epigenetic regulatory genes have been reported in HCC (Ozen et al., 2013). Deacetylation of histones via histone deacetylases (HDACs) results in transcriptional repression and heterochromatin formation (Yang and Seto, 2007). High expression of these enzymes has been reported in many types of cancer, including HCC (Li and Seto, 2016).

Research investigating novel approaches for the treatment and prevention of cancer has improved our understanding of the interactions between diet and gene regulation (Nosrati et al., 2017). Many dietary compounds have been shown to be useful in cancer prevention by modulating gene expression through multiple mechanisms (Hardy and Tollefsbol, 2011; Meeran et al., 2010). Sulforaphane (SFN), a bioactive isothiocyanate found in cruciferous vegetables, activates the nuclear factor NRF2, upregulating cytoprotective genes, including

* Corresponding author. Av. do Café, s/n, Faculdade de Ciências Farmacêuticas de Ribeirão Preto, 14040-903, Ribeirão Preto, SP, Brazil.
E-mail addresses: patrickwsantos@gmail.com (P.W.d.S. dos Santos), anaritatmachado@usp.br (A.R.T. Machado), degrandis.rone@gmail.com (R.A. De Grandis), diegoluisribeiro@usp.br (D.L. Ribeiro), kattuttis@gmail.com (K. Tuttis), mmorselli@g.ucla.edu (M. Morselli), afaissa@gmail.com (A.F. Aissa), matteop@mcdb.ucla.edu (M. Pellegrini), lusania@fcfrp.usp.br, lusania@fcfrp.usp.br (L.M.G. Antunes).

https://doi.org/10.1016/j.fct.2019.111047
Received 24 October 2019; Received in revised form 30 November 2019; Accepted 5 December 2019
Available online 12 December 2019
0278-6915/ © 2019 Elsevier Ltd. All rights reserved.